DEVELOPMENT AND APPLICATION OF NON-TAPERED ELECTROSPRAY EMITTERS FOR NANO-ESI MASS SPECTROMETRY

by

SHUQIN SU

A thesis submitted to the Department of Chemistry

In conformity with the requirements for

the degree of Doctor of Philosophy

Queen's University

Kingston, Ontario, Canada

September, 2008

Abstract

Nano-ESI mass spectrometry is an attractive analytical technique due to its high sensitivity and small sample consumption, which is especially important for research areas such as proteomics. However, current nano-ESI emitters become a bottleneck for nano-ESI to be widely applied because of problems such as clogging, poor robustness, large flow resistance, and poor spray efficiency for highly aqueous solutions. The objective of this thesis study is to address the problems associated with tapered emitters and provide alternative solutions by developing advanced nano-ESI emitters. Two strategies that were explored to improve the clogging resistance and robustness while maintaining comparable electrospray performances include the development of emitters with larger apertures and multiple channels.

Following these strategies, five types of emitters were fabricated without tapering either internal or external diameters, which include a roughened open tubular emitter, a porous membrane-assisted emitter, a microstructured multiple channel photonic crystal fiber (MSF) emitter, a packed ODS bead emitter, and an entrapped ODS bead emitter. The successful transformation of MSF fibers to nanoelectrospray emitters demonstrates a new practical approach to expand the application of nano-ESI because of its availability, compatibility, precisely controlled channel dimensions, variety of channel patterns, and feasibility for surface modification.

The fundamental mechanism of non-tapered emitters was studied at nano flow rates. The fact that a plume of mist, instead of single Taylor cone, is generated from multiple channel emitters at nano flow rates suggests multiple Taylor cones may be

formed. The calculated sensitivity gains from a MSF emitter compared to a single-tip tapered emitter are related to the number of the orifices containing on a MSF emitter.

The characterization of impacts of operational parameters on nanoelectrospray performances shows that non-tapered emitters are more robust and less dependent on the emitter's fine positioning. It was also found that unlike tapered emitters, non-tapered emitters can be positioned ten times further from the orifice of a mass spectrometer, which is greatly beneficial to online sample manipulation and purification. Furthermore, the electrospray efficiency of spraying highly aqueous solutions (*e.g.* 90%) was greatly improved through the hydrophobic modification of a MSF emitter exit.

Co-Authorship

The work discussed in this thesis was conducted by the author in the Department of Chemistry of Queen's University under the supervision of Dr. Richard D. Oleschuk. Part of the work described in Chapter 3 was co-supervised by Dr. Guojun Liu. Portions of the thesis have been published or submitted for publications in the following journals:

1. **Su, S.;** Marecak, D.; and Oleschuk, R. D., *Rapid Communications in Mass Spectrometry*, **2008**, 22, 2053 - 2062
2. **Su, S.** and Oleschuk, R. D., submitted to the *Canadian Journal of Chemistry*
3. Mugo, S.; **Su, S.;** Marecak, D.; Oleschuk, R. D.**,** submitted to *Analytical Chemistry*
4. Oleschuk, R. D.; **Su, S.;** Mugo, S.; Marecak, D., US provisional patent application, 61/ 064,712

Acknowledgements

I would like to thank my supervisor Richard Oleschuk for his guidance, encouragement, and inspiration during my entire study and research work. Without his support, I wouldn't be where I am today. I also thank my co-supervisor Dr. Guojun Liu for his co-supervision on my membrane project and for allowing me to use his lab resources during my research. I would also like to acknowledge my committee members Dr. Diane Beauchemin and Dr. Hugh Horton for all their help.

I would also like to thank everyone in the O-group for sharing and discussing ideas with me which made my study more valuable and enjoyable. Special thanks are given to the following individuals for their generous help. Dr. Terry Koerner and Dr. Stephen Lee trained me on nano-ESI interfaced mass spectrometers. Dr. Mohammed Bedair taught me how to use hot embossing to fabricate a polymer-based microchip. I also appreciate all the valuable discussions with Dr. Dale Marecak and enjoyed his fine work from a true crafts man's hand. Working with Sam on the photonic crystal fiber project was fascinating and I appreciate his dedication on eventually getting our best nanoelectrospray images. Dr. Graham Gibson greatly helped me in editing my English over years, which I appreciated very much. I also thank Michelle Douma, Adam Daley, Feng Sheng, Ruixi Xie, and Runkai Li for their friendship and support.

In addition, I want to especially thank Dr. Xiaohu Yan in Dr Liu's group for training me on preparing a polysulphone membrane. Also, I thank Dr. Gabrial for helping us use the microscope and getting electrospray images. Finally, I thank Ms. Jian Wang for her talent and generous help by taking the AFM images for me.

Dr. Yimen She helped me arranged my experiment on Q-TOF in the departmental mass spectrometry facility, which was greatly appreciated. I also enjoyed the discussions with Yimen and Ms. Jessie Sui.

I would like to thank NSERC (Natural Sciences and Engineering Research Council of Canada), Canadian Foundation for Innovation, Genome Prairie, Ontario Innovation Trust, MDS SCIEX, and Queen's university for providing the funding to support my research.

I would also like to thank my husband Yi Zhang, as well as my sons Winston and Victor for their love and support. I have learned lots of tips and tricks from Winston and Victor on making better cartoon models or animations to present the scientific findings or discussions through my study.

Statement of Originality

This thesis work is the first to categorize non-tapered emitters into open tubular emitters and multiple channeled emitters.

The original findings include the reports of a roughened open tubular emitter, a porous polymer membrane assisted emitter, and a photonic crystal fiber derived multiple channeled emitters, and their applications as nano-ESI emitters.

This thesis also reports the evaluation and characterization of these non-tapered emitters in terms of their operational parameters, robustness, and sensitivity. It is the first finding from this work that a non-tapered emitter should be positioned relatively further to the MS orifice compared to a conventional tapered emitter, which makes a great contribution for the effective utilization of non-tapered emitters. It is also original work to use Hank's solution to evaluate the robustness of an entrapped emitter and a crystal fiber emitter.

In addition, it is also an original work that these emitters were used in a Q-TOF to demonstrate protein identifications from a constant infusion.

I hereby certify that all of the work described within this thesis is the original work of the author except where otherwise indicated. Any published (or unpublished) ideas and/or techniques from the work of others are fully acknowledged in accordance with standard referencing practices.

Shuqin Su

August 2008

Table of Contents

List of Figures

List of Tables

List of Abbreviations

ACN	-	acetonitrile
AFM	-	atomic force microscope
API	-	atmospheric ionization
BDDA	-	1, 3-butanediol diacrylate
BK	-	bradykinin
BMA	-	butyl methacrylate
BME	-	benzoin methyl ether
BSA	-	bovine serum albumin
CCD	-	charged coupled devices
CE	-	capillary electrophoresis
CEC	-	capillary electrochromatography
CI	-	chemical ionization
CNF	-	carbon nanofiber
COC	-	cyclic olefin copolymer
CPS	-	counts per second
CTMS	-	chlorotrimethylsilane
Cyt-c	-	cytochrome c
Da	-	dalton
ESI	-	electrospray ionization
FAB	-	fast atom bombardment
FD	-	field desorption
FP	-	fluorinated polymer
FTICR	-	fourier transform ion cyclotron resonance
FWHM	-	full-width at half-maximum
HPLC	-	high performance liquid chromatography
i.d.	-	internal diameter
Ins	-	insulin
Kphos	-	potassium phosphate

LC	-	liquid chromatography
LE	-	leucine enkephalin
MALDI	-	matrix assisted laser desorption ionization
MeOH	-	methanol
MS	-	mass spectrometry
MS/MS	-	tandem mass spectrometry
MSF	-	microstructured silica fiber
m/z	-	mass to charge ratio
MW	-	molecular weight
o.d.	-	outer diameter
ODS	-	octadecyl silane
PAH	-	polyaromatic hydrocarbon
PC	-	polycarbonate
PD	-	plasma deposition
PEEK	-	poly ether ether ketone
PMMA	-	poly(methyl methacrylate)
PPM	-	porous polymer monolith
PSF	-	polysulphone
PTFE	-	polytetrafluoroethylene
Q-TOF	-	quadrupole time of flight
RSD	-	relative standard deviation
SD	-	standard deviation
SEM	-	scanning electron microscope
S/N	-	signal to noise ratio
SPE	-	solid phase extraction
2D-PAGE	-	two dimensional polyacrylate gel electrophoresis
THF	-	Tetrahydrofuran
TMSPMA	-	3-(trimethyoxysil)propyl methacrylate
μ-TAS	-	micro total analysis system
TIC	-	total ion current

TOF	-	time of flight
Tris	-	tris(dimethylphenylphosphine)(2,5-norbornadiene)rhodium(I) hexafluorophosphate
UPLC	-	ultra high pressure liquid chromatography
XIC	-	extracted ion current

Chapter 1

Introduction

1.1 Overview

The discovery of electrospray ionization (ESI) has made mass spectrometry not only a powerful detector for small molecules (e.g. drugs), but for large biomolecules such as proteins/peptides as well.[1] Electrospray ionization enables the formation of singly or multiply charged ions, which can be separated and detected by a mass spectrometer with a regular mass to charge (m/z) window. This makes it possible to detect molecular masses of hundreds to hundreds of thousands of Daltons such as proteins or peptides. The availability of the ESI technique has largely proliferated the application of mass spectrometry in research areas such as proteomics, biomarker discovery, drug discovery, combinatorial chemistry, pharmacokinetics, drug metabolism, clinical drug testing, forensics, the analysis of food/herbal nutrients/toxins, water quality, food contamination, and the study of petrofuel/biofuel compositions.[2-5] ESI-MS is now a basic tool used in probably every biological chemistry laboratory in the world.

One of the key reasons that ESI-MS is favored by bio-analytical laboratories is because of its capability of transforming ions from a liquid-phase to a gas-phase, which makes ESI an ideal match between sample manipulation and purification technologies such as solid phase extraction (SPE), liquid chromatography (LC) and microfluidic devices, and the versatile detection method of mass spectrometry.[6-8] Microfluidic devices (both chip-based and capillary-based), which are miniaturized analytical devices also

called micro total analysis system (μ-TAS), are capable of fully or partially integrating injection, sample cleanup, reaction, concentration, separation, and detection all on one glass or polymer chip.[9, 10] While the ultimate aim of μ-TAS is to include sample manipulation and detection on a single chip-sized device, simpler devices with partially integrated functionalities may have more advantages in some applications due to their robustness and better reliability. Compared to a chip-based device, a capillary-based device is simpler and can integrate functions such as desalting, pre-concentration and separation.[11-15] Following online LC or nano-LC, the analytes can be delivered through electrospray ionization into a mass spectrometer (MS) for enhanced detection.

Among the application areas of LC-ESI-MS or MS/MS, proteomics, which studies the relationship between protein expression profiles and disease status, has become a driving force for the development of advanced ESI technologies.[16-18] The emerging field of proteomics is envisioned as one of the most promising approaches for the development of non-invasive diagnostic tools to identify human diseases.[19-21] Proteomics seeks to create protein expression profiles for hundreds or thousands of proteins in a single assay. Challenges faced by current proteomic technologies include small sample amounts available for testing, limited throughput capabilities, the labour intensity nature of the technique, large sample volume requirements, large dynamic range of protein concentration, and the inability to measure low abundance proteins. New technologies are being developed to handle the challenges in this research area. Nano-ESI, which generates smaller droplets by spraying analytes into a MS ion source at flow rates less than 1000 nL/min, is one of the most remarkable advances in ESI technology

development.[22-24] Nano-ESI/MS or MS/MS, in combination with nano-LC/microfluidic devices, has successfully demonstrated improved sensitivity, selectivity and sample throughput through online sample cleanup, pre-concentration, and separation of analytes from complicated matrixes.[18, 25] Nano-LC/nano-ESI/MS or MS/MS has become a dominant analytical tool for the "bottom-up" protein analysis strategy, in which proteins of interests are digested by enzymes such as trypsin; the resulting "tryptic peptides" being used as a fingerprint for protein identification.[16]

As an interface, a nano-emitter is crucial to coupling a miniaturized sample manipulation system with a mass spectrometer. An ideal nano-emitter would be able to attain small flow rates for highly efficient separation and highly sensitive detection, meanwhile allowing high flow rates for fast sample loading and concentrating. Nano-emitters also need to be robust enough to achieve high throughput for routine analysis.[26-29] Traditionally, nano-ESI is generated from tapered-emitters with small apertures fabricated by pulling or etching techniques.[22, 26, 30-32] However, due to the nature of small apertures, tapered nano-emitters suffer from continuous clogging caused by salt deposits or solids from LC column bleed.[29, 33, 34] Common problems encountered with traditional tapered nano-emitters also include less accessible flow rates to match higher flow rates for fast on-line sample preparation. Furthermore, if there is a separation process necessary upstream of the emitter, any dead volume caused by an ESI emitter may lead to band broadening. The tradeoff of emitter robustness for higher sensitivity from traditional tapered nano-emitter has largely impeded the wide acceptance of nano-ESI/MS in more diverse application areas.

The development of efficient and robust nano-emitters to interface nano-LC and nano-ESI/MS is currently an active research area.[31, 32, 35-37] Further fundamental understanding of nano-ESI and the factors that affect nanoelectrospray behavior and performance would enable not only the development of more efficient and robust nano-emitters, but also the application of nanoelectrospray in broader areas. The objective of this thesis is to develop alternative nano-emitters to address existing problems associated with the tapered emitters, and apply them to protein/peptide analysis using a nano-LC/nano-ESI/MS system. This introduction includes some fundamental aspects of nanoelectrospray, including a brief literature review of the history and theory of nano-ESI, the design and fabrication techniques of various nano-emitters, instrumental components in a nano-LC/nano-ESI/MS system, and a brief introduction of nanoelectrospray applications in proteomics and other areas. The strategies/approaches used in the thesis for developing non-tapered nano-emitters are also introduced leading to more detailed discussions in the designated chapters. Through this study, significant progress has been achieved to solve some of the problems associated with the tapered nano-emitters.

1.2 The fundamental aspects of nanoelectrospray

1.2.1 The journey from electrospray to nanoelectrospray

The invention of the first mass spectrometer by Thomson in the early twentieth century opened a new chapter of molecular studies.[38, 39] In principle, if a molecule can be vaporized and ionized, its molecular mass can be determined according to its mass to

charge ratio after being accelerated and separated in an electro-magnetic field. It is feasible to vaporize or ionize small molecules by bombarding them with energetic particles such as electrons, photons, or ions of other atoms or molecules. However, as cited in Fenn's Nobel lecture in 2002: "a few years ago, the idea of making proteins or polymers fly seemed as improbable as a flying elephant." It was not easy to make large bio-molecules such as proteins/peptides, the big "elephant", fly without extensive fragmentation and decomposition since many of the bio-molecules are insufficiently volatile and thermally unstable.[40, 41] In the 1960s, the recognize of the relationship between information contained in DNA and the protein structures intensified the search for relatively "soft" ionization techniques, through which fragmentation and decomposition are greatly eliminated.[42] The major historical developments regarding "soft" ionization methods for mass spectrometry are listed in Table 1.1.

During the search for "soft" ionization methods, a number of such methods were developed, including chemical ionization and field desorption.[42, 43] Eventually, two main paths were followed, which led to the discovery of electrospray ionization (ESI) and matrix-assisted laser desorption/ionization (MALDI), the two dominant "soft" ionization techniques for biomolecule analysis by mass spectrometry today.[44] Unlike electrospray, MALDI and several other techniques such as plasma deposition (PD), and fast atom bombardment (FAB) are based on an energy-sudden approach from which sufficient rapid heating vaporizes complex molecules before they have time to decompose. Even though this approach is not the subject of this thesis, it is worth mentioning since it is also a commonly used ionization method for biomolecule analysis.

Table 1.1. Historical developments in "soft" ionization since MS invented[43]

Investigator(s)	Year	Contribution
Thomson	1899-1911	First mass spectrometer
Munson and Field	1966	Chemical ionization (CI)
Dole	1968	Electrospray ionization(ESI)
Beckey	1969	Field desorption (FD)
MacFarlane and Torgerson	1974	Plasma desorption (PD)
Barber	1981	Fast atom bombardment (FAB)
Tanaka and Karas	1983	Matrix-assisted laser desorption ionization (MALDI)
Fenn	1984	ESI on biomolecules
Mann and Wilm	1991	Nano-ESI
Fenn/Tanaka	2002	Nobel Prize for ESI on biomolecules

Electrospray on the other hand utilizes a phenomenon that produces fine droplets from the conical tip of a fluidic surface as fluid flows from a capillary under an external electric field.[6, 45] With solvent evaporation, these droplets repetitively undergo fission to become a fine mist. The electrospray technique has been used in applications ranging from coating a car with uniform paint, crop-dusting with insecticides, to nanotechnologies such as generating nano-particles and quantum dots, and micro-engineering through direct writing.[46, 47] Electrospray has also been used as a "soft" ionization technique in mass spectrometry, which not only produced a revolution in the detection of large bio-molecules, but also provided an efficient interface between separation technologies (*e.g.* liquid chromatography) and mass spectrometry.[42]

The pioneering work using electrospray as a "soft" ionization technique for macromolecule analysis was reported by Dole in 1968.[48] In Dole's original experiment, he demonstrated the possibility of generating gas-phase ions of macromolecules by electrospraying a diluted solution of nonvolatile solute species from the tip of an electrically charged capillary. His work defined the basic experimental parameters for electrospray and included the successful ionization of several high mass species such as polystyrene with average 510,000 Da. Unfortunately, his system couldn't produce sufficient desolvation for the charged droplets by using an evaporation chamber filled with nitrogen gas. Moreover, he did not realize the multiple-charging aspects of ESI and was not able to interpret the observed mass spectrum, which largely impeded his further exploration. However, Dole's work paved the road for Fenn's discovery, which eventually gave "wings to the big molecular elephant".[42]

When Fenn and his colleagues repeated Dole's electrospray experiment, they realized some flaws limiting the desolvation efficiency in Dole's original design and made some significant modifications.[42] In Fenn's setup, dry nitrogen gas was introduced at the exit of the emitter as a curtain gas to assist droplet desolvation in order to avoid solvent and other "junk" entering the vacuum system.[42] A convincing experimental result was reported for the first time where peptides and proteins with up to 40,000 Da molecular mass were measured in 1984.[49] Most dramatically, they discovered that through electrospray, multiply charged ions could be produced, which makes the measurement of large bio-molecules possible by the commercially available mass analyzers with limited mass range. Fenn's work outlined the fundamental aspects of

electrospray ionization, demonstrated its utility for the analysis of biomolecules, and provided an efficient interface for the combination of a liquid chromatographic separation with mass spectrometry.

After Fenn's 1988 seminal publication,[1] the MS community broadly recognized the potential of coupling LC and MS through an ESI interface to do biomolecule related studies. Over the past 20 years, ESI-MS applications have expanded at a breathtaking pace to include essentially every class of biomolecules. Electrospray ionization mass spectrometry (ESI-MS) has matured to become a versatile technology because of its unrivalled high sensitivity, selectivity, broad applicability and availability. The emerging ESI platform has largely proliferated the application of mass spectrometry in proteomics, which studies the relationship between protein expression profiles and disease status from the array of proteins in an organism, tissue, or cell at a given time.[19, 20, 50] In return, the need for greater sensitivity to better detect, identify, and quantify biomolecules in proteomics has become a primary driving force for the development of the advanced ESI technologies.[16-18] Since the volume of sample in proteomics is usually very small (a few microliters), the detection sensitivity becomes a limiting factor to obtain sufficient in-depth information with current proteome measurements.

Nanoelectrospray, which generates smaller droplets by spraying analytes into a MS orifice at flow rates less than 1000 nL/min, enhances the sensitivity of detection with very small sample consumption.[22, 33] Fenn noticed this effect as described in a paper published in Science in 1989.[1] However, it was Wilm and Mann who first quantitatively studied (published in 1994) the electrospray processes to predict the size of a droplet at

different flow rates.[51] Consistent with theoretical prediction, nanoelectrospray results in the formation of smaller droplets, which consequently leads to better desolvation and ionization of charged species from the ion source to the mass analyzer, providing distinctively high sensitivity. In addition, nano-ESI eliminates the nebulizing gas requirements, and greatly minimizes matrix effects due to the reduction of charge competition. At lower flow rates, sample utilization efficiency is higher due to the elongated acquisition time.[33] Since the emergence of nano-ESI, research in nanoelectrospray has been actively pursued in different directions such as the development of robust and reliable nano-ESI emitters,[52] the coupling of nano-ESI/MS to miniaturized sample manipulation devices,[53, 54] and the development of high throughput proteomics system involving nano-ESI.[33] However, the nano-ESI technique has not been widely accepted as a routine bio-analytical tool due to robustness concerns. Moreover, the mechanism of nanoelectrospray has yet to be fully understood because of the complicated multiple variables involved, which makes the practice of nano-ESI rather a "black box" for its users. This study hopes to shine some "light" into the "black box".

1.2.2 Mechanism of nanoelectrospray

In general, the electrospray process can be divided into three stages including droplet formation, droplet shrinkage, and gaseous ion formation as shown in Figure 1.1. However, debate remains on how gaseous ions form.[6, 33, 45] When a solution is delivered to the tip of an electrospray emitter under an electric field, the tip of solution forms a conical shape called a Taylor cone named after Dr. Taylor who theoretically described

this phenomenon in 1964.[55] In positive ESI mode, a positive potential is applied on the tip of the emitter, positive ions in the solution will accumulate on the surface of the conical cone. The electric forces on the emitter tip pull the liquid into a cone shape. When the electric forces overcome the surface tension, the liquid surface becomes unstable. The instability of the liquid surface causes the ejection of droplets.

One mechanism suggests that the evaporation of solvent from the initially formed droplet leads to a shrinkage in the size of the droplet. "Coulombic explosion" occurs at the Rayleigh limit, where the density of the charges on the droplet surface overcomes the surface tension holding the droplet together.[1] A series of smaller and lower charged droplets are formed. The evaporation and explosion processes are repeated until ions with a single or multiple charges are formed. The charges are statistically distributed among the analyte's available sites to form multiply charged ions.

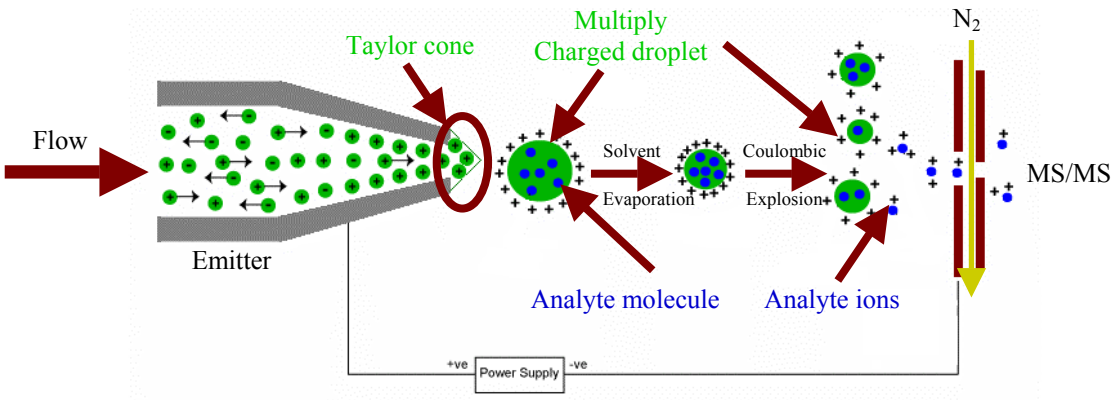

Figure 1.1. Schematic drawing illustrating the electrospray processes.

The second mechanism is based on the idea of Iribarne and Thompson, in which ions escape from highly charged droplets due to the same charged ions within a droplet.[56, 57] Fenn's explanation is based on the evaporation and repulsion theory. None of these theories, however, quantitatively describes the electrospray process and research is still continuing on the mechanism of ion formation.[58, 59]

Wilm and Mann quantitatively studied electrospray processes based on the original Taylor cone theory.[22] A relationship, illustrated in equation 1.1, was established to predict the size of an emission zone at the tip of a Taylor cone in a situation close to static equilibrium. A schematic diagram of a Taylor cone (zoom-in) and an illustration of the radius of the emission region are shown in Figure 1.2.

$$r_e = \left(\frac{\rho}{4\pi^2 \gamma \tan\left(\frac{\pi}{2} - \vartheta\right)\left[\left(\frac{U_a}{U_T}\right)^2 - 1\right]} \right)^{1/3} \times \left(dV/dt\right)^{2/3} \qquad (1.1)$$

Where: r_e is the radius of the emission region for droplets at the tip of a Taylor cone,

ρ is the density of a liquid

γ is the surface tension of a liquid

ϑ is the liquid cone angle ($\vartheta = 49.3°$ for a classical Taylor cone model at static equilibrium)

U_a is the applied spray voltage

U_T is the threshold voltage

dV/dt is the flow rate

Based on equation 1.1, the emission diameter on the tip of a Taylor cone, at which droplets are emerging, is proportional to the 2/3 power of the flow rate. This formula indicates that the emission diameter, and thus the size of the droplets is reduced when the flow rate is lowered. As the droplet size is reduced, desolvation becomes much easier because less energy is required to evaporate the solvent from the surface of the droplets. At flow rates of a few nanoliters per minute, droplets become small enough to result in almost immediate ion emission. This has become the fundamental theory for nanoelectrospray ionization.

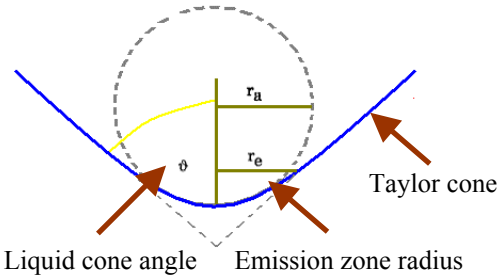

Figure 1.2. A schematic diagram of a Taylor cone (zoom-in) and an illustration of the radius of the emission region.[22]

The feature that distinguishes conventional ESI and nano-ESI is the size of droplets formed according to Wilm and Mann. However, it has to be mentioned that the above equation was derived under a condition that is close to static equilibrium, whereas electrospray occurs in a non-equilibrium condition. Furthermore, the nanoelectrospray theory was proposed using a model of a single tapered emitter tip, and emitters with different architectures may produce ions in an alternative manner. For instance, instead of observing a single Taylor cone, a plume of mist was observed during one of our studies

from multiple-channel emitters while spraying at low nano flow rates. Characterization of the nanoelectrospray behavior of various emitters with different architectures would be beneficial for the further understanding of nanoelectrospray mechanism.

1.2.3 Characterization of nanoelectrospray behaviour and its performance

Nanoelectrospray usually refers to flow rates in the range of 1 nL/min to 1000 nL/min.[33] In this study, we refer to flow rates from 10-50 nL/min as low nano flow rates; 50-100 nL/min as intermediate nano flow rates; and 100 to 500 nL/min as high nano flow rates.

Characterization of nanoelectrospray is mostly based on single-tip tapered emitters. The operational parameters of such a nano-emitter were initially described in a case of establishing a nanoelectrospray from a 1-2 μm emitter aperture at about a 20 nL/min flow rate.[22] The nano-emitter tip was positioned 1-2 mm in front of the orifice of the MS vacuum system and in line with the quadrupole axis to reduce ion losses, thus ensuring high sensitivity. These parameters became commonly recommended when using a tapered nano-emitter. However, in reality, the corresponding operational parameters to realize the expected electrospray performance are complicated due to many variables. Through the characterization of a nanoelectrospray behavior under different conditions, an optimized electrospray performance may be realized.

Electrospray behavior refers to the type of Taylor cone formed and the relative spray performance. Tapered emitters have been extensively studied by different groups to understand how their operational parameters affect nanoelectrospray behaviour.[33, 60, 61] In

general, factors such as emitter geometry, interface design (*e.g.* with or without sheath flow and applied heat), as well as electrospray voltage, solvent composition, flow rate, and the relative distance from an emitter tip to the MS orifice, have been found to affect the formation of a Taylor cone, a critical factor for establishing a stable nanoelectrospray.[62] The formation of a Taylor cone is a dynamic phenomenon involving interactions between liquid and the emitter exit, liquid and liquid, liquid and air, due to surface tension.[63] When applying high voltages to an emitter tip, the electric repulsion on the surface of a cone is balanced by the surface tension γ of a fluid. Furthermore, the electrospray voltage not only affects the electrospray performance but also determines if an electrospray is able to be initiated or not. In a static condition, pressures due to the electrostatic force and the surface tension must be equal for all points on the surface of a Taylor cone.[64] The threshold or onset voltage U_t, has a relationship, as illustrated in equation 1.2,[51] with the surface tension γ, electric constant ε_0, and the distance between the tip of a cone and the counter electrode r_1:

$$U_t = 0.863\left(\frac{\gamma r_1}{\varepsilon_0}\right)^{1/2} \qquad (1.2)$$

This equation shows that higher surface tension and longer distance from the counter electrode require higher threshold voltages. When an applied electric potential U_a is higher than the threshold voltage U_t, the static equilibrium is broken and a pointed cone forms rapidly from the liquid surface. The fluid is dispersed from the tip of the cone in the form of a narrow jet. The jet spreads into a fine mist of droplets, which shrink by solvent evaporation, and eventually form multiply-charged ions through "Coulombic

explosion" or repulsion. When the applied spray voltage is increased, the electrospray ion current will increase linearly in the stable spray region as shown by equation 1.3,[51] where R_f is the overall flow resistance:

$$I \propto \left(\frac{1}{R_f^{1/5}} \right) \left[\left(\frac{U_a}{U_t} \right)^2 - 1 \right]^{3/5} \tag{1.3}$$

Meanwhile, solvents with larger surface tension have higher threshold voltages, as shown in equation 1.2. Organic solvents generally have a smaller surface tension than water; therefore they spray more easily than water. In fact, the applied voltage needed to spray pure water may be high enough to cause an electrical discharge, especially in negative ion mode. As a result, spraying 100% aqueous solutions is problematic, which necessitates the development of specially designed emitters to assist electrospray of high aqueous solutions.

Flow rate (i.e. <1000 nL/min) differentiates nanoelectrospray from conventional electrospray and determines the size of the emission diameter for droplets emerging from the tip of a Taylor cone, as illustrated in equation 1. At higher flow rates, a jet of liquid emerges from the tip of a Taylor cone. As the flow rate is reduced, the cone jet becomes shorter due to smaller droplets formed. Higher sensitivity is expected at lower flow rates. Nanoelectrospray sensitivity is usually divided into two flow rate regions: a concentration sensitive regime, and a mass sensitive regime.[33] Within the concentration sensitive regime, the intensity of total ion current (TIC) or extracted ion current (XIC) stays almost constant at different flow rates when infusing solutions with the same concentration. It means that lowering the flow rate increases both sample utilization efficiency and

ionization efficiency. The point where the sample utilization and ionization efficiencies are maximal, is called the optimum flow rate. When the flow rate is lowered further, a mass sensitive region appears, and the TIC intensity decreases as the flow rate is lowered. In this region, the absolute number of ions contained in the solution determines the intensity of TIC, and the nanoelectrospray behaviour becomes unpredictable.

Various approaches were used to measure, compare or simply demonstrate the sensitivity of detection from nanoelectrospray MS. Electrospray ion current is used for the quantitative measurement of ionization efficiency and transmission efficiency individually. Practically, for a comparison of sensitivity at the same flow rate with the same analyte concentration, the intensity of TIC or XIC are the simplest methods. To indicate a change in sensitivity at different flow rates, signal change per unit amount of analyte more accurately reflects the sensitivity under different conditions. A signal response factor is calculated using the average TIC/XIC intensity divided by the amount of analyte consumed over a certain amount of acquisition period using the following equation 1.4:

$$RF = \frac{I}{\left[c \times \left(\frac{dV}{dt} \right) \times t \right]} \qquad (1.4)$$

Where: *RF* is the response factor; *I* is the average intensity of TIC/XIC (TIC in this case); *c* is the concentration of analyte; d*V*/d*t* is the flow rate; and *t* is the acquisition time.

In addition, factors such as spray voltage, flow rate, mobile phase composition, and emitter geometry are also believed crucial to determining Taylor cone modes, which affect the distribution of droplet sizes, the ionization efficiency, and the signal stability.

[60, 61, 65] However, it is not practical to measure a Taylor cone mode unless special tools are used, even though various spray modes have been observed and studied.[65] Pulsating mode, constant amplitude oscillation mode, cone-jet mode and multi-spray mode are common modes that might be observed during electrospray ionization under different conditions. Among them, the cone jet mode is the most effective mode from which stable electrospray signals are produced, while the constant amplitude oscillation mode changes dramatically depending on how the base of the Taylor cone wets the electrospray tip.

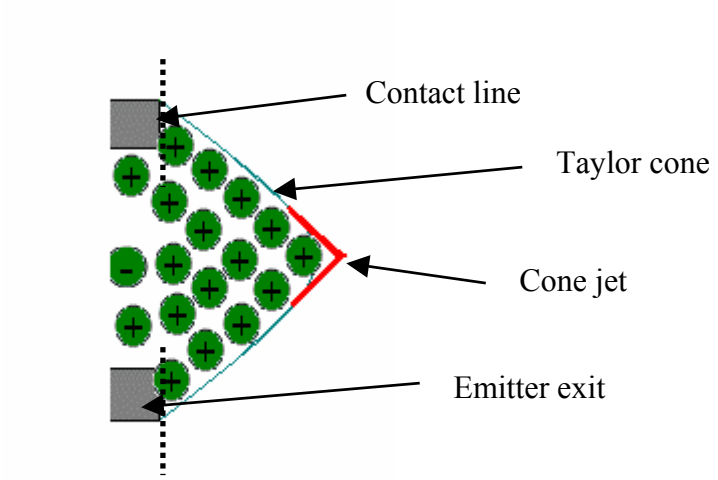

Figure 1.3. A schematic diagram of a Taylor cone showing the contact line between the Taylor cone base and the emitter exit surface.

As shown in Figure 1.3, the size of a Taylor cone base during electrospray is defined by the external, not the internal diameter of an emitter. The positional stability of a contact line between the liquid and the emitter tip was found to affect the stability of spray currents observed using Fourier spectra.[65] Malformation of a Taylor cone due to incomplete wetting of an emitter tip was found to have significant effects on spray current. Physical properties of emitter tips play an important role in current oscillations.

In particular, the position of a contact line has significant impact on the frequency of current oscillations. Very subtle changes in the position of a contact line greatly affect spray stability. Ultimately, not only the emitter geometry but also wetting properties of an emitter exit could be important factors to produce stable electrospray.

Furthermore, the relative distance between an emitter tip and the MS orifice affects the onset voltage of an electrospray as illustrated by equation 1.2. Theoretically, by positioning an emitter tip closer to the MS orifice, the applied spray voltage can be reduced. Moreover, the position of an emitter tip was found crucial to the reproducibility of electrospray performances. A vision-based monitor and an xyz stage are usually used to control the position of an emitter tip. However, this technique may cause bias in the position accuracy. A digital triggered control system was developed to switch the emitter position between data acquisition and rinse position to optimize the position of emitter accurately and efficiently. [66, 67]

In addition to the single-tipped emitter, recently, Richard Smith's group conducted a thorough study on the characterization of electrospray behaviour from an externally tapered emitter with 77 μm i.d. and 360 μm o.d. using an array of 23 electrodes for accurately measuring ionized and transmitted ion currents.[68] In addition to a flow profile (ion current versus flow rate), the impact of an emitter distance relative to the MS orifice on the ionization and transmission efficiency was investigated. According to their study, when the distance was increased from 1 mm to 2 mm, increased desolvation efficiency was observed, as indicated by increased analyte signal intensity. However, when the distance was increased further from 2 mm to 5 mm, the reduced

intensity suggested a reduction in transmission efficiency. Their experimental results are consistent with the recommended operational distance (within 1-2 mm) for a typical tapered emitter.

In this thesis, the nanoelectrospray emitters developed are all non-tapered and some of them utilize multiple electrospray channels. Since these types of nano emitters have dramatically different architectures compared to conventional tapered emitters, the operational parameters may be significantly different. Herein, the electrospray behaviour of these non-tapered emitters is investigated and compared to standard tapered emitters. The characterization and evaluation experiments were carried out over a wide range of flow rates (10 -500 nL/min), spray voltages (2.4 - 5.0 kV), and relative distances (5 - 25 mm) from an emitter tip to the MS orifice. The converted signal response factor and signal to noise ratio (S/N) was used for the comparison of sensitivity at each of the different conditions. Stability and reproducibility of electrospray were also evaluated. To visually demonstrate the distinguishable electrospray behaviour of non-tapered emitters from a tapered emitter, offline electrospray experiments were designed to capture the electrospray images at a low nano flow rate.

1.3 Development of novel nanoelectrospray emitters

1.3.1 Tapered nano-emitters

Traditionally, tapered emitters are used to achieve stable nano flow rates. A pulled, gold-coated glass capillary with a tip of 1-3 μm was the first nano-emitter developed by Wilm and Mann.[51] Various fabrication methods have been developed to

improve the reproducibility, robustness, durability, or conductivity of tapered emitters.[52, 69-78] These emitters have been fabricated by pulling or etching tips of fused silica capillaries to small apertures. Various tapering methods have been employed including internal diameter tapering, external diameter tapering, or both as illustrated in Figure 1.4.

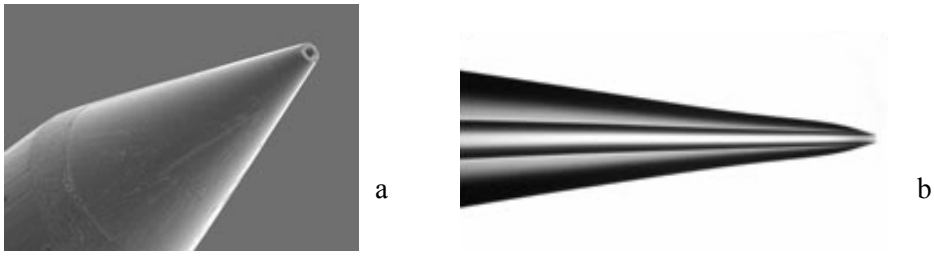

Figure 1.4. Representative tapered emitters. (a) Externally tapered emitter. (b) Both internally and externally tapered emitter.[80]

Most tapering technologies draw both internal and external diameters simultaneously, which makes it difficult to control the reproducibility of emitter tip fabrication.[33] Tapering internal diameters to small apertures is used to attain low flow rates for generating stable electrospray signals, while tapering outer diameter reduced the onset electrospray voltages from about 3.0 kV down to 1.0 kV or less. Lower spray voltages reduce the chances of electrical discharge, which may cause ion suppression.[78] Furthermore, tapered external diameters prevented the Taylor cone base from spreading on a hydrophilic surface of the emitter exit, which is beneficial for spraying highly aqueous solutions.[79] The early studies of the nanoelectrospray process suggested that the smaller the emitter apertures, the smaller the Taylor cone that forms, which leads to the production of smaller droplets.[51] As a result, the aim was to fabricate as small an emitter

aperture as possible for superior sensitivity. Very small emitter apertures (1-2 μm) can be opened either by touching a metal plate before the operation, or etched by HF to get more reproducible aperture sizes. [51, 78]

However, emitters with internal diameters of less than 20 μm are not practical and tend to be clogged by debris during fabrication or precipitates and particles bled from chromatographic media.[33, 58, 78] This can ultimately limit sample throughput, especially for proteomics where hundreds of samples are run on a mass spectrometer each day. In addition, when designing a nano-ESI emitter the flow rates that an emitter can handle also need to be taken into consideration. The ideal combination of nano-LC and nano-ESI/MS involves two processes[36, 81-83]: first, the relatively fast sample loading, pre-concentration, and clean-up by capillary LC at relatively high flow rates (usually > 1 μL/min); and second, the slower sample introduction into a mass spectrometer for high sensitivity detection at relatively low flow rates (usually < 500 nL/min). Variable flow strategies have been developed to balance the needs.[36] However, the flow resistance from a very small aperture limits the flow rate range, which usually requires switching valves and flow splitters. This type of configuration adds extra dead volume due to the multiple connections, which tends to cause band broadening during separation. Furthermore, it makes the operation more complicated because of the switching valves and multiple stages of the flow operation involved. As a result, nano-ESI emitters with larger flow rate range capabilities are desirable.

1.3.2 Robust non-tapered nano-emitters

Essentially, two major limitations lie in the design of a typical tapered emitter. The narrow aperture of the emitter tip limits the flow resistance, and a single-tip provides no backup in case of clogging. To overcome the disadvantages associated with the tapered emitters, approaches such as the development of emitters with larger apertures (i.e. open tubular emitters), and/or the fabrication of emitters with multiple electrospray channels or arrays of emitters, have been explored.[59, 78, 79] The initial investigation of open tubular capillaries was done by Covey and other researchers, which depicted (as shown in Figure 1.5) a relationship between optimum flow rate from 1-1000 nL/min and the size of emitter apertures with inner diameters from 1-50 μm.[33]

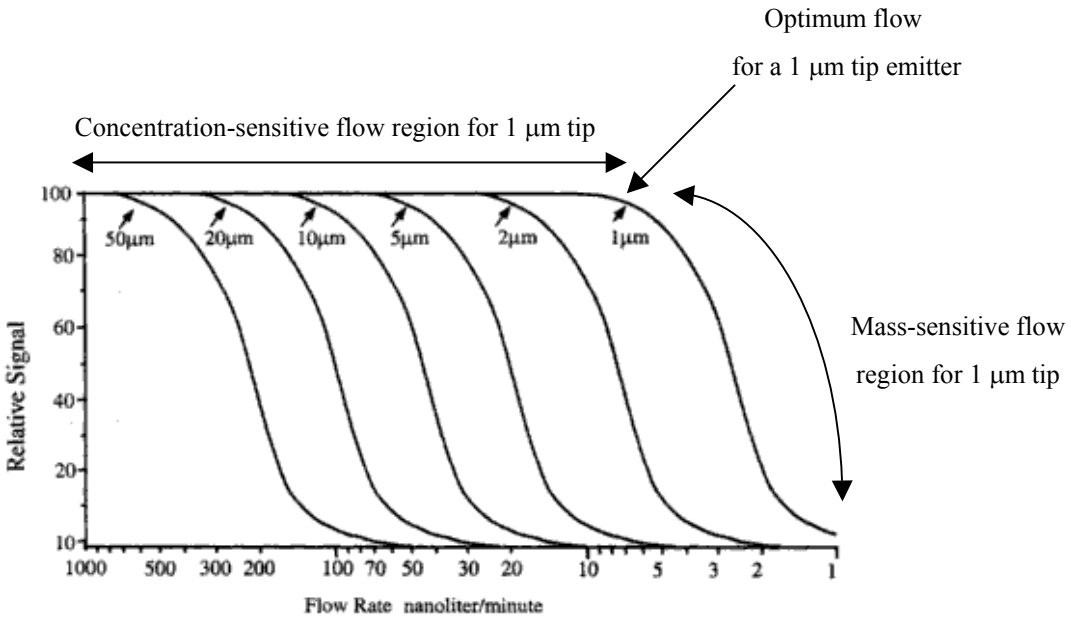

Figure 1.5. Flow profiles of open tubular capillaries with different internal diameters.[33]

These emitters with relatively large apertures (up to 50 μm i.d.) were fabricated by cleaving fused silica capillaries without further efforts to shape the tips other than generally preparing as square a cut as possible. With this emitter geometry the minimum flow rate that can be maintained with a stable electrospray is higher than 500 nL/min. Capillaries with internal diameters larger than 50 μm (e.g. 75 μm i.d.) are usually used for conventional electrospray with flow rates larger than 1 μL/min.

Recently, nanoelectrospray from a relatively large capillary aperture (55 μm) has been proposed on an emitter model containing a multiple plumed ESI emitter array of carbon nanofibers (CNFs) around the capillary orifice.[59] A schematic drawing of a CNF emitter is shown in Figure 1.6. In the simulated ESI experiment, each CNF served as an individual electrospray emitter resulting from the ends of the CNF tips having higher potentials under an electric field. The liquids, supplied through capillary forces, were delivered from virtual reservoirs placed between the CNFs. The study concluded that this type of emitter could generate multiple nanoelectrosprays through a relatively large open tube. Through this study, fused silica emitters with relatively large open tubular apertures (360 μm o.d. and 20 μm to 75 μm i.d.) demonstrated the capability of generating stable nano-electrospray (50-500 nL/min) through roughening the exit surface of a fused silica capillary, as discussed in Chapter 2.

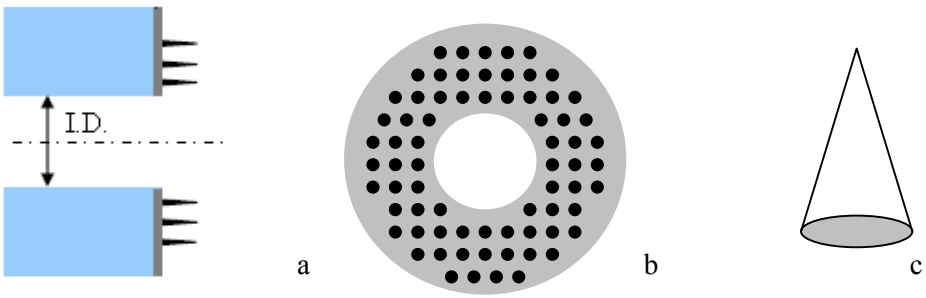

Figure 1.6. Schematic diagram of modeled open tubular emitter with array of CNFs around the capillary orifice: (a) vertical cross-section of the emitter model, (b) CNFs array around the orifice, (c) geometry of an individual CNF.

The second approach involves in the fabrication of emitters with multiple electrospray channels or arrays of emitters. Initially proposed by Tang et al., a multiple electrospray emitter, fabricated using a micro-ablation technique, was to increase the detection sensitivity, but at relatively large flow rates (> 1 μL/min).[84] Figure 1.7 shows the multi-emitter and the multiple electrospray image generated.

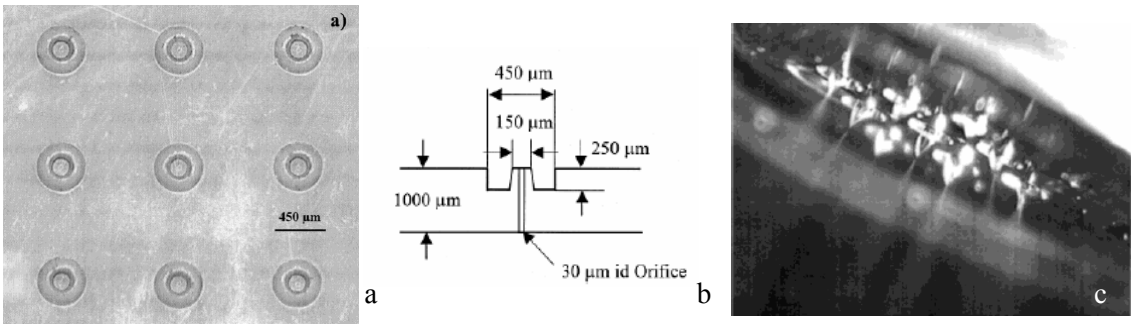

Figure 1.7. The multiple emitter designed by Tang. *et.al*., (a) Top view of the multi-emitter, (b) dimension of individual orifice, (c) Image of multiple electrospray.[84]

Our group has extended the multiple electrospray concepts by forming multiple electrospray channels in tubular capillaries without either internal or external tapering. These multiple channel emitters were fabricated by either forming porous polymer monolith (PPM) or entrapping microspheres by polymers in the capillary columns, from which multiple spray channels were generated.[15, 85, 86] When spraying from these emitters, the multiple channels formed largely eliminated the tendency of clogging and improved robustness. Furthermore, we have demonstrated increased sensitivity at relatively low flow rates due presumably to the formation of multiple Taylor cones. The non-tapered emitters also showed stable nanoelectrospray signals without external tapering. Besides the enhanced spray stability and robustness, these emitters integrate chromatographic functionality through either PPM or entrapped microspheres. However, it is fairly difficult to define and characterize the dimensions of the multiple channels formed by these technologies. To demonstrate the merits established from the multiple channel nanoelectrospray emitters, a novel method was developed to fabricate multi-path electrospray emitters with more defined channels. These uniform channels were obtained by gluing hydrophobic porous polymer membranes, (such as polysulphone (PSF) and polycarbonate (PC) membranes), which contain pores with well-defined sizes, onto the exit aperture of fused silica capillaries or microfluidic chips. The development of this type of emitter and the comparison of electrospray performance of emitters fabricated from membranes with different pore sizes is discussed in Chapter 3.

Moreover, a commercialized photonic crystal fiber was borrowed from its intended application in telecommunications for the purpose of generating multiple

electrospray. This emitter solves many of the problems encountered with the traditional tapered emitters, as well as most of the recently attempted strategies for improving nano-emitter stability, sensitivity, robustness, and ease of fabrication. The multiple channels available for the fluid flow make the MSF emitter highly resistant to clogging. This type of emitter may finally make nanoelectrospray ionization a routine tool for mass spectrometry analysis. Chapter 4 discusses the characterization of multiple channel MSF emitters.

1.3.3 Nano-emitter for highly aqueous solutions

One of the challenges for electrospray is the poor ionization efficiency of spraying highly aqueous solutions due to the high surface tension of water.[87] Electrospraying aqueous samples efficiently is significant since a highly aqueous solvent is often necessary at the beginning of a reversed phase LC separation gradient. Furthermore, in structural proteomics, some samples can not tolerate significant organic solvent content without denaturation, hence necessitating working in aqueous environments. However, highly aqueous solutions are notoriously difficult to spray with a large-aperture hydrophilic silica tip owing to the high surface tension of both emitter exit and water.[79] On the hydrophilic exit surface of a fused silica emitter, especially on a relatively large contact area between the fluid and the emitter exit, the Taylor cone base tends to spread, which may cause the malformation of the cone surface. This results in an unstable electrospray process leading to poor ionization efficiency for aqueous spraying.

An ESI emitter that can function with high sensitivity under highly aqueous conditions would provide a useful proteomic tool.

Tapered-emitters, however, prevent the cone base from spreading making them a relatively good choice to spray highly aqueous solutions.[87] Since a larger cone base tends to form on the large exit of a non-tapered emitter, the wettability of the surface on a non-tapered emitter exit will significantly affect the stability of a cone base. Solutions for this problem have involved modifying the emitter surface's wettability to be more hydrophobic to prevent the liquid from spreading. Tojo et al. developed an electrospray emitter coated by a fluorinated polymer (FP) with low surface energy.[79, 88] The emitter body was made of fused silica capillary (20 μm i.d. and 150 μm o.d) with only the external diameter tapered. The outer wall of the tip and the entire inner wall were coated with FP coating, making the tip unwettable (contact angle 122°). Stable electrospray performance was demonstrated from this type of emitter at 400 nL/min and 800 nL/min flow rates, and the hydrophobic coating made spraying aqueous solutions easier.

During this study, a hydrophobic silylation reagent was used to chemically modify the exit surface of the MSF emitter to enable the electrospray of 99.9% aqueous solution (0.1% of formic acid) with enhanced stability and sensitivity compared to tapered fused silica emitters. Detailed discussions are in Chapter 4.

1.3.4 Integrated nano-emitter

An integrated emitter enables more functions than simply electrospray. Typical nano-LC/nano-ESI/MS systems involve pre-concentration, desalting, analytical

separation, ionization through a nano-ESI emitter, and detection by a mass spectrometer.[13, 25, 89] To achieve pre-concentration, reverse-phase microspheres selectively trap analytes through solid phase extraction (SPE) before their elution for analysis, which increases the analyte selectivity, separation efficiency, and detection sensitivity. Salts and detergents (*e.g.* contained in trypsin digested proteins) may suppress ions of interest, or clog the emitter tip over time. Removing large amount of salts is often necessary, even though nano-ESI has a certain degree of tolerance to salts. The pre-concentration column and separation column may be hyphenated with or integrated into an emitter in a nano-LC – nano-ESI/MS system. However, if there is a separation process necessary in the upper stream of an emitter, any dead volume caused by an ESI emitter may lead to a band broadening especially at nanoliter per minute flow rates. Integrating various functionalities into a single emitter is a trend for the development of nanoelectrospray emitters.[90-97]

To functionalize an emitter, reverse-phase chromatographic materials are packed or formed in-situ inside tapered and non-tapered emitters.[90, 94, 96] Microsphere chromatographic particles, as used in the conventional HPLC packed columns, are still attractive because of their diverse sources, wide availability, well defined categories, and well understood mechanisms.[98, 99] The commonly used particle sizes are 3-5 μm due to the pressure limitation associated with conventional HPLC pumps. With the availability of UPLC (Ultra high pressure LC), using smaller particles such as sub 2 μm particles largely increases the separation efficiency.[100] It is reported that 5 μm sized reverse phase media was packed against the small aperture in an emitter needle to analyze femotemole

amounts of a peptide mixture. However, it was observed that this necessitates a high degree of technical expertise for both the needle assembly as well as the particle packing. On the other hand, when packing particles in a capillary with a relatively large aperture, a frit was necessary in order to retain the particles and prevent them from moving. It is difficult however, with the current technology, to achieve highly permeable and mechanically strong frits, which are critical to electrospray applications that do not also lead to significant bubble formation. [98]

Monolithic stationary phases, which are formed in-situ inside of the capillary, is increasingly considered as a viable alternative for microsphere particles in HPLC columns.[93, 94, 96] A solution containing monomers and porogen is introduced into the capillary. Upon polymer initiation, the polymer grows and phase separates from the porogenic solvent resulting in an interconnected network of polymer nodules. The polymer surface chemistry can be modified using different monomers. The pore size can also be tailored by using different monomer and porogenic solvent compositions.[101, 102] Because of the high permeability and compatibility with high flow rates, a monolithic column can be made longer to yield high separation efficiency.[103] Moreover, the possibility of preparation of monolith in-situ makes it easier to transfer the separation technology onto microfluidic devices.[104] However, the reproducibility of the fabrication processes is still problematic.[98] The fundamental mechanisms of monolithic-based mass transfer and band-dispersion are still not well understood, due to the different and complicated morphology of monoliths. In general, the application of monoliths remains relatively limited to date.

Entrapping particles inside a capillary is an approach that combines the advantages of both the packed column and the monolithic column.[86] Entrapped emitters demonstrate superior stability and reproducibility compared to conventional packed columns. A temporary frit was first used and then removed once the particles were fixed by the polymer formed. A silica-based porous matrix was formed inside of a capillary column to support the packed particles. An entrapped microsphere (3 μm ODS) emitter was developed through photo-initiated polymerization by our group. The enhanced stability stems from the network between the microspheres through polymer at specific bead-bead and bead-capillary points. The entrapped ODS emitter was successfully used in CEC for the PAHs' separation. To be used as an integrated emitter in a nano-LC-nano-ESI/MS system, the impact of polymerization on emitter's robustness, induced backpressure, microsphere surface morphology, and chromatographic properties were studied, as discussed in Chapter 5. The nanoelectrospray behavior of entrapped emitters was also investigated.

1.4 Instrumental components of nano-LC-nano-ESI/MS

1.4.1 Instrumental components

The instrumental components for nano-LC-nano-ESI/MS can be simplified into a diagram block shown in Figure 1.8. It can be categorized into the sample manipulation and introduction system, the mass spectrometer, and the ion source assembly. Liquid samples can be introduced into the electrospray interface through a LC, nano-LC, CE/CEC, or microfluidic devices. The introduction of fluids can be operated discretely or

continuously. For a discrete sample introduction, a sample is first filled in the emitter tip and then a finely controlled gas flow is used to push the fluid from the emitter exit, which yields 10 to 30 nL/min flow rate. To introduce sample continuously into the system, a regular LC pump was used with the assistance of splitting valves, especially when coupling with tapered emitters. Nano-LC pumps are able to generate a continuous flow at microliter per minute to nanoliter per minute flow rates. Current nanoLC pumps use microfluidic flow control to generate precise HPLC gradients at nanoliter-per-minute flow rate, and are able to maintain flow rate precision at even 10 nL/min.[105] The newly developed nano-LC system also allows sample loading at higher flow rates (e.g. 30 μL/min) for significant time saving and flexibility.

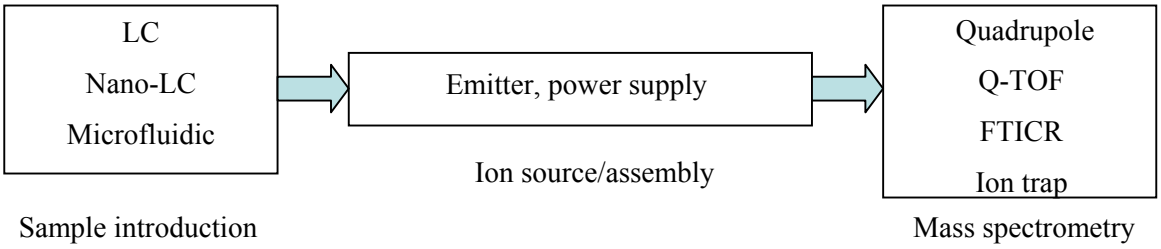

Figure 1.8. A block diagram showing the instrumental components in a continuous sample introduction system coupled with mass spectrometer.

Various mass analyzers such as quadrupole, magnetic sector, Fourier transform ion cyclotron resonance (FTICR), quadrupole ion trap, time of flight (TOF), and their tandem systems, have been coupled with LC systems successfully through electrospray interfaces for different purposes. Quadrupole, TOF and their combination Q-TOF are the most popular mass analyzers used for electrospray. [20, 50, 106] The principal advantage of

using a single quadrupole is that it is relatively reliable, low cost, and offers both qualitative and quantitative analytical capabilities. The limitation is that it can only produce low resolution mass spectra. TOF on the other hand is capable of very high resolution, speed, and sensitivity. It allows for accurate mass measurements. For structure analysis and for improved target compound selectivity through selected reaction monitoring, triple quadrupole or hybrid instruments such as Q-TOF are used to allow further fragmentation in the collision cell from the selected precursor ions. [107]

1.4.2 Ion source assembly

The very heart of the instrumental components for nanoelectrospray technology relies on the design of efficient interface devices and strategies to increase desolvation for improved ionization efficiency. This emerging nanoelectrospray technique makes it possible to generate aerosol without using assisting techniques such as nebulizing gas, heat, or ultrasounds. Nanoelectrospray is indeed a "pure" electrospray technique, dependent strictly on the electrostatic means and, because of this, the emitter diameters, the position of the emitter, and the applied potentials are critical to nanoelectrospray performance. This is in contrast to conventional electrospray where the external sources play important roles in generating electrospray.[108]

One of the challenges in the development of an efficient nanoelectrospray ion source is the application of electric potential to the solution that exits from a small dimensioned tip. Techniques include: coating the emitter tip with conductive material such as gold, platinum, or conductive polymers; using sheath flow liquid; inserting a fine

wire into the capillary tip; using a metal union or a liquid junction upstream of the emitter tip.[33, 68, 70, 71, 90, 109] In some applications, a liquid junction proves more practical as it is an easier and more robust approach. A micro-cross or a micro-tee unit is used for a liquid junction, as shown in the schematic drawing in Figure 1.9. The voltage is applied through the metal wire in contact with the liquid within the junction, where two other horizontal unions are connected with a sample introduction line on one side and with an emitter on the other side.

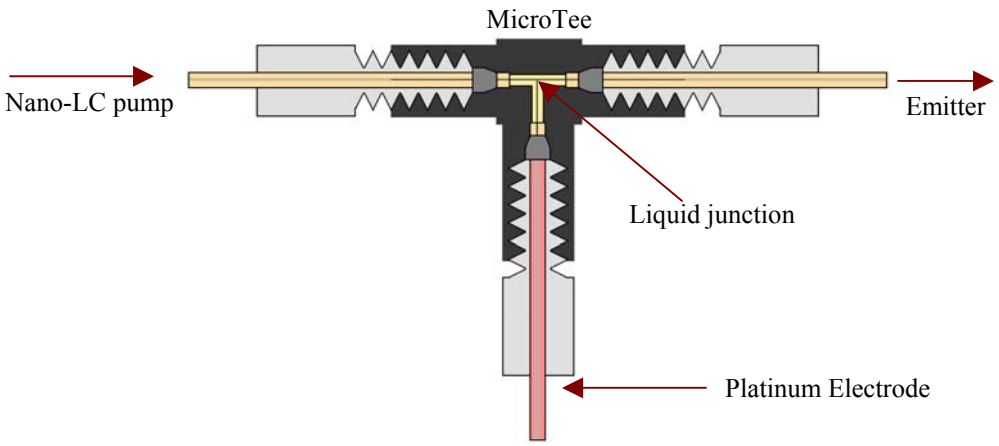

Figure 1.9. Schematic diagram of a MicroTee providing a liquid junction.

1.4.3 Interface configurations

In an application that requires on-line sample pre-treatment, other than direct analysis, a pre-concentration column and separation column may be hyphenated or integrated into the emitter in a nano-LC-nano-ESI/MS system.[91, 110, 111]

A hyphenated nano-LC-nano-ESI/MS configuration usually connects single function components such as: pre-concentration/desalting columns (micro-SPE), separation columns (nano-LC), and electrospray emitter together.[112-114] Pre-concentration

columns are frequently implemented to facilitate large volume injection of diluted sample mixtures onto micro-columns without loss in column performance. A typical hyphenated nano-LC-nano-ESI/MS configuration was demonstrated in the setup as shown in Figure 1.10a.

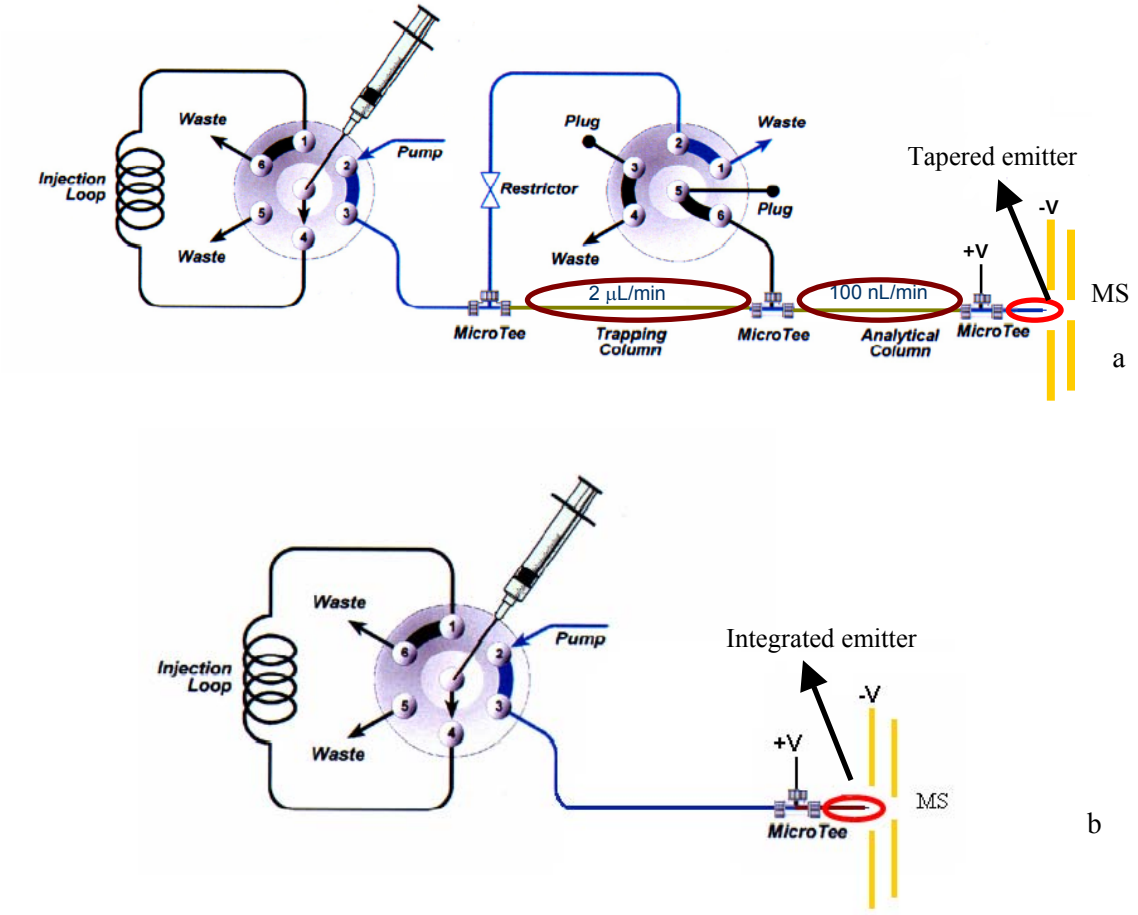

Figure 1.10. Schematic diagrams of hyphenated (a) and (b) integrated configurations. (a) an example of a hyphenated system with a 50 to 100 µm i.d. and 8 – 10 mm length of trapping column for sample concentration, and a 100 µm i.d. and 6 – 7 cm length of separation column coupled to a 75 µm i.d. emitter with a 5 µm tapered electrospray tip (see reference[37] for details regarding valve positions and operation modes); (b) an integrated nano-LC-nano-ESI/MS system.

Column switching and flow splitting techniques were used to allow variable flow rates in order to overcome the flow resistance induced from the small apertures of tapered-emitters. During the analytical process, a 2 μL/min flow rate was used for fast sample loading onto the trapping column by bypassing the analytical column, and the flow direction was controlled by a second valve; 100 – 125 nL/min flow rates were used for analytical separation and the elution of analytes from the separation column into the MS ion source for analysis. However, it became a challenge for a hyphenated configuration to achieve high separation efficiency because, at low flow rates, the dead volumes and flow distortions due to column connections cause band broadening. A dead volume of 1 μL would result in a 10 min elution delay for a system flow rate of 100 nL/min.[33]

Although a hyphenated configuration allows more choices for coupling different LC columns, the induced dead-volume may cause band broadening during the separation. To overcome this problem, an integrated configuration that combines functionalities such as pre-concentration, desalting, separation, and electrospray ionization can be integrated into one capillary, as illustrated in Figure 1.10b.[93-97] The need for flow restrictors, splitters, and MicroTees for connections is reduced significantly, which simplifies the system operation and maintenance. By integrating a SPE column, a separation column and an electrospray emitter, the dead volume is largely reduced and therefore increased separation efficiency is achieved, allowing a large number of proteins, including low abundance proteins, to be identified from a trypsin digested sample.

In this study, a packed and an entrapped ODS bead emitter are applied in an integrated system. Their capability for desalting, preconcentration and separation were evaluated. Diluted protein/peptide solutions were used to test the loading capacity of entrapped bead columns in terms of analyte amount per gram of stationary phase. In addition, the trapping efficiency of entrapped beads was evaluated for proteins/peptides with different hydrophobicity (Chapter 5).

1.5 Applications of nanoelectrospray

Nano-LC/nano-ESI/MS or MS/MS have significantly increased sensitivity and selectivity for the analysis of small amounts of proteins/peptides.[18, 115, 116] However, due to the problems and difficulties associated with current nanoelectrospray emitters, nanoelectrospray technology remains limited to study areas such as proteomics. With the availability of robust and reliable nano-emitters, essentially any application area currently using conventional ESI could feasibly be configured into nanoelectrospray.

1.5.1 Proteomics

With the completion of the human genome in 2002, scientists realized that gene expression itself won't be able to provide enough information to fully understand diseases.[21] As a result, more attention has been directed to the study of the proteome, which is directly related to the status of human health at the protein level. Proteomics, which studies the changes of protein expression patterns, has become a rapidly growing area. Protein expression profiling encompasses not only protein identification, but also

quantification information, protein folding structure, protein-protein interaction and their post-translations.[20]

"Bottom-up" protein fingerprinting is one of the most popular strategies used in proteomics.[117, 118] As shown in the workflow diagram (Figure 1.11), proteins contained in tissue, cells, the blood stream, or body fluids from healthy individuals and patients are first separated using 2D PAGE. The suspected protein or protein mixture spot is cut and then tryptically digested into peptides. Through database matching, proteins are then identified from their peptide fingerprint obtained by nano-LC-nano-ESI/MS/MS analysis. After clinical validation, some of the target proteins may be used as biomarkers for disease diagnosis and treatment therapies.

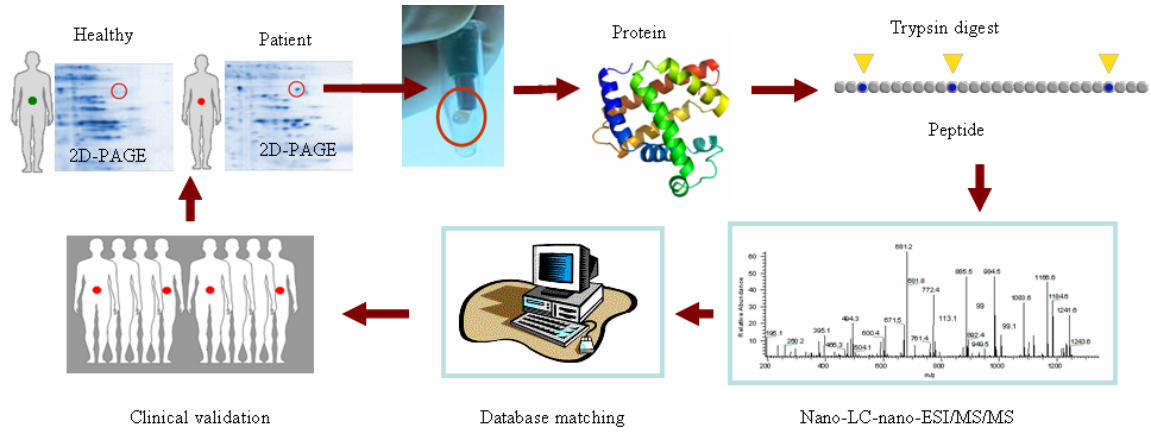

Figure 1.11. The workflow diagram of "Bottom-Up" proteomics.

In contrast to existing diagnostic assays, which examine protein biomarkers one at a time, clinical proteomics need to detect hundreds or even thousands of different proteins simultaneously in a single experiment.[19, 119, 120] Furthermore, tissue, cells, blood,

or body fluids are usually used for protein identifications in clinical proteomics. The blood and body fluid are more desirable for clinical practice because they can be accessed more easily and in a less invasive fashion. However, obtaining accurate and reproducible protein expression profiles from biological samples poses challenges due to their complexity. The dynamic range of proteins is one of the biggest challenges. For example, within plasma, the dynamic range of proteins spans 9 orders of magnitude. High abundance proteins such as albumin and immunoglobulin account for about 60-90% of the plasma proteins, while low abundance proteins such as cytokines, which are important to the proteomics study can, unfortunately, be masked by albumin. The large number of expressed proteins in a single cell requires high throughput and high resolution protein analytical techniques. The interferences due to the complex matrix make it difficult to obtain reproducible expression results. In addition, the mixture of proteins is not stable; some of the proteins may be modified during the sample treatment and separation processes. Therefore, rapid processes for handling the protein separation are required.

Nano-LC/nano-ESI/MS/MS is attractive to clinical proteomics because of its high sensitivity, small sample consumption, low cost, and potentially high throughput and automation.[2, 121-125] Developing miniaturized devices coupling ESI/MS, which allow the integration of multi-functions, use a small sample volume, offer robustness, rapidity and low cost, and enable high sensitivity/selectivity, high throughput, and accurate quantification, will continue to be an active research area for clinical proteomics.[53, 54] Although real proteomic samples were not used in this study, standard proteins/peptides

samples were used to demonstrate the possibilities for non-tapered nanoelectrospray emitters in proteomic facilities (Chapter 5).

1.5.2 Non-proteomics

The drawbacks of traditional tapered nano-emitters have largely impeded the wide application of the nano-LC/nano-ESI/MS technology. Non-proteomic laboratories usually prefer standard LC/ESI/MS operation rather than nano-LC/nano-ESI/MS because of the ease of operation and the higher reliability of LC-ESI/MS.

During this study, significant progress has been achieved to solve problems associated with the traditional tapered nano-emitters. With the availability of the robust nano-ESI emitters with both a single function and integrated functions, it is possible to operate a nano-LC/nano-ESI/MS as easily as a regular LC/ESI/MS experiment. Areas such as pharmacokinetics, drug metabolism, and combinatorial chemistry have already benefited from the nanoelectrospray technologies.[126-128] Robust nanoelectrospray techniques may also find a new niche in emerging research areas including but not limited to the concerns of pharmaceutical environmental contamination, the bio-diesel industry, clinical drug testing, forensics, the analysis of food/herbal nutrients/toxins, water quality, and food contamination.[4, 5, 129-132] In addition to increased sensitivity, the miniaturized analytical system also allows "greener" operation in analytical laboratories with the reduced consumption of sample, solvent, energy, and reduced waste generation, which will become increasingly valued by industries.[133] The outlook of these applications for advanced nanoelectrospray emitters is discussed in Chapter 6.

1.6 Summary

The objectives of this thesis study are depicted in this chapter for the development and application of robust non-tapered nano-ESI emitters. Background information is given for the better understanding of the purposes of the study. Fundamental theory of ESI and nano-ESI, practical aspects on instrument compositions, configurations and operational parameters, and the current and potential application areas of nano-ESI are laid out, which are related to the concepts, the themes, and the experimental designs during the thesis study. The thesis aims at improving the robustness and clogging resistance associated with traditional tapered emitters. A thorough literature review was conducted on the ESI fundamental mechanism, its characterization, emitter fabrication techniques, different techniques to improve the emitter robustness, sensitivity, multiple-functionalities, and the spraying of highly aqueous solutions. Strategies to solving these problems by either using larger open aperture emitter or multiple channel emitters were introduced.

1.7 Reference

(1) Fenn, J. B.; Mann, M.; Meng, C. K.; Wong, S. F.; Whitehouse, C. M. *Science (Washington, DC, United States)* **1989**, *246*, 64-71.

(2) Smyth, W. F.; Brooks, P. *Electrophoresis* **2004**, *25*, 1413-1446.

(3) Zuehlke, S.; Duennbier, U.; Heberer, T. *Chemosphere* **2007**, *69*, 1673-1680.

(4) Smyth, W. F.; Rodriguez, V. *Journal of Chromatography, A* **2007**, *1159*, 159-174.

(5) Eide, I.; Zahlsen, K. *Energy & Fuels* **2007**, *21*, 3702–3708.

(6) Fenn, J. B.; Mann, M.; Meng, C. K.; Wong, S. F.; Whitehouse, C. M. *Mass Spectrometry Reviews* **1990**, *9*, 37-70.

(7) Smith, R. D.; Loo, J. A.; Loo, R. R. O.; Busman, M.; Udesth, H. R. *Mass Spectrometry Reviews* **1991**, *10*, 359-452.

(8) Liu, C.; Verma, S. S. *Journal of Chromatography, A* **1999**, *835*, 93-104.

(9) Oleschuk, R. D. Harrison, D. J. *Trends in Analytical Chemistry* **2000**, *19*.

(10) Xie, J.; Miao, Y.; Shih, J.; Tai, Y.-C.; Lee, T. D. *Analytical Chemistry* **2005**, *77*, 6947-6953.

(11) Shen, Y.; Zhao, R.; Belov, M. E.; Conrads, T. P.; Anderson, G. A.; Tang, K.; Pasa-Tolic, L.; Veenstra, T. D.; Lipton, M. S.; Udseth, H. R.; Smith, R. D. *Analytical Chemistry* **2001**, *73*, 1766-1775.

(12) Luo, Q.; Shen, Y.; Hixson, K. K.; Zhao, R.; Yang, F.; Moore, R. J.; Mottaz, H. M.; Smith, R. D. *Analytical Chemistry* **2005**, *77*, 5028-5035.

(13) Luo, Q.; Page, J. S.; Tang, K.; Smith, R. D. *Analytical Chemistry* **2006**, ACS ASAP.

(14) Xie, R.; Oleschuk, R. *Electrophoresis* **2005**, *26*, 4225-4234.

(15) Koerner, T.; Xie, R.; Sheng, F.; Oleschuk, R. *Analytical Chemistry* **2007**, *79*, 3312-3319.

(16) Jacobs, J. M.; Smith, R. D. *Separation Methods in Proteomics* **2006**, 363-385.

(17) Smith, R. D.; Tang, K.; Shen, Y. *Molecular BioSystems* **2006**, *2*, 221-230.

(18) Luo, Q.; Tang, K.; Yang, F.; Elias, A.; Shen, Y.; Moore, R. J.; Zhao, R.; Hixson, K. K.; Rossie, S. S.; Smith, R. D. *Journal of Proteome Research* **2006**, *5*, 1091-1097.

(19) Hochstrasser, D. F.; Corthals, G.; Zimermann, C.; Scherl, A.; Bougueleret, L.; Colinge, J.; Masselot, A.; Binz, P.-A.; Muller, M.; Bairoch, A.; Appel, R. D.; Sanchez, J.-C.; Rose, K. *Advances in Mass Spectrometry* **2004**, *16*, 19-32.

(20) Oda, Y. *Biobencha* **2002**, *2*, 65-73.

(21) Yates, J. R., III *Nippon Iyo Masu Supekutoru Gakkai Koenshu* **1998**, *23*, 11-19.

(22) Wilm, M.; Mann, M. *Analytical chemistry* **1996**, *68*, 1-8.

(23) Wilm, M.; Shevchenko, A.; Houthaeve, T.; Breit, S.; Schweigerer, L.; Fotsis, T.; Mann, M. *Nature* **1996**, *379*, 466-469.

(24) Koerner, R.; Wilm, M.; Morand, K.; Schubert, M.; Mann, M. *Journal of the American Society for Mass Spectrometry* **1996**, *7*, 150-156.

(25) Shen, Y.; Tolic, N.; Masselon, C.; Pasa-Tolic, L.; Camp, D. G., II; Hixson, K. K.; Zhao, R.; Anderson, G. A.; Smith, R. D. *Analytical Chemistry* **2004**, *76*, 144-154.

(26) Smith, D. R.; Sagerman, G.; Wood, T. D. *Review of Scientific Instruments* **2003**, *74*, 4474-4477.

(27) Barnidge, D. R.; Nilsson, S.; Markides, K. E. *Analytical Chemistry* **1999**, *71*, 4115-4118.

(28) Bergquist, J.; Nilsson, S.; Wetterhall, M.; (Forskarpatent I Uppsala Ab, Swed.). Application: WO, 2001.

(29) Guzzetta Andrew, W.; Thakur Rohan, A.; Mylchreest Iain, C. *Rapid Communications in Mass Spectrometry* **2002**, *16*, 2067-2072.

(30) Van, B. G. J.: U.S. Patent 3,015,656, 2003.

(31) Liu, J.; Knapp, D. R.; (Musc Foundation for Research Development, USA). Application: US, 2006, pp 5pp.

(32) Le Gac, S.; Rolando, C.; Arscott, S. *Journal of the American Society for Mass Spectrometry* **2006**, *17*, 75-80.

(33) Covey, T. R.; Pinto, D. *Practical Spectroscopy* **2002**, *32*, 105-148.

(34) Koerner, T.; Turck, K.; Brown, L.; Oleschuk Richard, D. *Analytical Chemistry* **2004**, *76*, 6456-6460.

(35) Liu, C. C.; Zhang, J.; Dovichi, N. J. *Rapid Communications in Mass Spectrometry* **2005**, *19*, 187-192.

(36) Vissers, J. P. C.; Blackburn, R. K.; Moseley, M. A. *Journal of the American Society for Mass Spectrometry* **2002**, *13*, 760-771.

(37) Meiring, H. D.; Van der Heeft, E.; ten Hove, G. J.; De Jong, A. P. J. M. *Journal of Separation Science* **2002**, *25*, 557-568.

(38) Thomson, J. J. *Chem. News J. Ind. Sci. FIELD Full Journal Title:Chemical News and Journal of Industrial Science* **1911**, *103*, 265-268.

(39) Thomson, J. J. *Philos. Mag. (1798-1977) FIELD Full Journal Title:Philosophical Magazine (1798-1977)* **1899**, *48*, 547.

(40) Fenn, J. B. *Prix Nobel* **2003**, 154-184.

(41) Fenn, J. B. *Abstracts of Papers, 225th ACS National Meeting, New Orleans, LA, United States, March 23-27, 2003* **2003**, ANYL-010.

(42) Fenn, J. B. *Journal of Biomolecular Techniques* **2002**, *13*, 101-118.

(43) Borman, S. R., H., Siuzdak, G. *Today's Chemist at Work* **2003**, *www.tcawonline.org*, 47-49.

(44) Allen, M. H.; Grindstaff, D. J.; Vestal, M. L.; Nelson, R. W. *Biochemical Society transactions* **1991**, *19*, 954-957.

(45) Mann, M.; Fenn, J. B. *Mass Spectrom.* **1992**, *1*, 1-35.

(46) Yamagata, Y.; Tanioka, A.; Matsumoto, H. *Plastics Age Encyclopedia, Shinpo Hen* **2004**, 95-101.

(47) Salata, O. V. *Current Nanoscience* **2005**, *1*, 25-33.

(48) Dole, M.; Mack, L. L.; Hines, R. L.; Mobley, R. C.; Ferguson, L. D.; Alice, M. B. *Journal of Chemical Physics* **1968**, *49*, 2240-2249.

(49) Yamashita, M.; Fenn, J. B. *Iyo Masu Kenkyukai Koenshu* **1984**, *9*, 203-206.

(50) Yates, J. R., III *Journal of Mass Spectrometry* **1998**, *33*, 1-19.

(51) Wilm, M. S.; Mann, M. *International Journal of Mass Spectrometry and Ion Processes* **1994**, *136*, 167-180.

(52) Maziarz, E. P.; Lorenz, S. A.; White, T. P.; Wood, T. D. *Journal of the American Society for Mass Spectrometry* **2000**, *11*, 659-663.

(53) Smith, L. A.; Sobek, D.; Editors *Lab-on-a-Chip: Platforms, Devices, and Applications. (Proceedings of the SPIE International Conference held 26-28 October 2004, in Philadelphia, Pennsylvania.) [In: Proc. SPIE-Int. Soc. Opt. Eng.; 2004, 5591]*, 2004.

(54) Wood, T. D.; Moy, M. A.; Dolan, A. R.; Bigwarfe, P. M., Jr.; White, T. P.; Smith, D. R.; Higbee, D. J. *Applied Spectroscopy Reviews* **2003**, *38*, 187-244.

(55) Taylor, G. I. *Proc.. Roy. Soc.Lond. 1964* **1964**, 280-283.

(56) Iribarne, J. V.; Dziedzic, P. J.; Thomson, B. A. *International Journal of Mass Spectrometry and Ion Physics* **1983**, *50*, 331-347.

(57) Thomson, B. A.; Iribarne, J. V. *J. Chem. Phys. FIELD Full Journal Title:Journal of Chemical Physics* **1979**, *71*, 4451-4463.

(58) Zeng, J.; Sobek, D.; Korsmeyer, T. *Transducers '03, International Conference on Solid-State Sensors, Actuators and Microsystems, Digest of Technical Papers, 12th, Boston, MA, United States, June 8-12, 2003* **2003**, *2*, 1275-1278.

(59) Sen, A. K.; Darabi, J.; Knapp, D. R. *Microfluidics and Nanofluidics* **2007**, *3*, 283-298.

(60) Skazov, R. S.; Nekrasov, Y. S.; Kuklin, S. A.; Simenel, A. A. *European Journal of Mass Spectrometry* **2006**, *12*, 137-142.

(61) Eshraghi, J.; Chowdhury, S. K. *Analytical Chemistry* **1993**, *65*, 3528-3533.

(62) Lee, S. S. H.; Douma, M.; Koerner, T.; Oleschuk, R. D. *Rapid Communications in Mass Spectrometry* **2005**, *19*, 2671-2680.

(63) Chen, H.-W.; Li, M.; Zhou, J.-G.; Fei, Q.; Jiang, J.; Jin, Q.-H.; Zhang, T.-M.; Zhang, X. *Gaodeng Xuexiao Huaxue Xuebao* **2006**, *27*, 1439-1442.

(64) Smith, K. L.; Alexander, M. S.; Stark, J. P. W. *Journal of Applied Physics* **2006**, *99*, 64909.

(65) Parvin, L.; Galicia, M. C.; Gauntt, J. M.; Carney, L. M.; Nguyen, A. B.; Park, E.; Heffernan, L.; Vertes, A. *Analytical Chemistry* **2005**, *77*, 3908-3915.

(66) Valaskovic, G. A.; Murphy, J. P., III; Lee, M. S. *Abstracts of Papers, 225th ACS National Meeting, New Orleans, LA, United States, March 23-27, 2003* **2003**, ANYL-224.

(67) Valaskovic, G. A.; Murphy, J. P.; Lee, M. S. *Journal of the American Society for Mass Spectrometry* **2004**, *15*, 1201-1215.

(68) Page, J. S.; Kelly, R. T.; Tang, K.; Smith, R. D. *Journal of the American Society for Mass Spectrometry* **2007**, *18*, 1582-1590.

(69) Wood, T. D.; Lorenz, S. A.; Maziarz, E. P., III *Proceedings of SPIE-The International Society for Optical Engineering* **2000**, *3926*, 79-86.

(70) Wood, T. D.; Maziarz, P. E., III; Lorenz, S. A.; White, T. P.; (The Research Foundation of State University of New York, USA). Application: WO, 2001, pp 39 pp.

(71) Wetterhall, M.; Nilsson, S.; Markides, K. E.; Bergquist, J. *Analytical Chemistry* **2002**, *74*, 239-245.

(72) White, T. P.; Wood, T. D. *American Biotechnology Laboratory* **2002**, *20*, 16, 18.

(73) Wood, T. D.; Bigwarfe, P. M., Jr.; Smith, D. R.; White, T. P. *Abstracts of Papers, 225th ACS National Meeting, New Orleans, LA, United States, March 23-27, 2003* **2003**, ANYL-223.

(74) Wetterhall, M.; Klett, O.; Markides, K. E.; Nyholm, L.; Bergquist, J. *Analyst* **2003**, *128*, 728-733.

(75) Zhai, J.; Shui, W.; Xu, X.; Yu, Y.; Bao, H.; Chen, X.; Yang, P. *Rapid Communications in Mass Spectrometry* **2004**, *18*, 1177-1179.

(76) Yamada, N.; Sayama, Y.; Ando, T.; Aoki, M.; Suzuki, E.; Hirayama, K.; (Ajinomoto Co., Inc., Japan; Eisho Kinzoku Co., Ltd.). Application: JP, 2004, pp 15 pp.

(77) Liu, J.; Ro, K. W.; Busman, M.; Knapp, D. R. *Analytical Chemistry* **2004**, *76*, 3599-3606.

(78) Kelly, R. T.; Page, J. S.; Luo, Q.; Moore, R. J.; Orton, D. J.; Tang, K.; Smith, R. D. *Analytical Chemistry* **2006**, *78*, 7796-7801.

(79) Tojo, H.; (Japan). Application: WO, 2004, pp 36 pp.

(80) Poon, T. C. W.; Johnson, P. J. *Clinica Chimica Acta* **2001**, *313*, 231-239.

(81) Liedtke, S.; Moseley, M. A.; Vissers, J. P. C. *LaborPraxis* **2000**, *24*, 42-43.

(82) Liu, Y.-j.; Mou, S.-f. *Huanjing Huaxue* **2002**, *21*, 98-99.

(83) Aitken, A. *Proteomics Protocols Handbook* **2005**, 375-383.

(84) Tang, K.; Lin, Y.; Matson, D. W.; Kim, T.; Smith, R. D. *Analytical Chemistry* **2001**, *73*, 1658-1663.

(85) Koerner, T.; Turck, K.; Brown, L.; Oleschuk, R. D. *Analytical Chemistry* **2004**, *76*, 6456-6460.

(86) Xie, R.; Oleschuk, R. *Analytical Chemistry* **2007**, *79*, 1529-1535.

(87) Chowdhury, S. K.; Chait, B. T. *Analytical Chemistry* **1991**, *63*, 1660-1664.

(88) Tojo, H. *Journal of Chromatography, A* **2004**, *1056*, 223-228.

(89) Shen, Y.; Moore, R. J.; Zhao, R.; Blonder, J.; Auberry, D. L.; Masselon, C.; Pasa-Tolic, L.; Hixson, K. K.; Auberry, K. J.; Smith, R. D. *Analytical Chemistry* **2003**, *75*, 3596-3605.

(90) Robins, R. H.; Guido, J. E. *Rapid Communications in Mass Spectrometry* **1997**, *11*, 1661-1666.

(91) Amirkhani, A.; Wetterhall, M.; Nilsson, S.; Danielsson, R.; Bergquist, J. *Journal of Chromatography, A* **2004**, *1033*, 257-266.

(92) Dahlin, A. P.; Bergstroem, S. K.; Andren, P. E.; Markides, K. E.; Bergquist, J. *Analytical Chemistry* **2005**, *77*, 5356-5363.

(93) Peh, T. K. G.; (Avago Technologies General Ip (Singapore) Pte. Ltd., Singapore). Application: US, 2005, pp 6 pp.

(94) Xie, C.; Ye, M.; Jiang, X.; Jin, W.; Zou, H. *Molecular and Cellular Proteomics* **2006**, *5*, 454-461.

(95) Lindberg, P.; Dahlin, A. P.; Bergstroem, S. K.; Thorslund, S.; Andren, P. E.; Nikolajeff, F.; Bergquist, J. *Electrophoresis* **2006**, *27*, 2075-2082.

(96) Liu, J.; Ro, K.-W.; Nayak, R.; Knapp, D. R. *International Journal of Mass Spectrometry* **2007**, *259*, 65-72.

(97) Luo, Q.; Page, J. S.; Tang, K.; Smith, R. D. *Analytical Chemistry* **2007**, *79*, 540-545.

(98) Eeltink, S.; Decrop, W. M. C.; Rozing, G. P.; Schoenmakers, P. J.; Kok, W. T. *Journal of Separation Science* **2004**, *27*, 1431-1440.

(99) Stella, C.; Rudaz, S.; Gauvrit, J.-Y.; Lanteri, P.; Huteau, A.; Tchapla, A.; Veuthey, J.-L. *Journal of Pharmaceutical and Biomedical Analysis* **2007**, *43*, 89-98.

(100) Nguyen, D. T. T.; Guillarme, D.; Rudaz, S.; Veuthey, J.-L. *Journal of Separation Science* **2006**, *29*, 1836-1848.

(101) Soga, N. *Mirai Zairyo* **2004**, *4*, 66-69.

(102) Williams, J. L. *Catalysis Today* **2001**, *69*, 3-9.

(103) Svec, F.; Stachowiak, T. B. *Handbook of Capillary and Microchip Electrophoresis and Associated Microtechniques (3rd Edition)* **2008**, 1297-1326.

(104) Ro, K. W.; Nayak, R.; Knapp, D. R. *Electrophoresis* **2006**, *27*, 3547-3558.

(105) http://www.eksigent.com/hplc/products/nanoLC/LC2DU.php.

(106) Lapolla, A.; Fedele, D.; Seraglia, R.; Traldi, P. *Mass Spectrometry Reviews* **2006**, *25*, 775-797.

(107) Morris, H. R.; Paxton, T.; Panico, M.; McDowell, R.; Dell, A. *Journal of Protein Chemistry* **1997**, *16*, 469-479.

(108) Wilm, M.; Mann, M. *Analytical chemistry* **1996**, *68*, 1-8.

(109) Viberg, P.; Nilsson, S.; Skog, K. *Analytical Chemistry* **2004**, *76*, 4241-4244.

(110) Schilling, M.; Nigge, W.; Rudzinski, A.; Neyer, A.; Hergenroeder, R. *Lab on a Chip* **2004**, *4*, 220-224.

(111) Sung, W.-C.; Makamba, H.; Chen, S.-H. *Electrophoresis* **2005**, *26*, 1783-1791.

(112) Walles, M.; Gu, Y.; Dartiguenave, C.; Musteata, F. M.; Waldron, K.; Lubda, D.; Pawliszyn, J. *Journal of Chromatography, A* **2005**, *1067*, 197-205.

(113) Gooley, A. A.; Nguyen, C. H. T.; Hunter, W. S.; Ramsden, R. J.; (Proteome Systems Intellectual Property Pty. Ltd., Australia; Shimazu Corporation). Application: JP, 2002, pp 7 pp.

(114) Pelzing, M.; Neususs, C. *Electrophoresis* **2005**, *26*, 2717-2728.

(115) Toll, H.; Oberacher, H.; Swart, R.; Huber, C. G. *Journal of Chromatography, A* **2005**, *1079*, 274-286.

(116) Wang, Y.; Zhang, J.; Gu, X.; Zhang, X.-M. *Journal of Chromatography, B: Analytical Technologies in the Biomedical and Life Sciences* **2005**, *826*, 122-128.

(117) Millea, K. M.; Krull, I. S.; Cohen, S. A.; Gebler, J. C.; Berger, S. J. *Journal of Proteome Research* **2006**, *5*, 135-146.

(118) Du, X.; Callister, S. J.; Manes, N. P.; Adkins, J. N.; Alexandridis, R. A.; Zeng, X.; Roh, J. H.; Smith, W. E.; Donohue, T. J.; Kaplan, S.; Smith, R. D.; Lipton, M. S. *Journal of Proteome Research*, ACS ASAP.

(119) Shimizu, A.; Nakanishi, T.; Kishikawa, M.; Miyazaki, A. *Journal of Chromatography, B: Analytical Technologies in the Biomedical and Life Sciences* **2002**, *776*, 15-30.

(120) McComb, M. E.; Lim, A.; Berg, E. A.; Connors, L. H.; Skinner, M.; Costello, C. E. *Abstracts of Papers, 224th ACS National Meeting, Boston, MA, United States, August 18-22, 2002* **2002**, ANYL-121.

(121) Nakanishi, T. *Farumashia* **1997**, *33*, 996-1000.

(122) Nakanishi, T.; Shimizu, A. *Nippon Iyo Masu Supekutoru Gakkai Koenshu* **1994**, *19*, 177-183.

(123) Caprioli, R. M. *Nippon Iyo Masu Supekutoru Gakkai Koenshu* **1996**, *21*, 33-46.

(124) Aldred, S.; Grant, M. M.; Griffiths, H. R. *Clinical Biochemistry* **2004**, *37*, 943-952.

(125) Wilm, M.; Shevchenko, A.; Houthaeve, T.; Breit, S.; Schweigerer, L.; Fotsis, T.; Mann, M. *Nature* **1996**, *379*, 466-469.

(126) Van Pelt, C. K.; Zhang, S.; Fung, E.; Chu, I.; Liu, T.; Li, C.; Korfmacher, W. A.; Henion, J. *Rapid Communications in Mass Spectrometry* **2003**, *17*, 1573-1578.

(127) Wickremsinhe, E. R.; Singh, G.; Ackermann, B. L.; Gillespie, T. A.; Chaudhary, A. K. *Current Drug Metabolism* **2006**, *7*, 913-928.

(128) Biederman, K. J.; Lee, H.; Haney, C. A.; Kaczmarek, M.; Buettner, J. A. *The Journal of Peptide Research: Official Journal of the American Peptide Society* **1999**, *53*, 234-243.

(129) Richardson, S. D. *Analytical Chemistry (Washington, DC, United States)* **2007**, *79*, 4295-4323.

(130) Banik, K. K.; Hossain, S. *Indian Journal of Environmental Protection* **2006**, *26*, 926-932.

(131) Zahlsen, K.; Eide, I. *Energy & Fuels* **2006**, *20*, 265-270.

(132) Durden, D. A. *Journal of Chromatography, B: Analytical Technologies in the Biomedical and Life Sciences* **2007**, *850*, 134-146.

(133) He, Y.; Tang, L.; Wu, X.; Hou, X.; Lee, Y.-I. *Applied Spectroscopy Reviews* **2007**, *42*, 119-138.

Chapter 2

Development of Roughened Open tubular Nano-ESI Emitters

2.1. Overview

Single-tip tapered emitters with less than 20 μm diameter apertures often encounter problems such as frequent clogging and larger flow resistance due to the nature of the smaller aperture.[1] One of the strategies for solving problems associated with tapered emitters has included using emitters with open tubular tip from non-tapered internal diameters or simply larger apertures. Emitters with larger apertures (> 50 μm i.d.) prepared by directly cutting fused silica capillaries without further treatment are generally not able to produce stable sprays at nano flow rates (especially < 500 nL/min). Although a capillary with an array of carbon nanofibers (CNFs) around its orifice was proposed to facilitate nanoelectrospray through a relatively large open tube (55 μm i.d.), currently the design has only been simulated and a functioning device based on this principle has yet to be presented.[2]

In this study, an "end roughened" non-tapered fused silica emitter is reported to establish a stabilized electrospray from an open aperture (75 μm i.d. and 360 μm o.d.) at flow rates between 50 nL/min and 500 nL/min. The emitter was fabricated simply by grinding the exit orifice surface of a fused silica capillary with sandpaper. Grinding increases both the surface roughness and wettability (probed by AFM and contact angle measurements), which are shown to contribute to improved electrospray performance. The roughened emitter extends the usable flow rate range to as low as 50 nL/min, which

is not feasible with non-roughened open tubular emitters of similar compositions and dimensions.

2.2. Experimental

2.2.1. Reagents

Glacial acetic acid, methanol and acetonitrile (HPLC grade) were all purchased from Fisher Scientific (Ottawa, ON, Canada) and used without purification. O-(2-aminopropyl)-O'-(2-methoxyethyl) polypropylene glycol 500 (Jeffamine) and leucine enkephalin were purchased from Sigma-Aldrich (Oakville, ON, Canada) and also used without purification. Deionized water was obtained from a Milli-Q filtration system (Bedford, MA, USA). Trypsin was purchased from Calbiochem (Mississauga, ON, Canada).

2.2.2. Fabrication of surface roughened non-tapered open tubular emitters

Fused-silica capillaries with UV transparent 360 μm o.d., 75 μm i.d. (Polymicro Technologies, Phoenix, AZ, USA) were cut to the length of 3-6 cm. One of the capillary exits was ground manually using PEPA P#1000 to 4000 grit silicon carbide sanding paper (Struers, Copenhagen, Denmark) as shown in Figure 2.1a. Sanding was done end-on to minimize rounding of the tip, and involved back and forth hand motions with some rotating of the capillary between strokes. The sanding debris was blown from the capillary with compressed air or nitrogen, and then the roughened emitter was flushed with either methanol or ethanol as shown in Figure 2.1b, and dried prior to use. The

emitter was then checked under microscope to ensure it was debris free as shown in Figure 2.1c.

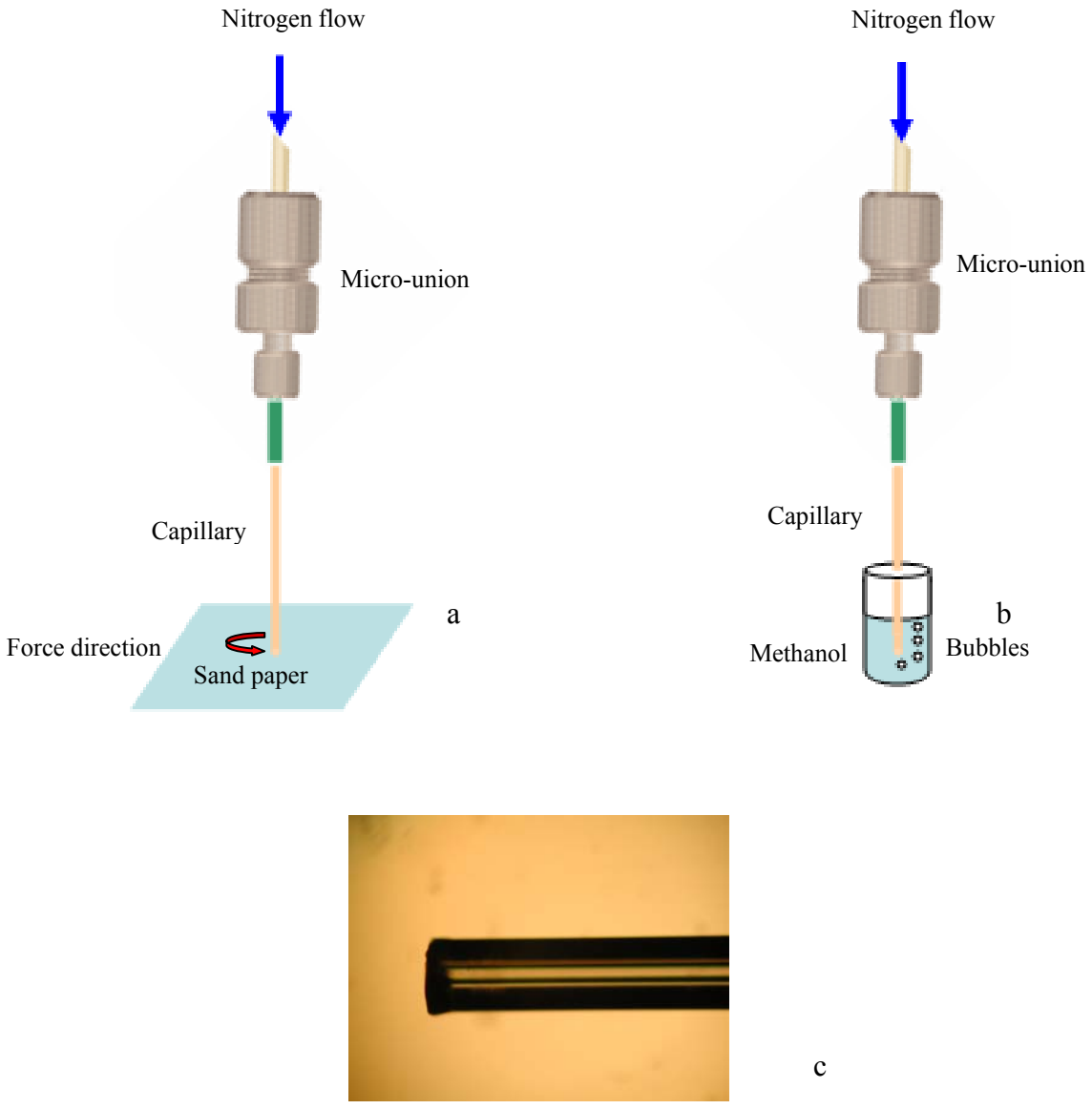

Figure 2.1. Schematic drawing of fabrication processes of roughened emitter. (a) Sanding emitter exit under nitrogen flow. (b) Removing debris by submerging emitter exit in methanol while purging with nitrogen. (c) A roughened emitter under microscope for checking debris.

An alternative method was used to fabricate a roughened emitter by first sealing one end of the emitter exit with melted crystal bond (a trade name with ingredients of ethylene glycol and phthalic anhydride) as shown in Figure 2.2a. The sealed capillary exit was ground using sandpaper without nitrogen purging. The sealed crystal bond inside of the capillary was then washed away by acetone leaving an open tubular emitter without any debris as shown in Figure 2.2c. This method was found having less chance of leaving debris from sanding in the capillary channel.

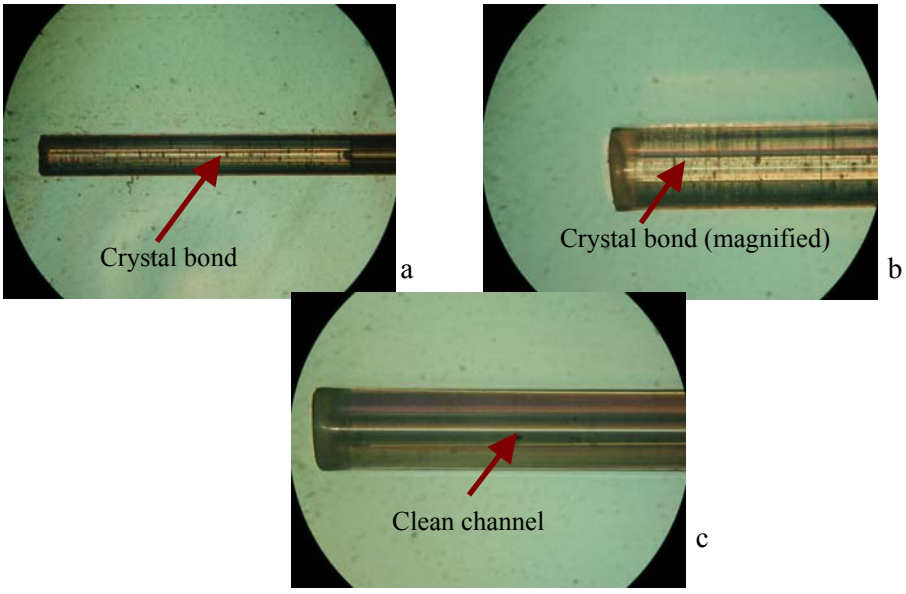

Figure 2.2. Microscope images from fabricating a roughened emitter by crystal bond sealing. (a) Crystal bond at one end of emitter exit. (b) Magnified image of (2a). (c) Clean channel after removing of the crystal bond by acetone.

2.2.3. AFM images

An atomic force microscope (AFM, Veeco, Nano-scope A, USA) was used to probe the surface morphology of emitter exits for both the roughened emitter and a cleaved emitter (both with 75 μm i.d. and 360 μm o.d.). The roughened emitter was

prepared following the fabrication protocol described above (Figure 2.1). Capillary sections (2 mm) with roughened and cleaved ends were taped to the sample holder of an AFM. The surface morphology of the two capillary exits was then scanned (schematic drawing shown in Figure 2.3) using two ranges (30 μm x 30 μm and 8 μm x 8 μm) to directly compare surface roughness.

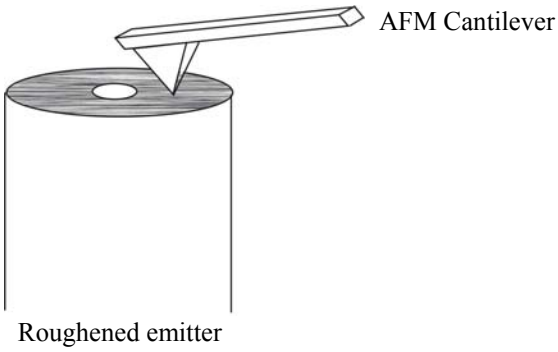

Figure 2.3. Schematic drawing of AFM tip scanning an emitter exit surface.

2.2.4. Contact angle measurement

A video contact angle surface analysis system (VCA OptimaXE, AST Products, Inc., Billerica, MA, USA, shown in Figure 2.4) was used for the contact angle measurement of an unmodified and a roughened glass plate to examine the surface wetting prior to and following grinding. Treated and control plates were submerged into soapy water in an ultrasonic bath for 30 minutes. They were then rinsed thoroughly with distilled water and sonicated again in distilled water for another half hour to ensure that all detergent residues were removed. Afterwards, the plates were rinsed with

methanol/ethanol and dried with compressed air. A droplet of testing solution was released onto the glass plate through a flat-tip needle, controlled by turning a screw (on the VCA instrument) against a syringe plunger. Droplet volume consistency was controlled by positioning the needle and turning the plunger in a reproducible manner. The static contact angle images were captured using a built-in precision camera immediately following the release of the droplet from the needle tip. The five-point method was used to determine the tangent lines for the measurement of the contact angles. The average contact angle was calculated from three separate spots on each surface.

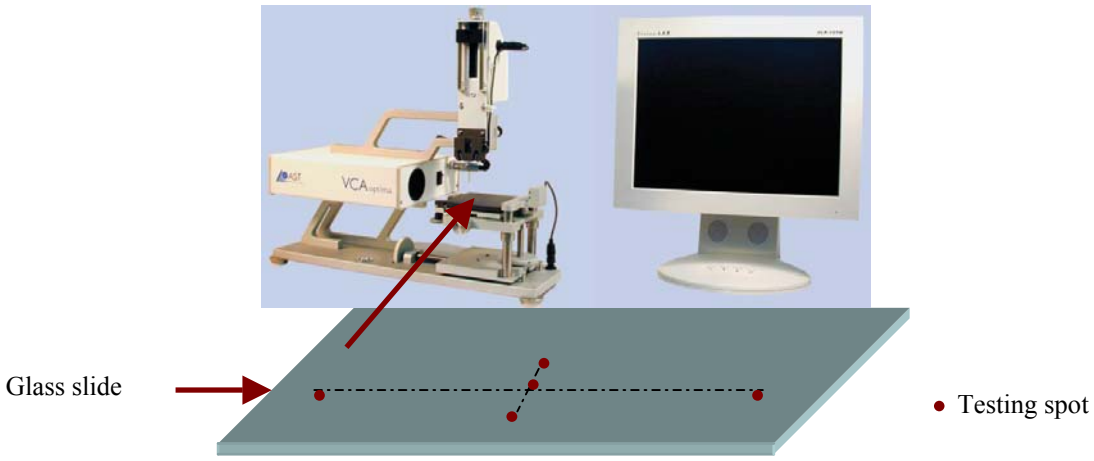

Figure 2.4. Layout of contact angle measurement.[3]

2.2.5. Offline electrospray

As shown in a schematic drawing shown in Figure 2.5, a roughened emitter was set in a MicroTee (Upchurch, S.P.E., Toronto, ON, Canada) which was in turn mounted

onto an x-y-z stage (Proxeon, Odense, Denmark). A CCD camera was used to record images through an ATI multimedia program. A high voltage supply (Micralyne, Edmonton, AB, Canada) was controlled by PC via μTK software and supplied the necessary electrospray potential. A small metal plate (3 cm x 3 cm), used as a counter electrode, was positioned 1 cm in front of the emitter. The positive high voltage was connected via a platinum wire electrode in contact with the mobile phase (liquid junction) within the MicroTee. A syringe pump (Harvard, PA, USA) infused 1 μM leucine enkephalin solution in 70% methanol to the ground emitter, and electrospray images were recorded at different flow rates.

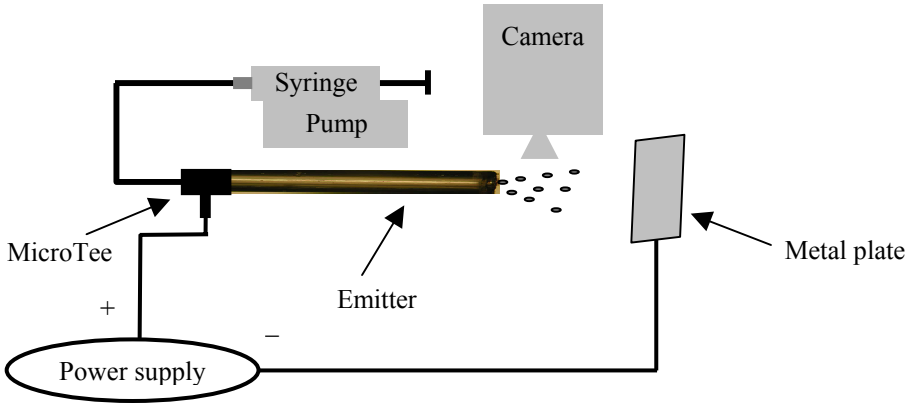

Figure 2.5. A schematic diagram of an offline electrospray setup.

2.2.6. Online electrospray

Mass spectra were acquired with a m/z range of 400 to 1000 on an API 3000 triple-quadrupole mass spectrometer (MDS, Sciex, ON, Canada). The setup of

electrospray ion source is shown in Figure 2.6. A nanospray interface (Proxeon, Odense, Denmark) was installed with two CCD cameras, a MicroTee and an x-y-z stage. An emitter was first mounted onto the tee on the stage, then CCD cameras and the x-y-z stage were used to finely position the emitter. The relative distance between the emitter and the mass spectrometer orifice was maintained at 0.5 cm to 1.5 cm. Spray voltages between 2.5 kV and 3.5 kV were applied through a metal wire inserted into the liquid junction within the MicroTee. One end of the MicroTee was connected to a nano-LC pump (Eksigent, CA, USA) with 15 cm of capillary (360 μm o.d. and 30 μm i.d.). Positive ion mode was used for the detection of both the Jeffamine and leucine enkephalin samples. The curtain gas flow rate was set at 0.3 L/min and both the declustering potential and focusing potential were kept at 60 V and 250 V respectively. Quadrupole peak width (set to yield unit mass resolution of 0.7 a.m.u. at FWHM) and scan time (one spectrum per second, 1Hz) were kept constant for all experiments. No additional desolvation methods were employed.

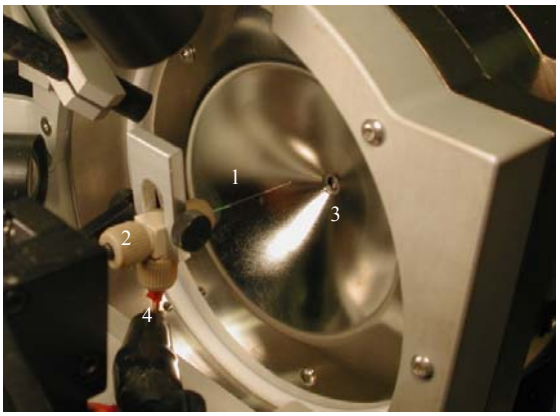

1.Emitter
2.MicroTee
3.MS orifice
4.Electrode

Figure 2.6. The configuration of electrospray ion source.

2.3. Results and discussion

2.3.1. Fabrication of surface roughened open tubular emitters

In this study, a non-tapered open tubular emitter was developed for nano-ESI by simply roughening the exit surface of a fused silica capillary. Unlike the traditional tapered emitter, which possesses a narrow aperture at the tip (usually less than 20 μm) to support electrospray at nano flow rates, the roughened emitter allows nano-ESI from a larger bore aperture (75 μm i.d. and 360 μm o.d.) without tapering either internal or external diameters. Tapered emitters are fabricated by pulling, micromachining, or chemical etching to allow electrospray at flow rates below 1 μL/min.[4-9] In general, the smaller the emitter tip is, the lower the flow rate that can be used to generate a stable electrospray. Superior sensitivity is achieved at flow rates as low as a few nanoliters per minute from very small sized aperture emitters (1 to 5 μm).[10] However, as the tip aperture is reduced below 20 μm, clogging from salt deposits, solids from column bleed, and debris resulting from capillary cutting becomes a constant concern and a significant problem.[2] In essence, emitter robustness is traded for higher sensitivity, which has impeded the wider acceptance of nanospray as a routine analytical technique.[1] Furthermore, the flow resistance from the small aperture can limit the range of the accessible flow rates where it is often desirable to conduct sample preparation (i.e. loading, desalting and preconcentration) at relatively high flow rates, while it is advantageous to conduct MS analysis at much lower flow rates.[11]

To overcome the disadvantages associated with the tapered emitters, approaches such as the development of emitters with larger apertures, and/or the fabrication of

emitters with multiple electrospray channels or arrays of emitters, have been explored as discussed in section 1.3.2. Figure 2.7a illustrated such an emitter with multiple fluid flow paths formed by entrapped functionalized silica spheres. A schematic drawing of a simulated CNF emitter is shown in Figure 2.7b. In this thesis study, a roughened emitter (as illustrated in Figure 2.7c) is also demonstrated to have the capability of generating stable nano-electrospray through a relatively large open tubular aperture (360 µm o.d. and 20 µm to 75 µm i.d.).

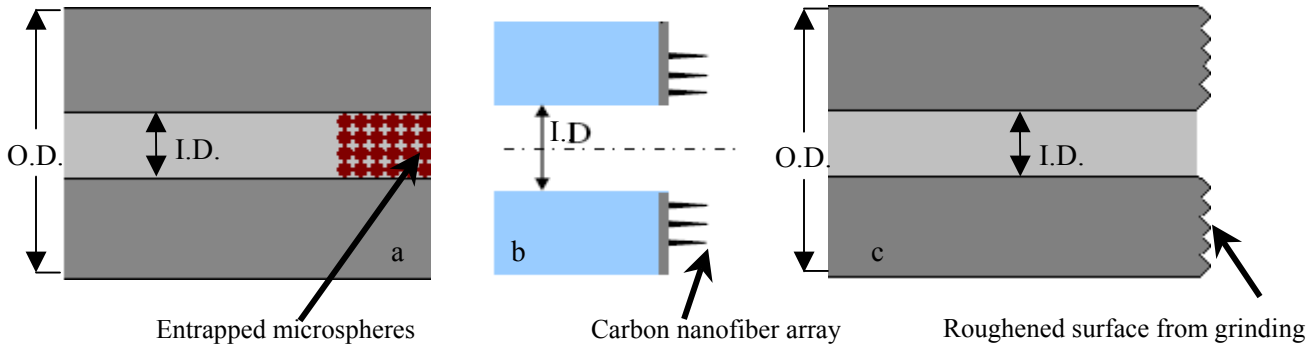

Figure 2.7 Schematic drawing of the horizontal cross sections of different types of non-tapered emitters: (a) Bead-entrapped emitter; (b) CNF emitter[2]; (c) Roughened emitter

Emitters were fabricated by roughening the exit aperture of fused silica capillaries. During the fabrication of emitters, precautions were taken to use similar grinding conditions (pace, grinding time, directions and applied forces) for each emitter. Several emitters were prepared using different grit sand papers and it was found that emitters fabricated with 4000 grit sand paper were the most consistent (data not shown). A comparison of the electrospray behaviour of both unmodified and surface roughened

fused silica emitters shows that enhanced TIC stability is obtained with surface roughened emitters (Figure 2.8).

When spraying from an unmodified cleaved capillary with 75 μm i.d., an unstable Taylor cone is observed at and below 500 nL/min flow rates. As fluid accumulates on the conical surface of a Taylor cone, the cone is broken frequently because the base of the cone is not able to maintain its shape. Clusters of larger droplets are emitted, which contribute to unstable TIC signals ("spitting" shown in Figure 2.8a) and ion suppression (Figure 2.8c). Following the ejection of a relatively large droplet, the surface re-balances and a new cycle begins. The combination of repeated cycles results in pulses or spikes in the TIC signal. When spraying from a roughened emitter, it is more facile to sustain a stable electrospray and the minimum attainable flow rate for a stable electrospray is extended to 50 nL/min. The liquid appeared to be more evenly distributed over the conical surface. "Spitting" was not observed from the roughened emitter and ionization efficiency was improved compared to the unmodified emitter (Figure 2.8b and 2.8d).

The differences in electrospray behavior shown by the unmodified and surface roughened emitters indicate that the surface roughness of the emitter exit impacts the formation of a Taylor cone and the ESI stability. In a previous study it was noted that lightly sanding a metal emitter improved spray performance.[12] The improved electrospray characteristics were ascribed to multiple points of electrospray nucleation. However, when using fused silica emitters, the improved electrospray performance likely stems from the modified wetting characteristics of the roughened emitter exit, which results in a more stabilized Taylor cone base.

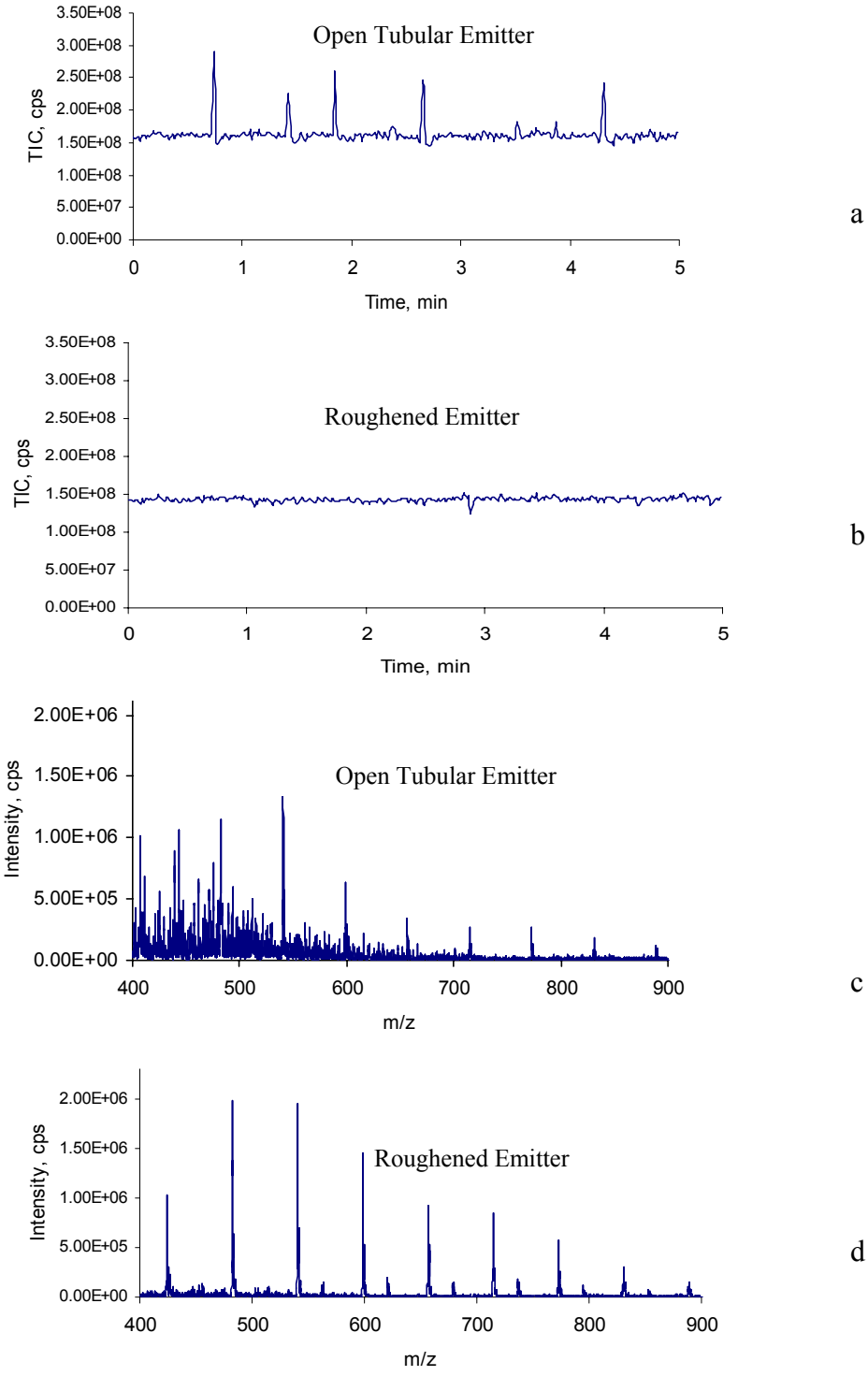

Figure 2.8. Comparisons of electrospray performance from an unmodified capillary emitter (a, c) and a roughened emitter (b, d) by infusing 1 μM Jeffamine in 70% MeOH, 500 nL/min flow rate and +2.8 kV spray potential. a and b: five minute TIC traces. c and d: extracted mass spectrum from 1s of the TIC spectrum.

The surface morphology of an unmodified emitter and a roughened emitter was characterized by directly probing the capillary exit surface with an AFM tip (Figure 2.9).

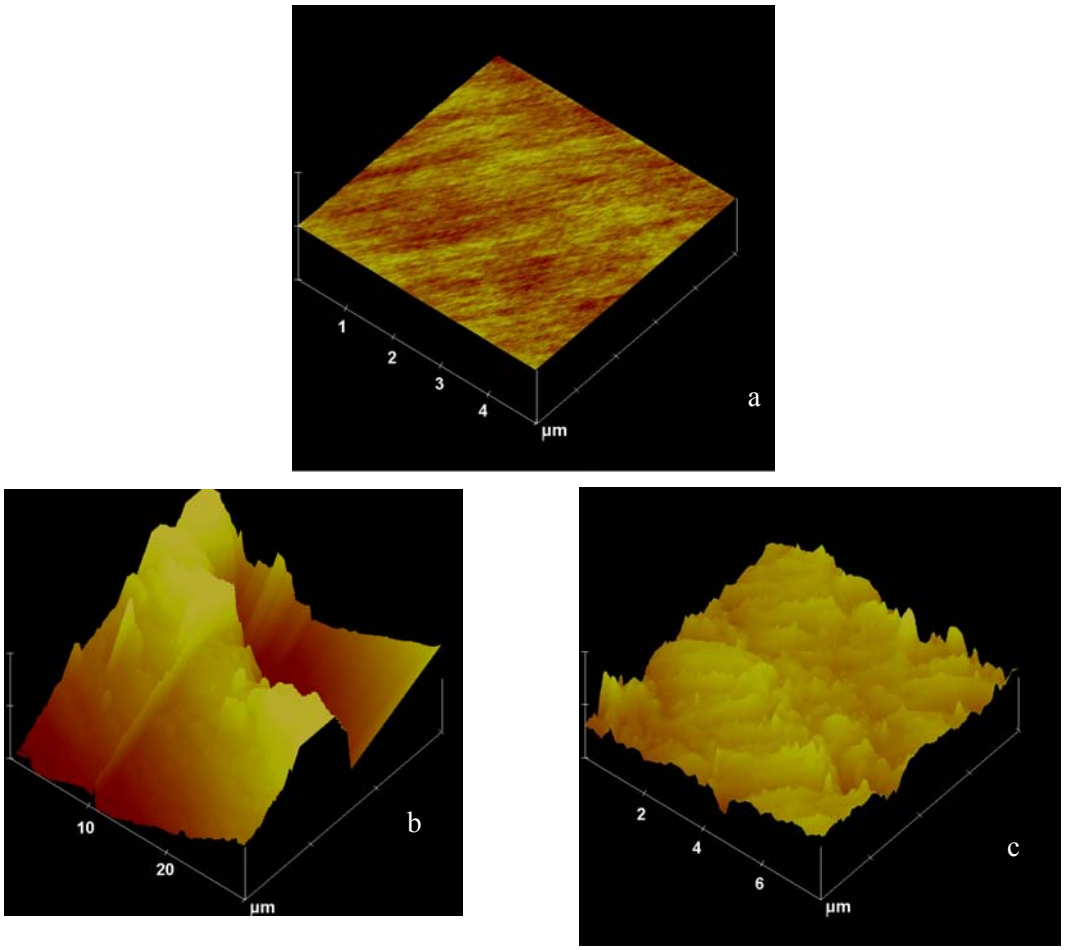

Figure 2.9. Comparison of the surface roughness before and after grinding: (a) AFM image of the top view (5 µm scanning range) of the emitter exit before grinding; (b) AFM image of the top view (30 µm scanning range) of the emitter exit after grinding; (c) AFM image of the top view (8 µm scanning range) of the emitter exit after grinding.

Surface roughness analysis of a directly cleaved emitter shows a very smooth surface with an estimated roughness of 0.5 nm (Figure 2.9a). Smaller scanned regions were examined but did not show any additional features (data not shown). The dynamic

processes involved during sanding however produce a complex surface topography on the roughened emitter. The AFM image at a scanning range of 30 μm X 30 μm showed a number of ridges (10 μm to 15 μm in width and 5 μm in height), resulting from sanding, with an estimated mean roughness (Ra) of 400 nm (Figure 2.9b). A decrease in the scanning range showed further structural details of smaller ridges (2-3 μm in width and less than 1 μm in height) in Figure 2.9c.

The effect of surface roughness on the wetting properties of a surface is complex and has not yet been fully characterized. However, there are a number of studies that have advanced the understanding.[13-15] When a drop of liquid spreads out on an ideally smooth and chemically homogenous surface, the surface tension and surface energy follow Young's relation. The shape of a drop on a solid surface is determined by three forces pulling at the three-phase contact lines, which are the common borderlines between the solid, the liquid, and the corresponding equilibrium vapor. The interactions across the three interfaces determine the contact angle, which reflects the surface energy of the smooth solid surface. The surface structures of a roughened surface affect the dynamic behavior of the contact line and the shape of the drop.[14] When a drop of fluid sits on a roughened hydrophilic solid surface, it is more likely to be involved in a Wenzel contact state in which a droplet penetrates the spaces between asperities or surface structures. Figures 2.10a and 2.10b illustrate the differences in contact angle for both a smooth and roughened hydrophilic surface. A decreasing contact angle indicates a transition from a higher energy state to a lower energy state, where the droplet becomes more stable. Chow proposed that for a given surface composition and a liquid with a

fixed equilibrium contact angle, an increase in surface roughness reduces the contact angle and broadens the three phase contact lines, which results in a more stabilized droplet surface.[15]

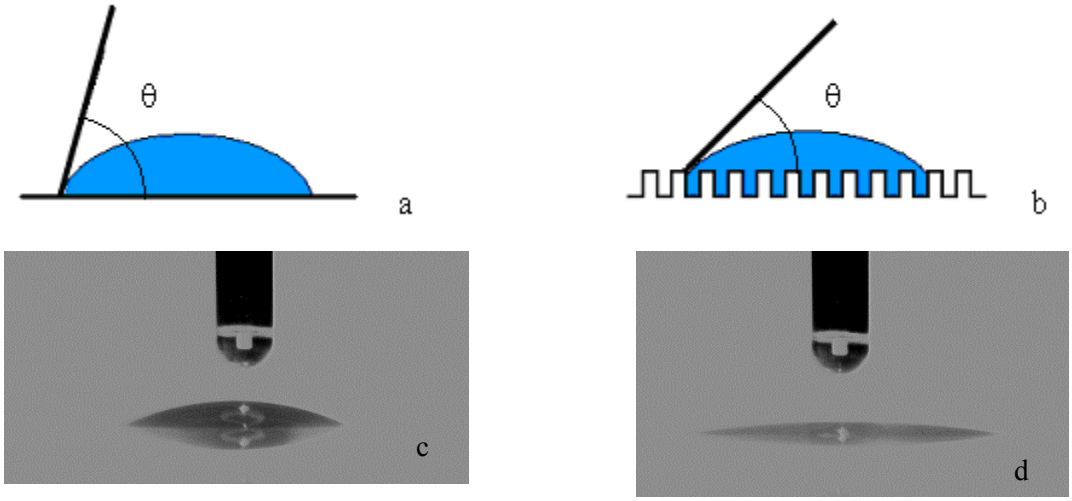

Figure 2.10. (a and b) schematic drawing of contact angles of a water droplet on: (a) a smooth hydrophilic surface; (b) a rough hydrophilic surface. (c and d), comparison of contact angles before and after sanding by 4000 grit silicon carbide sanding paper using 7:3 (v/v) water vs methanol as testing solutions: (c) image of contact angle on a plain glass plate; (d) image of a reduced contact angle on a roughened glass plate.

The effect of surface roughness on solution contact angle was conducted on unmodified glass plates and glass plates roughened with 4000 grit silicon carbide sanding paper. Solutions containing different ratios of water, methanol and 0.1% of acetic acid, prepared to mimic electrospray solvent conditions, were used for contact angle analysis. With increased surface roughness, a decrease in contact angle was observed for each of the three testing solution compositions listed in Table 2.1. Representative images for comparison have been included (Figure 2.10c and 2.10d) using a 7:3 (v/v)

water/methanol solution. Similar trends were observed at 100% aqueous solution and higher organic composition solutions. However, it became difficult to measure the contact angles of solutions containing > 50% methanol due to rapid spreading/evaporation. Smaller contact angles suggest better wettability and correlate with better emitter performance in regards to Taylor cone and TIC stability.

Table 2.1. Comparison of contact angles on non-modified and roughened surfaces at different solvent compositions.

Surface	Contact angle, °	SD, °	RSD, %
Non-modified surface			
100% aqueous	39	0.98	2.53
70% aqueous	31	1.41	4.56
50% aqueous	17	4.16	24.72
Roughened surface (by 4000 grit sand paper)			
100% aqueous	11	0.78	7.03
70% aqueous	8	0.65	7.67
50% aqueous	ND	ND	ND

Note: ND- non determinable

3.3.2. Stabilized electrospray at different nano flow rates

Stable Taylor cones were observed in both offline and online electrospray experiments with roughened emitters (75 μm i.d. and 360 μm o.d.) at flow rates as low as 50 nL/min. Figure 2.11 shows offline electrospray images taken by continuously infusing 1 μM leucine enkephalin in 70% methanol and 0.1% acetic acid at a spray voltage of 2.8

kV. Pointed cone jets were visible at both 500 nL/min and 300 nL/min flow rates, but gradually became less visible as the flow rate was reduced below 100 nL/min. Figure 2.11b shows a magnified image of an electrospray Taylor cone from Figure 2.11a. As discussed in section 1.2.2, the emission diameter on the tip of a Taylor cone, from where droplets are emerging (shown in Figure 2.11b and 2.11c), is proportional to the 2/3 power of the flow rate, which indicates that the emission diameter, and thus the size of the droplets is reduced when the flow rate is lowered. These fundamental aspects of nanoelectrospray are consistent with Taylor cone observations produced by the roughened emitter. (Note: a stable electrospray was not possible from an unmodified tip of the same dimension so no comparison below 500 nL/min was possible.)

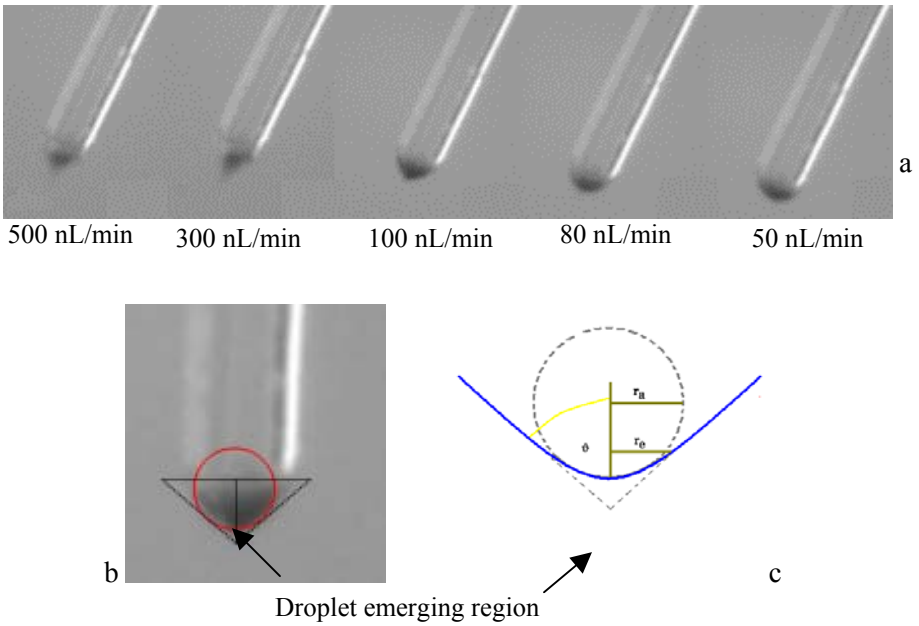

Figure 2.11. (a) Offline spray images show the decreased emission zone from 500, 300, 100, 80 and 50 nL/min flow rates; (b) a magnified offline electrospray image; (c) a schematic diagram of an electrospray Taylor cone at a condition close to static equilibrium.

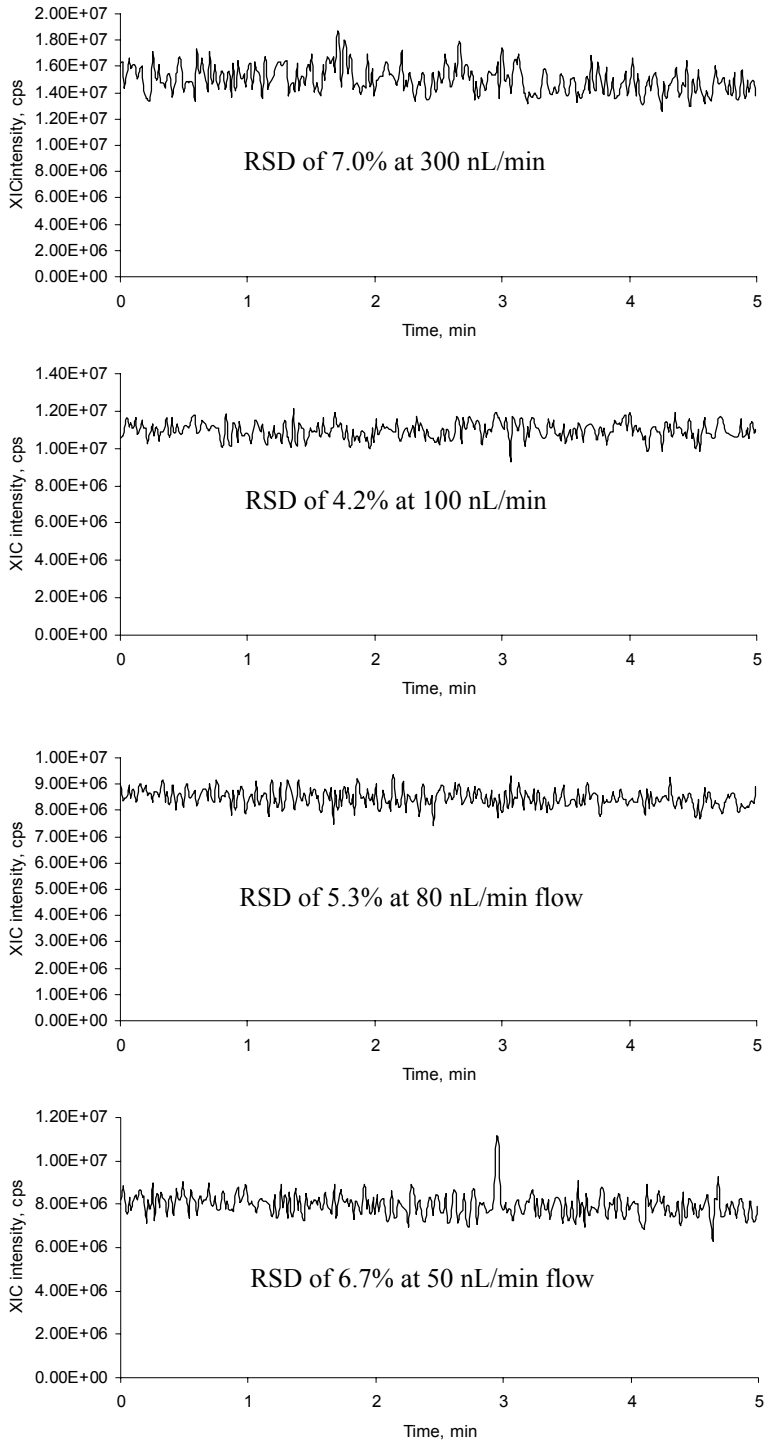

Figure 2.12. Stabilized electrospray ion currents obtained from a roughened emitter with 75 μm i.d. and 360 μm o.d. by infusing 1 μM leucine enkephalin in 70% MeOH at (a) 300 nL/min, (b) 100 nL/min, (c) 80 nL/min and (d) 50 nL/min flow rates (and 2.8 kV spray voltage.

The Taylor cone, stabilized by the roughened surface, enabled online electrospray of 1 μM leucine enkephalin at less than 500 nL/min flow rates from a large aperture open tubular emitter (75 μm i.d.). The RSD's of the average extracted ion currents from 545 to 565 m/z (1 μM leucine enkephalin) were all less than 7% between 50 nL/min and 300 nL/min flow rates, as shown in Figure 2.12a to 2.12d.

2.3.3. Effects of solvent composition on electrospray performance

In many protein and peptide applications, electrospray is used downstream of the HPLC separation column where a solvent gradient is employed to enhance chromatographic separation efficiency.[16, 17] The changes in solvent composition lead to changes in electrospray ionization and ion production.[18] Methanol and acetonitrile are the most popular solvents used for the separation and identification of proteins and peptides and we chose to characterize the performance of a roughened emitter at different concentrations of these two organic solvents. The results show that solvent composition affects the electrospray stability and sensitivity with the roughened emitter (Figure 2.13a). As the fractional composition of organic solvent increases, the TIC signal variation also increases. An example, shown as error bars in Figure 13a, indicates that increasing the fraction of methanol in water solution from 3:7 (v/v) to 9:1 (v/v), causes the electrospray to become less stable (the RSD of the TIC intensity increases from 5% to 30%).

However, it may be noted that even with the largest oscillation at 90% methanol (Figure 2.13b) under certain spray conditions, the sensitivity of detection is maintained in

a reasonable range (Figure 2.13c). The lowest signal to noise ratio obtained from a spot of TIC traces (shown in Figure 2.13b) is 16 for the m/z peak at 482.5. The square wave-like TIC profile may have resulted from a cycling of a liquid build-up on the emitter end followed by a period of low end volume after the drop was spit off the tip. This effect was most dominant when the tip was close to the orifice and the resulting potential difference was a stronger influential force than the surface tension for the specific solvent mixture.

The stability of the electrospray at higher organic concentrations may be improved by balancing the forces on the surface of a Taylor cone, which are produced by the applied potential and surface tension of the liquid. Since a liquid with a higher fraction of organic solvent has decreased surface tension, to offset its impact one can either increase the relative distance between the emitter tip and the mass spectrometer orifice, or decrease the electrospray potential. It was found that by increasing the relative distance from 0.5 cm to 1.5 cm, TIC signals became more stable (i.e. variations decreased from 30% to 10% as shown in Figure 2.13b) using a solution 9:1 (v/v) of methanol in water. The electrospray stability did not change dramatically when the spray potential was decreased from 2.8 kV to 2.45 kV, although this may have been due to the relatively small voltage change (i.e. 350V) (Note: a Taylor cone did not properly form if the spray potential was smaller than 2.4 kV under these conditions). Acetonitrile showed a similar trend to that of methanol.

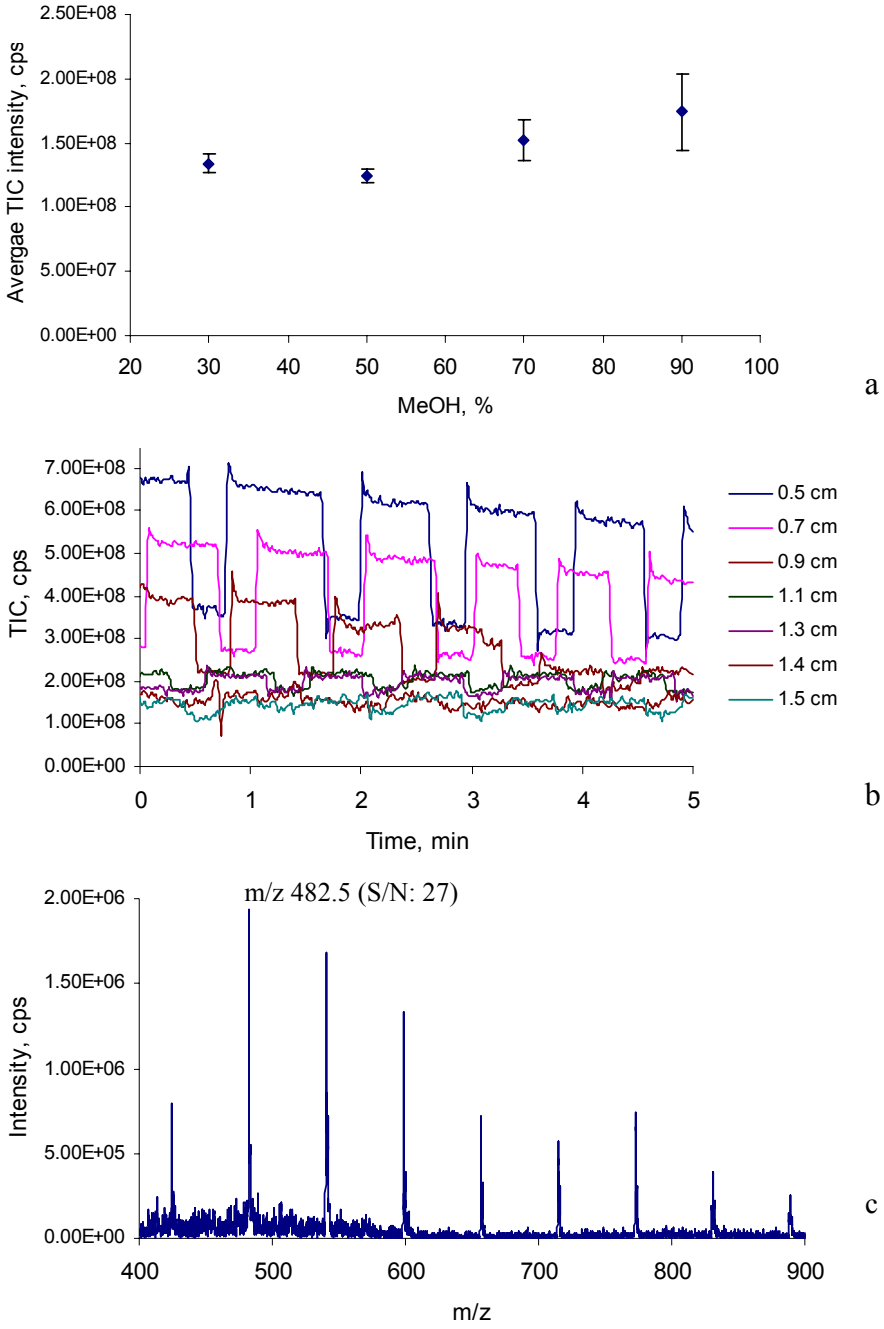

Figure 2.13. (a) Impact of different methanol concentrations on spray sensitivity and stability with a roughened emitter infusing 1 μM Jeffamine solution at 500 nL/min, + 2.8 kV spray voltage. (b) Changes in the electrospray stability by increasing the relative distance between the spray tip and the mass spectrometer orifice (at 90% methanol). (c) Representative extracted mass spectrum from normal spray region in Figure 2.13b.

The limitation of a roughened open tubular emitter is that as the aqueous concentration is increased to greater than 70%, it became difficult to consistently generate a stable electrospray (RSD's > 50%) due to the increased surface tension, larger Taylor cone volume and more problematic desolvation.

2.3.4. Sensitivity and reproducibility

The sensitivity of ESI/MS is determined by the ionization efficiency and mass transmission efficiency between the ion source and the mass detector. In this study the distance between an emitter tip and the mass spectrometer orifice was fixed. As a result, ionization efficiency was the main factor affecting the sensitivity. When reducing the flow rate from 300 nL/min to 50 nL/min, sensitivity improved as expected due to the enhanced ionization efficiency resulting from the formation of small charged droplets. To compare the change in sensitivity as the flow rate changed, a signal response factor was calculated using the average XIC (extracted ion current) intensity divided by the amount of leucine enkephalin consumed over a 5 minute acquisition period. The calculated signal response factors at different flow rates were plotted against corresponding flow rates as shown in Figure 2.14a. The higher signal response at lower flow rates with the same amount of analyte consumption indicates that the sensitivity increases exponentially when flow rates are reduced from 300 nL/min to 50 nL/min. As shown in the mass spectrum, which was extracted between m/z 545 and 565 from a one second TIC trace acquired at a 50 nL/min flow rate, 5 femtomoles of leucine enkephalin was detected with a signal to noise ratio (S/N) of 48 (Figure 2.14b).

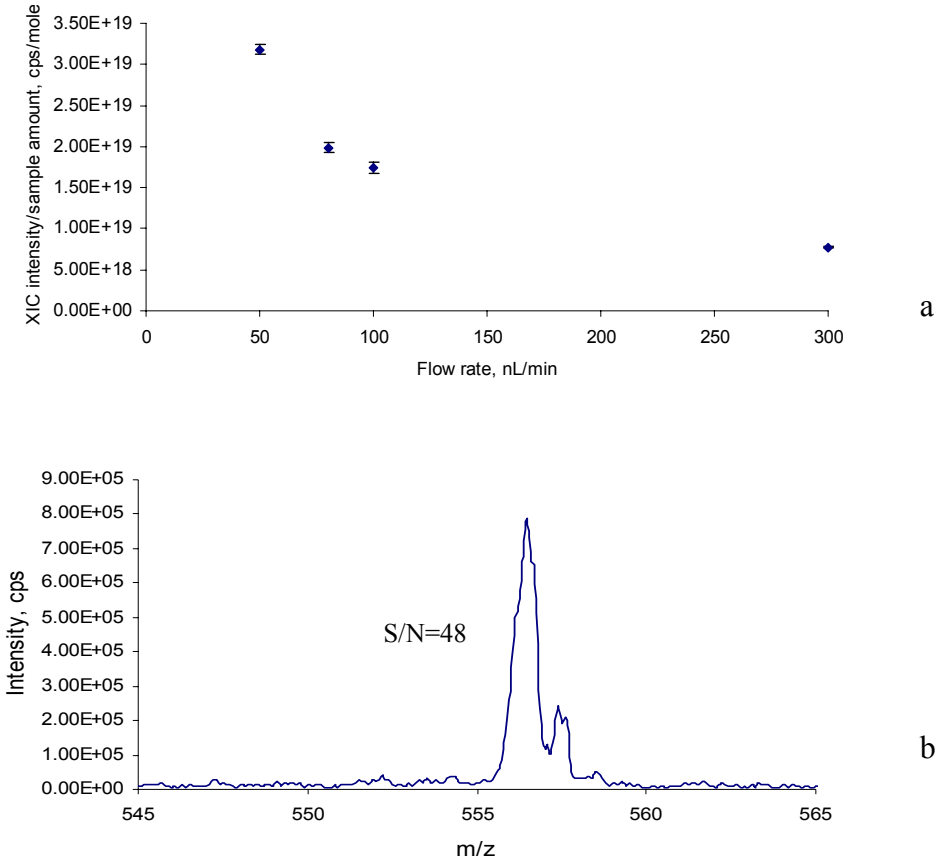

Figure 2.14. (a) XIC intensity (M.W. = 556) per unit amount of leucine enkephalin consumed at different flow rates using a roughened emitter. (b) mass spectrum generated from a 1 s TIC trace acquired by infusing 1 μM leucine enkephalin in 70% MeOH at 50 nL/min at + 2.8 kV applied potential.

Generating unambiguous protein identification information, especially quantitative information, relies heavily on the reproducibility and reliability of electrospray emitters used. Conventional pulled nanospray emitters require each emitter to be optimized and several may need to be tried before one sprays in a suitable fashion. Following initial optimization, the emitter position and the operational condition were maintained throughout. Each new emitter was simply installed and sprayed. Three

emitters were fabricated in a similar fashion, and electrospray performance of each of the individual emitters was tested under the same conditions. Typically, the reproducibility of the electrospray signals generated, were < 5% RSD (run to run) and < 7% from emitter to emitter (n=3) as shown in Figure 2.15.

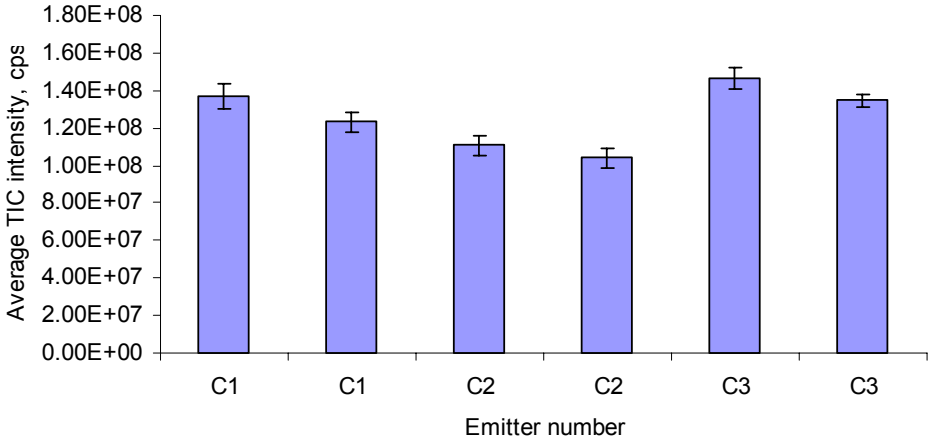

Figure 2.15. Reproducibility of roughened emitters from different batches and from different runs

2.4. Summary

A robust roughened open tubular emitter was developed by grinding the emitter exit aperture of a fused silica capillary. The stability of a Taylor cone is enhanced by the increased emitter surface roughness, and the minimum flow rate at which ESI was stable was extended to 50 nL/min without tapering either the internal or external diameters. At a 50 nL/min flow rate, 5 femtomoles of leucine enkephalin was detected with a signal to noise ratio of 48. Achieving a stable nanoelectrospray at low flow rates from relatively large sized aperture emitters would provide more flexibility for the integration of high flow approaches and low flow techniques into the same configuration. These allow for

the highly sensitive detection by MS at relatively low flow rates without trading off its robustness or flexibility of use at higher flow rates. Roughened open tubular emitters may be used as a routine, clog resistant tool in nanoelectrospray mass spectrometry for high throughput proteomics and drug discovery.

2.5. References

(1) Covey, T. R., Pinto, D. *Practical Spectroscopy Series* **2002**, *32*, 105-148

(2) Sen, A. K.; Darabi, J.; Knapp, D. R. *Microfluidics and Nanofluidics* **2007**, *3*, 283-298

(3) http://www.astp.com/vca/vca_optima.html

(4) Wilm, M.; Mann, M. *Analytical chemistry* **1996**, *68*, 1-8

(5) Kelly, R. T.; Page, J. S.; Luo, Q.; Moore, R. J.; Orton, D. J.; Tang, K.; Smith, R. D. *Analytical Chemistry* **2006**, *78*, 7796-7801

(6) Bruce, J. E.; Anderson, G. A.; Wen, J.; Harkewicz, R.; Smith, R. D. *Analytical Chemistry* **1999**, *71*, 2595-2599

(7) Fong, W. Y. K. Dissertation, Chinese University of Hong Kong, HK, 2001

(8) Melvin, A. WO Patent 3,034,464, February 2003

(9) Liu, J.; Ro, K. W.; Busman, M.; Knapp, D. R. *Analytical Chemistry* **2004**, *76*, 3599-3606

(10) Valaskovic, G. A.; Utley, L.; Lee, M. S.; Wu, J.-T. *Rapid Communications in Mass Spectrometry* **2006**, *20*, 1087-1096

(11) Vissers, J. P. C.; Blackburn, R. K.; Moseley, M. A. *Journal of the American Society for Mass Spectrometry* **2002**, *13*, 760-771

(12) Guzzetta Andrew, W.; Thakur Rohan, A.; Mylchreest Iain, C. *Rapid Communications in Mass Spectrometry* **2002**, *16*, 2067-2072

(13) Parvin, L.; Galicia, M. C.; Gauntt, J. M.; Carney, L. M.; Nguyen, A. B.; Park, E.; Heffernan, L.; Vertes, A. *Analytical Chemistry* **2005**, *77*, 3908-3915

(14) Bico, J.; Tordeux, C.; Quere, D. *Europhysics Letters* **2001**, *55*, 214-220

(15) Chow, T. S. *Journal of Physics: Condensed Matter* **1998**, *10*, L445-L451

(16) Suter, M. J.; DaGue, B. B.; Moore, W. T.; Lin, S. N.; Caprioli, R. M. *Journal of chromatography* **1991**, *553*, 101-116

(17) Markillie, L. M.; Lin, C.-T.; Adkins, J. N.; Auberry, D. L.; Hill, E. A.; Hooker, B. S.; Moore, P. A.; Moore, R. J.; Shi, L.; Wiley, H. S.; Kery, V. *Journal of Proteome Research* **2005**, *4*, 268-274

(18) Lee, S. S. H.; Douma, M.; Koerner, T.; Oleschuk, R. D. *Rapid Communications in Mass Spectrometry* **2005**, *19*, 2671-2680

Chapter 3

Porous Polymer Membranes Assisted Nano-ESI Emitters

3.1 Overview

In addition to spraying from larger aperture tubes as discussed in Chapter 2, emitters with multiple electrospray pathways are becoming a more attractive option for generating nanoelectrospray because of their lower chance of clogging, higher sample throughput, and the improved sensitivity.[1-3] Multiple electrospray pathways can be generated from an array of tips fabricated by either simply manipulating capillary tubes parallel to each other or using micro-fabrication techniques such as photolithographic patterning, plasma etching, or laser ablation.[4,5] Tang reported a multiple electrospray emitter by fabricating an array of emitters on a polycarbonate substrate.[6] The multiple pathways for electrospray were also generated by drilling holes on a hydrophobic plate.[7] However, these multiple electrospray emitters were designed to allow an increased sensitivity only at a relatively large scale of flow rates (>1 μL/min). For generating electrospray at nano-level flow rates, our group developed emitters with multiple pathways by forming porous polymer monolith (PPM) or entrapping microspheres inside of the capillary channel.[2,3]

Emitters with multiple pathways can be fabricated into either a capillary-based emitter or a chip-based emitter. A capillary-based emitter such as PPM filled or microsphere entrapped can be used in an integrated configuration for sample desalting, pre-concentration and separation as well.[3,8] Furthermore, chip-based emitters were also

developed to allow the integration of more complicated functionalities as well as an increased throughput.[9,10] Plastic materials are the choice for making disposable chips because they are cheaper. However, electrospray from the flat exit of a plastic chip channel is a challenge due to the liquid spreading. A capillary-based emitter can be inserted into the channel of a microchip to assist with the electrospray.[11] Although this technique has demonstrated good electrospray performance, it tends to leave a large dead volume which results in broadening of separation bands. Micro-fabrication techniques were used to form sharp tips to eliminate the spreading but these techniques are usually complicated and expensive.[12] Moreover, coating or bonding hydrophobic materials on the exit surface of a chip-based emitter demonstrated an alternative solution to address the problem. CF_4 coating by plasma deposition was used to increase the hydrophobicity on an emitter exit, but it could only last a short time before it was damaged.[13] A porous membrane was reported to enhance the hydrophobicity of an emitter exit surface by thermally bonding poly-tetrafluoroethylene (PTFE) onto the exit surface of a PC microchip.[14] A piece of PTFE membrane with 50 μm thickness and an average pore size of 0.22 μm was bonded onto a chip exit surface at about 150 °C by manually applying a force of 40 N for 10 s. However, it was found difficult to precisely control the temperature and the force used to allow a permanent bonding of membrane without deforming the channel exit during thermal bonding.

In addition, membranes with uniform pore sizes are also developed in numerous ways. In the 'track-etched' polymer membranes, cylindrical pores of uniform size are formed through a two-step procedure.[15] In the first step, a thin polycarbonate film is

exposed to collimated, charged particles from a nuclear pile. As these particles pass through the polycarbonate material, they leave sensitized tracks. In the second step, the polymer tracks are dissolved with an etching solution to form cylindrical pores. Varying the temperature, the strength of the etching solution, and the exposure time produces precisely controlled pore sizes. This unique process allows for increased control over pore size and the density of the membrane.

Yan *et.al.* developed a method by casting a polymer film on a template of a sacrificial pillar array.[16] The pillars are removed after film formation, leaving behind a porous membrane with cylindrical pores that span the complete thickness of the membrane (5 mm). The pore size may be tuned by adjusting the diameter of the templating pillars from 100 nm to 10 mm.

Porous polymer membranes are mainly used for filtration and purification. With the ability of creating ever-smaller, monodisperse pores, sophisticated applications of porous materials have been expanded to the areas as diverse as drug delivery, enantiomer separation, DNA and biomolecule separation, lithography, chemical sensoring, etc.[17-19] Porous polymer membranes with uniform pore sizes are used in this project to investigate its potential application in assisting electrospray by forming multiple electrospray pathways through these defined pores.

By bonding a piece of porous membrane on the exit of a capillary channel, the fluid flowing from the single channel (i.e. 75 mm) is split into multiple streams from the pores on membrane as shown in schematic drawing in Figure 3.1. Porous polymer membranes including polysulphone (PSF) and polycarbonate (PC), which have precisely

defined pore sizes, are used for the fabrication of both capillary-based emitter and a microchip based emitter. A novel technique is developed in this project to fabricate an emitter with multiple electrospray pathways by simply gluing a piece of porous polymer membrane onto the exit of a fused silica capillary or a channel exit of a polymer microchip under an optical microscope. Electrospray performance was evaluated at various operational conditions. The correlation between the sensitivity and pore sizes of membranes bonded on different emitters was investigated.

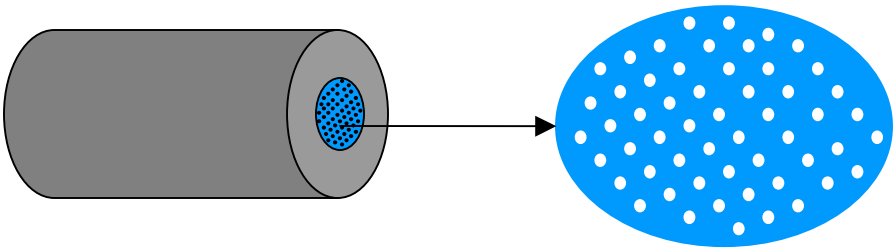

Figure 3.1. Schematic drawing of an emitter with multiple electrospray channels at the end of an open tube.

3.2 Experimental

3.2.1 Reagents and materials

Zinc nitrate hexahydrate, $Zn(NO_3)_2 \bullet 6H_2O$ (98%), hexamethylenetetramine, $C_6H_{12}N_4$ (99%), and glass plates coated with polycrystalline F-SnO_2 were purchased from Hartford Glass Inc. (USA). Polysulfone (Udel® P3500) was a gift from Solvay Advanced Polymers and was purified by precipitation fractionation using THF as a solvent and methanol as a precipitant. The weight-average molar mass *Mw* of the fractional sample was determined by light scattering using the specific refractive index increment of 0.201 ml/g measured in THF and was 9.0×10^4 g/mol. The polydispersity index *Mw/Mn* of the

sample was 1.42 as determined by size exclusion chromatography based on poly (methyl methacrylate) standards (*Mn* is the number average molecular weight). PSF membrane was prepared according to the procedures described elsewhere.[16] Whatman PC membrane was purchased from Fisher Scientific (Ottawa, ON, Canada). Fused-silica capillaries (360 μm o.d., 75 μm i.d.) were purchased from Polymicro Technologies (Phoenix, AZ, USA). Markrolon PC sheets were purchased from Sheffield Plastic Inc (Scarborough, ON, Canada). Epoxy resin was purchased from Varian, Canada. Glacial acetic acid, methanol (HPLC grade) and acetonitrile were all purchased from Fisher Scientific (Ottawa, ON, Canada) and used without purification. O-(2-aminopropyl)-O-(2-methoxyethyl) polypropylene glycol 500 (jeffamine) were purchased from Sigma-Aldrich (Oakville, ON, Canada) and also used without purification. Milli-Q water was obtained from Millipore (Bedford, MA, USA).

3.2.2 Preparation and characterization of PSF porous polymer membranes

PSF porous membrane was prepared by a patterning method which uses ZnO pillar arrays as a template. We used this method due to in house expertise in the Liu group in our department. The detailed procedure was described by Yan *et al*.[16] Briefly, as shown in the schematic drawing in Figure 3.2, ZnO pillars were prepared by immersing a SnO_2 coated glass plate into a solution containing $Zn(NO_3)_2 \bullet 6H_2O$ and $C_6H_{12}N_4$ (1:1 molar amount) at 90°C for 18 hrs following the reaction:

$$2Zn(NO_3)_2 + C_6H_{12}N_4 + 8H_2O \longrightarrow 2ZnO + 4NH_4NO_3 + 6H_2CO$$

A 2-3 mm dam was then built by epoxy resin along the periphery of a glass plate bearing ZnO pillars. 1.5 ml of 3.3 mg/ml PSF in THF solution was added onto a plate within the dam. After the THF evaporated, the PSF spherical end capping on the pillar was etched off by soaking the plate bearing PSF membrane in THF/methanol (v/v =1:1). The plate was then immersed into 0.5 M HCl to dissolve the pillars after the THF/methanol evaporated. Finally, the porous membrane was detached from the glass plate as ZnO was dissolved.

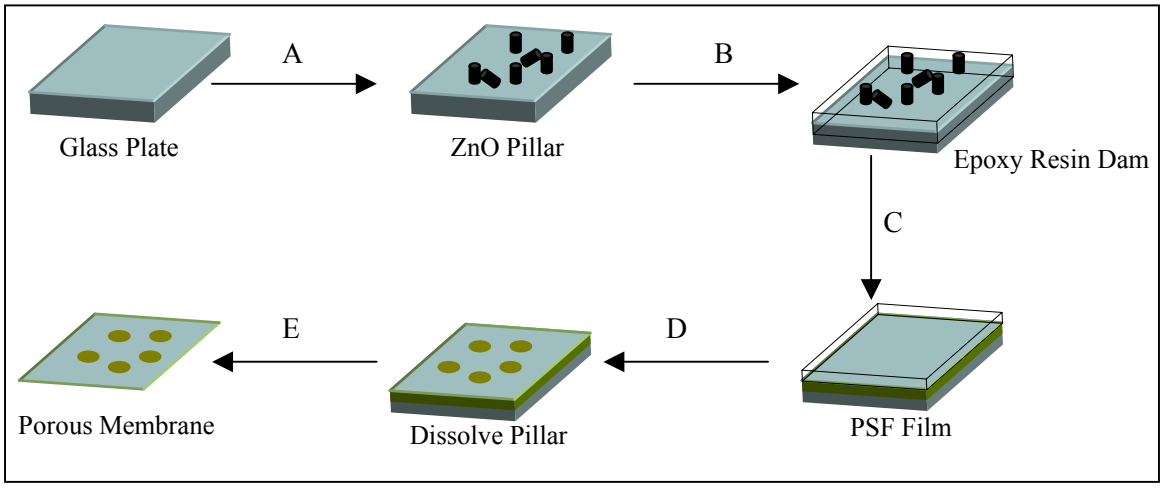

Figure 3.2. Schematic drawing of the preparation procedure of a PSF membrane.

Figure 3.3 shows the SEM image of ZnO pillars (a) with about 1 μm in width (b) and 6-7 μm in length (c). By casting polyfulfone solution onto these pillars, a 1 μm pore sized membrane can be obtained as shown in figure 3.3d.

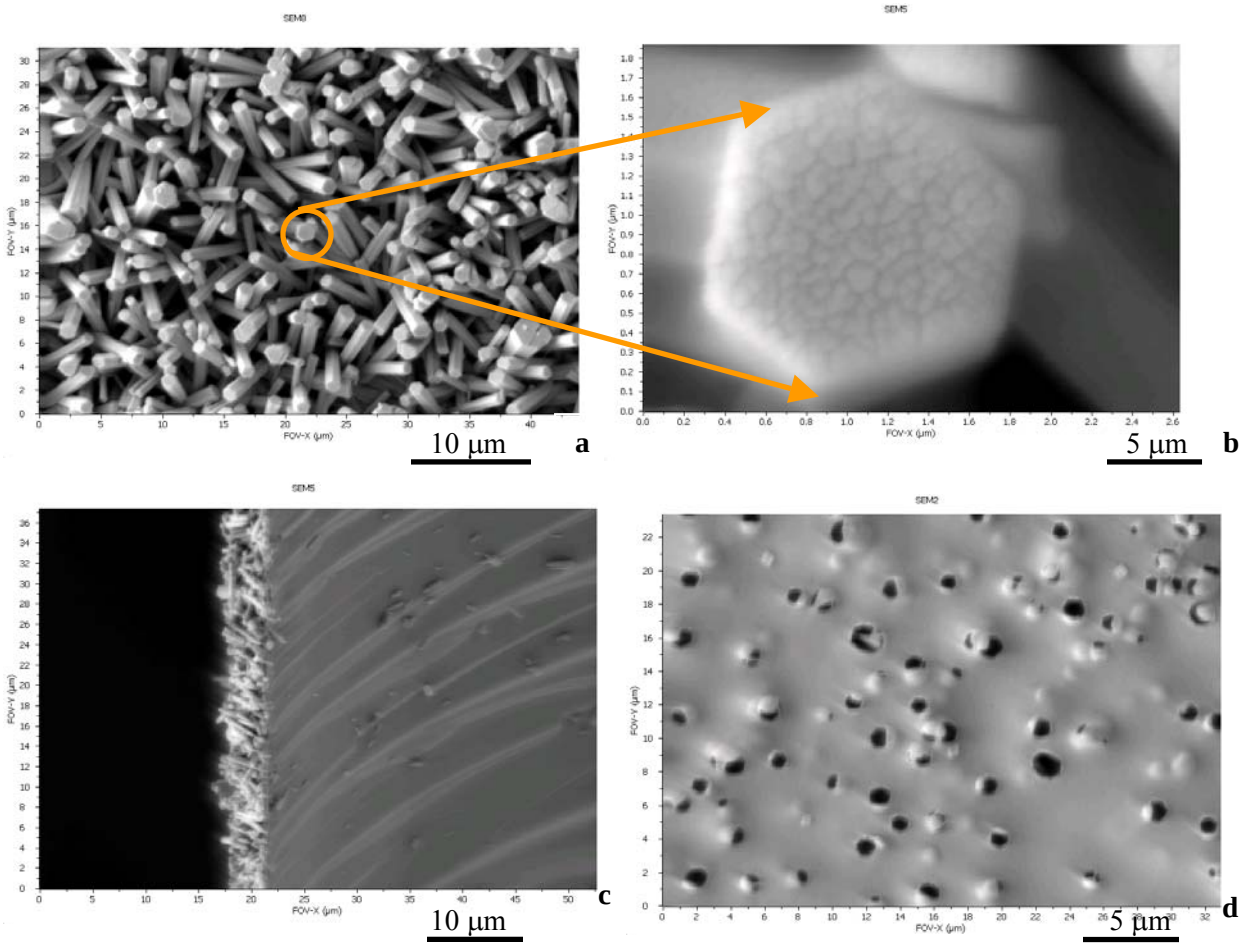

Figure 3.3. SEM images (a) top view of ZnO pillar template for porous membrane preparation, (b) one pillar in large magnification, (c) side view of ZnO pillar template, (d) PSF membrane with about 1 µm pores.

3.2.3 Fabrication of a capillary-based multi-pathway electrospray emitter

360 µm o.d. and 75 µm i.d. UV-transparent fused silica capillaries were used for the emitter fabrication in a setup as shown in the schematic drawing in Figure 3.4. Emitters were cut 4 cm to 6 cm in length, and their exits were checked under a microscope before testing. PSF membranes with 1.0 µm sized pores and PC membranes

with 0.22 μm, 1.0 μm and 5.0 μm sized pores were used for the emitter fabrication respectively. A thin layer of freshly mixed epoxy resin was applied onto a capillary exit using a sharp needle under an optical microscope. The capillary was flipped downsides and then stamped the glued exit onto a piece of membrane. The extra membrane along the capillary edge was taken away using a tweezer after the resin was dried. Figure 3.5 shows SEM images of membrane bonded emitter exit at different magnifications.

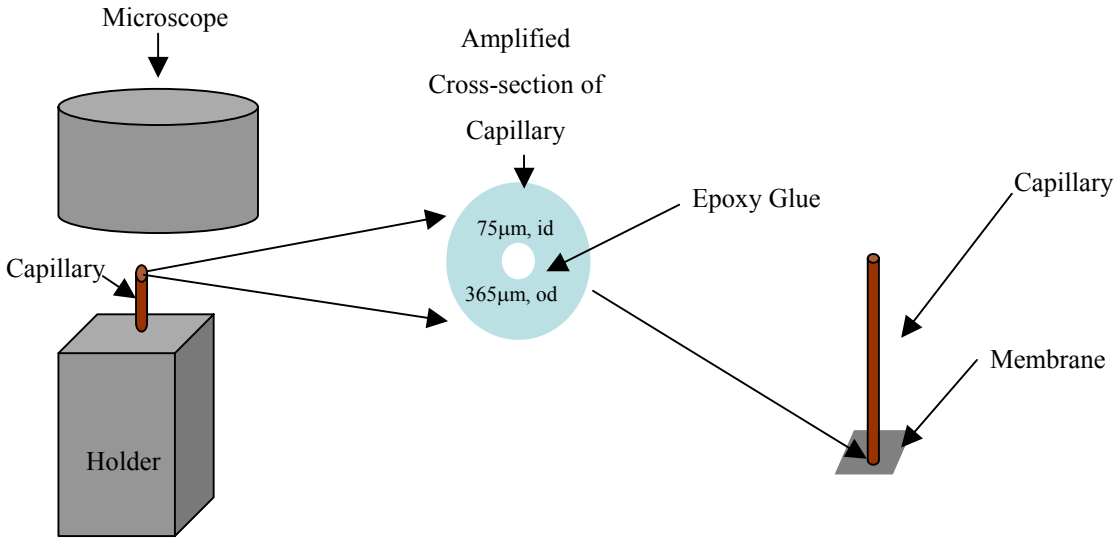

Figure 3.4 Schematic drawing of fabrication procedure for a porous polymer membrane glued emitter.

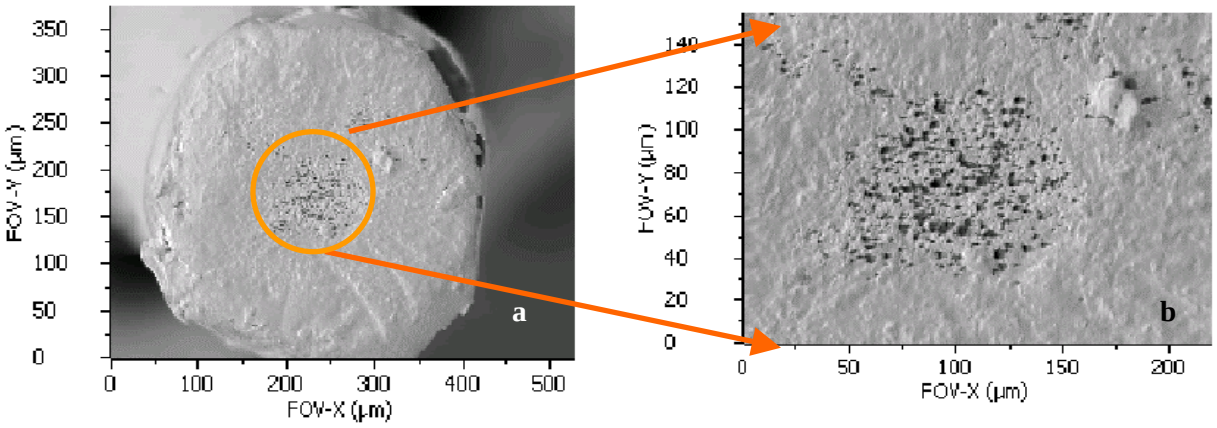

Figure 3.5. SEM images (a) top view of membrane bonded capillary exit, (b) larger magnification of bonded membrane.

3.2.4 Fabrication of a chip-based multi-path electrospray emitter

The method of hot embossing, as described elsewhere,[20] was used to fabricate a chip-based emitter from PC sheets as shown in the schematic diagram in Figure 3.6. Briefly, a fused silica capillary with 20 µm i.d and 150 µm o.d. was used as a master piece to create a channel by stamping the capillary onto a PC sheet at 150°C, 2000 N for 830 s. A channel was left on the surface of the PC sheet after peeling off the capillary. The channel was inspected under an optical microscope to ensure it was free of debris. A capillary with 20 µm i.d and 150 µm o.d. was inserted one-third into the channel through one exit for delivering the fluid into the chip channel. The other piece of PC sheet was then covered on the top of the bottom sheet bearing the positioned delivery capillary. Two pieces of PC sheets were bonded together under 145°C, 2000 N for 500 s. The chip exit was shaped to a narrower end so that it was easier to access the MS orifice. A piece

of porous membrane was then glued onto the chip exit using the method described above for the fabrication of a capillary-based emitter.

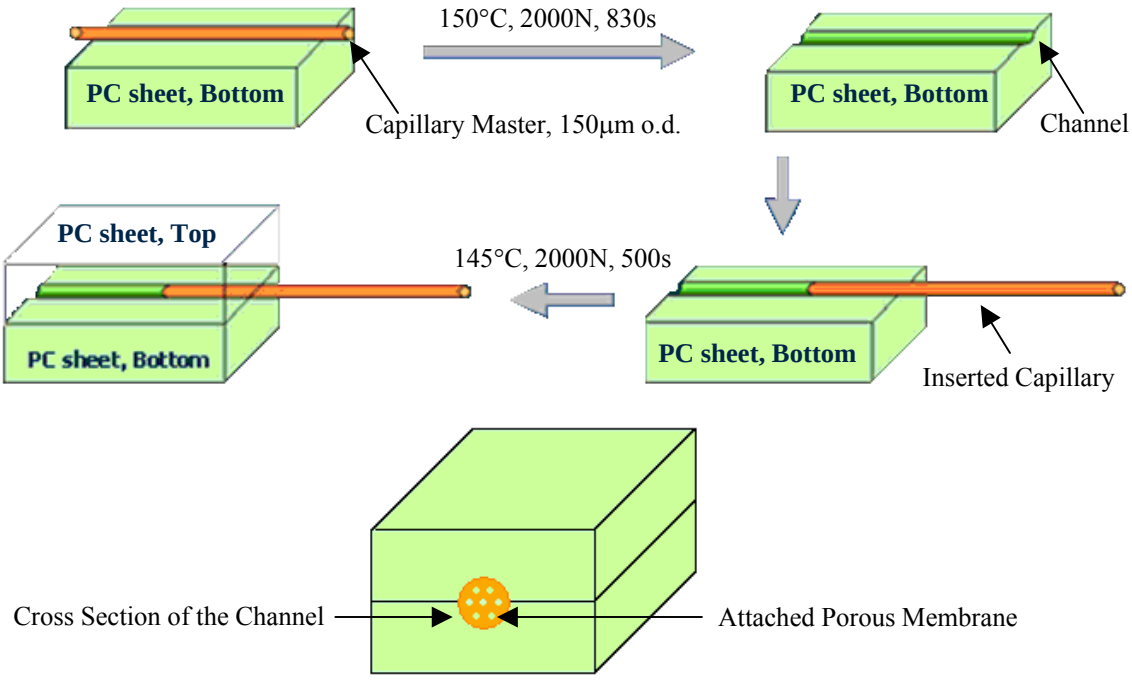

Figure 3.6. Diagram of fabrication of microchip-based emitter with membrane bonded on channel exit.

3.2.5 Offline and online electrospray mass spectrometry

Both offline and online Electrospray were conducted with the same instrumental setup as described in section 2.2.5 and 2.2.6 for a capillary-based emitter. For a chip-based emitter, it was first fixed on a home-made flat plastic holder, which was then mounted onto the x-y-z stage. A metal union was used to connect a delivery capillary to the chip channel and a capillary from a nano-LC pump. The metal union was also used for the connection with the electrode. CCD cameras and the x-y-z stage were used to finely position the chip-based emitter.

3.2.6 Investigation of electrospray performance

The influence of flow rates, spray voltages, and solvent compositions on the electrospray stability, sensitivity and the reproducibility was evaluated. A nano-pump was used to control flow rates from 50 nL/min to 500 nL/min. Spray voltages from 2.4 kV to 3.5 kV were applied through a metal wire inserted into the liquid junction within the micro tee. Standard solutions of 1 μM polypropylene (jeffamine) were prepared in methanol/acetonitrile with 10% - 90% water and 0.1% acetic acid. 1 μM leucine enkephalin was prepared in 70% methanol and 0.1% acetic acid. Data acquisition was set to scan between 400-1000 m/z. The intensity of the total ion current (TIC) was used to represent the sensitivity of the detection. The stability of the electrospray was indicated by the relative standard deviation (RSD %) of the TIC intensities calculated by dividing the standard deviation (SD) of the TIC data points against the average of TIC intensities. Signal to noise ratio (S/N) was calculated by dividing the background subtracted analyte peak heights against the standard deviation of the background signals.

3.3 Results and discussion

3.3.1 Fabrication of multi-path electrospray emitters using porous polymer membranes

A novel method to fabricate a multi-path electrospray emitter is reported by simply gluing a porous polymer membrane over the exit aperture of either a fused-silica capillary or a PC microfluidic chip. Various fabrication methods have been developed to fabricate emitters with an array of tips, channels, or simply holes to form multiple

electrospray paths.[21-23] The technique of laser etching was used by Tang to form an array of emitters on polycarbonate substrates at a relatively large scale. This multiple electrospray emitter demonstrated a 2- to 3-fold of enhancement in the detection sensitivity by ESI-MS at a microliter per minute flow rate.[6] For electrospray at nanoliter per minute flow rates, emitters with multi-paths have been fabricated with PPM or by entrapping microspheres inside of a capillary or microfluidic channel.[2-3] The patterned emitters not only enhanced sensitivity but reduced the tendency to clog as well. Clogging was largely reduced due to the multiple paths generated from macro-pores of PPM and interstices between the entrapped microspheres. PPM can also be formed inside of a glass or plastic microfluidic chip to assist the electrospray from a chip-based emitter.[20]

An alternative approach used a porous poly-tetrafluoroethylene (PTFE) membrane attached with thermal bonding to enhance the hydrophobicity of the exit surface of a PC microfluidic chip.[14] Multiple fluidic paths were formed as a result of the tortuous pores of the PTFE membrane. The liquid spreading at the exit aperture was reduced. However, as a result of thermal bonding, the authors found that the pore size (average 0.22 μm) and the pore distribution of a membrane were modified during bounding due to the bonding force and high temperature. It was not easy to precisely control the temperature and force to allow a permanent bonding of membrane without deforming the channel exit or sealing the pores on the membrane.

In this project, PSF and PC membranes with precisely defined non-tortuous pore sizes (0.2 – 5.0 μm) were used on both fused silica and plastic materials to fabricate capillary-based and chip-based emitters with multiple electrospray paths. A piece of

membrane was glued onto the fused-silica capillary exit by first applying epoxy resin on the capillary exit, and then simply stamping the glued exit onto a piece of membrane. The experimental result showed that following careful application of a very thin layer of epoxy resin onto the capillary exit under an optical microscope, enough membrane pores remained intact for electrospray. The electrospray performance was enhanced for both PSF and PC membrane assisted emitters due to the multiple electrospray paths obtained. Furthermore, the hydrophobic nature of these porous polymer membranes prevented the liquid from spreading across the entire emitter exit aperture. PMMA, COC, and PC substrates were used to fabricate a chip-based emitter using hot embossing method respectively, and the PC sheet was found to be the most compatible material with the gluing procedure. Membranes bonded to PMMA and COC devices frequently peeled from the substrate after several hours of spraying.

3.3.2 Electrospray from a membrane assisted capillary–based emitter

Stable electrospray are generally difficult to be produced at nano flow rates (e.g. < 1000 nL/min) from emitters with larger apertures (> 50 μm i.d.) prepared by directly cutting fused silica capillaries without further treatment. By roughening the emitter exit surface, the minimum flow rate to generate and maintain a stable electrospray was extended down to 50 nL/min from a 75 μm open tubular emitter.

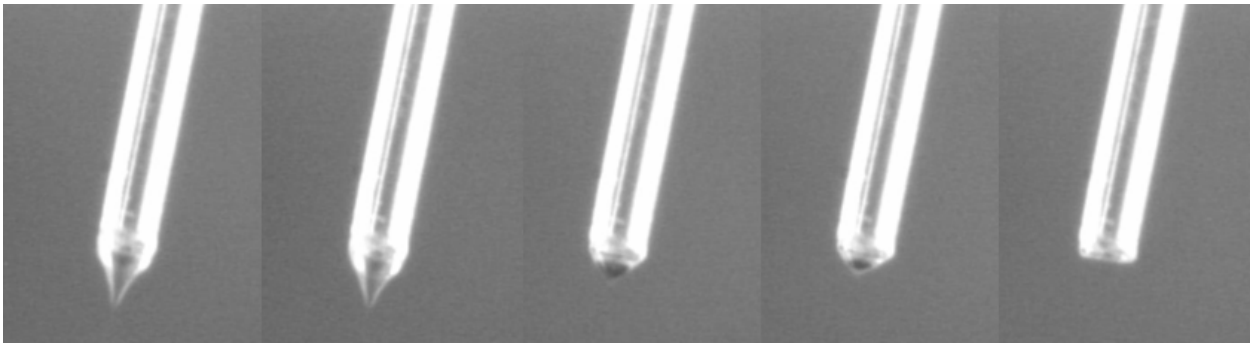

500 nL/min 300 nL/min 80 nL/min 50 nL/min 20 nL/min

Figure 3.7. Offline electrospray images from membrane assisted emitters (PSF membrane bearing 1 μm sized pores) at different flow rates through continuously infusing 1 μM leucine enkephalin in 70% methanol and 0.1% acetic acid at a spray voltage of 2.8 kV.

In this thesis, through attaching a piece of porous polymer membrane at a capillary exit (75 μm i.d. and 360 μm o.d.), stable electrospray Taylor cones were observed from both offline and online electrospray at flow rates from 20 nL/min to 500 nL/min. Figure 3.7 shows offline electrospray images taken from an emitter bonded with a piece of PSF membrane bearing 1 μm sized pores. Pointed cone jets were visible at both 500 nL/min and 300 nL/min flow rates, but gradually became less visible as the flow rate was reduced below 100 nL/min. No visible Taylor cone was observed at flow rate of 20 nL/min. Taylor cone observations produced by membrane assisted emitters are consistent with the fundamental aspects of nanoelectrospray, which suggested a reduced emission diameter, and thus a reduced size of droplets when lowering the flow rates.

Online electrospray experiments further confirmed the formation of stabilized Taylor cones through the assistance of porous polymer membrane as observed from

offline experiments. A comparison of electrospray performance between an open tubular emitter with a 75 μm i.d and a PSF membrane assisted emitter was conducted using a 1 μM jeffamine solution. The results show that both the stability and sensitivity of electrospray signals were enhanced for the membrane assisted emitter compared to that of the open tubular emitter, as shown in Figure 3.8. When utilizing an open tubular emitter at 500 nL/min, a stable signal could not be obtained at any position or applied voltage. Instead, a "spitting" mode predominated that manifested itself by the formation of large clusters rather than a cone jet mode, which resulted in signal spikes during electrospray as shown in Figure 3.8a, and caused MS signal suppression as shown in Figure 3.8b. Conversely, the stability and sensitivity were improved (shown in Figure 3.8c and 3.8d) using a porous membrane assisted emitter. The signal to noise ratio increases for all peaks of the jeffamine standard within the mass window from 400 to 900 m/z. For a peak at 482.4 m/z, an S/N ratio increases from 6 to 34 as indicated in Figure 3.8b and 3.8d.

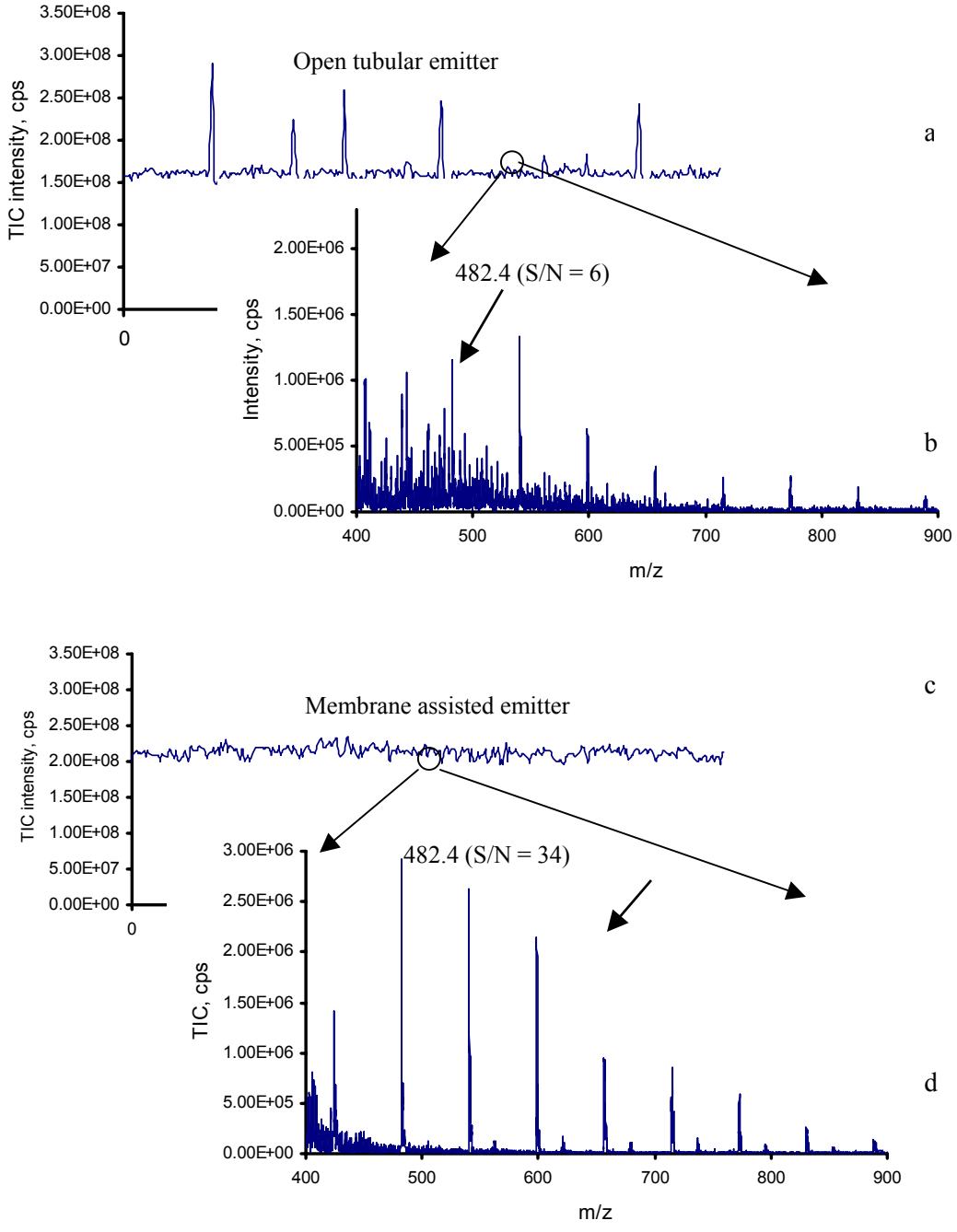

Figure 3.8. Comparison of electrospray stability and sensitivity from an open tubular emitter and a membrane assisted emitter by infusing 1 μM jeffamine in 70% MeOH at 500 nL/min flow rate and 2.8 kV spray voltage. (5a and 5c) TIC trace; (5b and 5d) the mass spectrum of 1s elution as assigned from TIC signals, respectively.

Furthermore, for a given emitter geometry, the spray voltage, solvent composition, flow rate, and the relative distance between an emitter tip and a MS orifice all have a strong influence on electrospray behavior.[8] The effects of these electrospray parameters on performances were evaluated by maintaining the emitter position relative to a MS orifice, and systematically adjusting the ESI parameters. The study showed that 2.4 kV voltage was necessary to initiate the electrospray process and increasing the electrospray voltage further resulted in increased ion current until 3.5 kV (Figure 3.9a) where ion suppression was caused by corona discharge.

The influence of solvent composition on electrospray performance was also investigated. Methanol, acetonitrile and water are the most common solvents used during reverse phase separations for protein and peptide analysis. Typically, proteins are separated by eluting them from columns through gradually changing the composition of the mobile phase. As the organic concentration increases, the surface tension of the mobile phase decreases, which results in improved ionization efficiency and increased TIC intensities (Figure 3.9b).

However, signals become unstable with 90% methanol. Moreover, when the organic component was less than 20%, it was difficult to get an efficient or stable electrospray. The RSD of TIC intensity increased from 5% for a 3:7 (v/v) MeOH/water solution to 16% for a 1:9 (v/v) MeOH/water solution. This was due to the larger surface tension of water and a substantially larger Taylor cone base formed on the exit aperture of a membrane assisted emitter compared to that from a tapered tip.

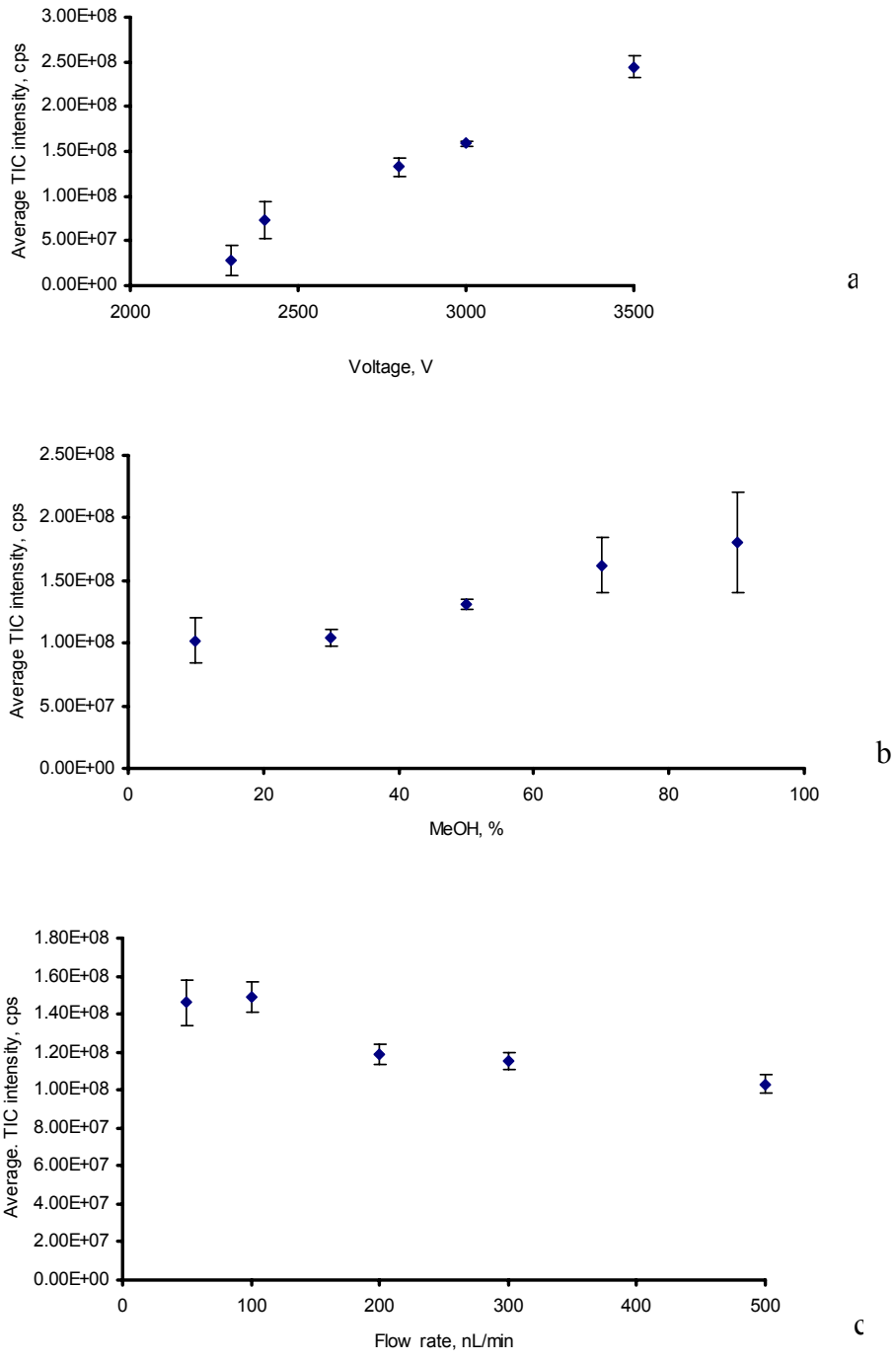

Figure 3.9. Impact of spray voltage, solvent composition and flow rate on electrospray performance using a PSF membrane assisted emitter with a 1 μM jeffamine solution. (a) TIC intensities at different spray voltages with 1:1 (v/v MeOH/water) and 500 nL/min flow rate. (b) TIC intensities with different methanol compositions at a 500 nL/min flow rate and 2.8 kV spray voltage. (c) TIC intensities at different flow rates with 1:1 (v/v) MeOH/water solution and 2.8 kV spray voltage.

Although, with the aid of a hydrophobic porous membrane, electrospray from higher aqueous solution became feasible, ion suppression resulted in reduced sensitivity when the organic component was lower than 10%. Different compositions of acetonitrile in water showed a similar trend to that of methanol (data not shown). Utilizing a PSF membrane assisted emitter at 2.8 kV spray voltage with 50% methanol solution, stable electrospray was easily obtained at flow rates ranging from 50 nL/min to 500 nL/min (Figure 3.9c), which was impossible for an open tubular emitter (such as 75 μm o.d.) at less than 500 nL/min flow rates.

Further studies to examine the correlation between membrane pore sizes and sensitivity were conducted over the same flow rate range using emitters fabricated with commercial PC membranes. The TIC intensity can be used for the direct comparison of sensitivities because the TIC signals were generated from the same amount of analytes. This is based on the assumption that electrospray is generated with the same ion transfer and ionization efficiency. A comparison of electrospray performance from three emitters bonded with commercial polycarbonate membranes was conducted using a solution of 1 μM jeffamine in 70% methanol at 500 nL/min flow rate and 2.8 kV spray voltage. These membranes contain well defined and distributed pores with sizes of 0.2 μm, 1.0 μm and 5.0 μm, respectively. For each emitter, five replicates were tested for the comparison (Table 3.1). As shown in table 3.1, the emitter with a 0.2 μm pore sized membrane gave a slightly higher TIC intensity than that of the other two. The TIC intensities for emitters with 1.00 μm and 5.00 μm pore sized membranes were not statistically different. The stability of the electrospray signals is all less than 6% RSD. However, no obvious

correlation was found between the size of the pores and the sensitivity of the detection. Even though good electrospray performance was demonstrated from emitters with different pore sized membranes, it is practical to use the smaller pore sized membrane for the fabrication since it is more robust and more facile to manipulate.

Table 3.1. Comparison of electrospray performances from emitters with different pore sized membranes

Emitter ID	Pore sizes	Trial 1	Trial 2	Trial 3	Trial 4	Trial 5	Average
Emitter 1	**0.2 μm**						
Mean TIC, cps		2.13E+08	1.98E+08	1.91E+08	1.83E+08	1.83E+08	1.94E+08
SD, cps		7.21E+06	7.04E+06	9.01E+06	7.84E+06	7.88E+06	7.80E+06
RSD, %		3.4	3.6	4.7	4.3	4.3	4.0
Emitter 2	**1.0 μm**						
Mean TIC, cps		1.17E+08	1.12E+08	1.20E+08	1.17E+08	1.22E+08	1.18E+08
SD, cps		6.91E+06	6.37E+06	5.93E+06	6.79E+06	6.78E+06	6.56E+06
RSD, %		5.9	5.7	4.9	5.8	5.5	5.6
Emitter 3	**5.0 μm**						
Mean TIC, cps		1.21E+08	1.24E+08	1.17E+08	1.41E+08	1.30E+08	1.27E+08
SD, cps		3.23E+06	2.69E+06	4.15E+06	3.76E+06	3.52E+06	3.47E+06
RSD, %		2.7	2.2	3.5	2.7	2.7	2.8

The reproducibility of the fabrication of porous polymer membrane assisted emitters was demonstrated by making five emitters bonded with polycarbonate membranes bearing 1.0 μm sized pores. The RSD of the average TIC intensities between the five membrane assisted emitters is about 11% as shown in Figure 3.10. Highly

accurate skills are required for applying glue onto capillary exits under a microscope in order to control a good reproducibility for the fabrication of this type of emitter.

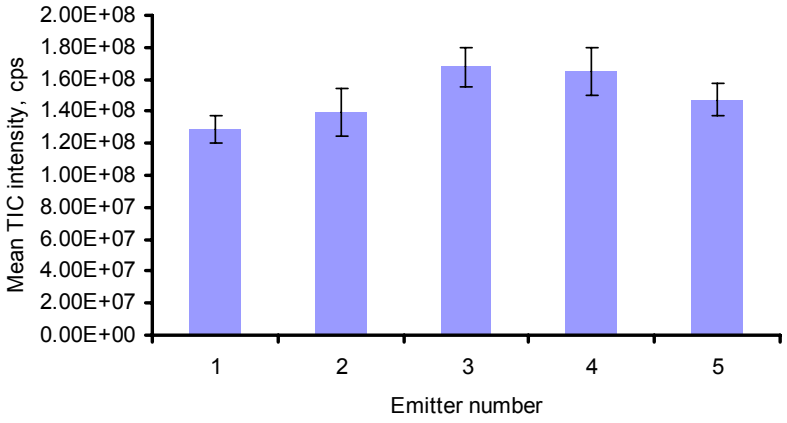

Figure 3.10. Reproducibility for five different membrane assisted emitters, TIC intensity was acquired with 1 μM jeffamine in 70% MeOH at 500 nL/min, 2.8 kV spray voltage, emitters were fabricated by polycarbonate membrane with 1.0 μm sized pores.

3.3.3 Electrospray from a membrane assisted microchip

Preliminary experiments were conducted to investigate the electrospray performance of a chip-based membrane bonded emitter. Electrospray performance from emitters with an open chip channel and a membrane bonded chip channel were compared by infusing a solution of 1 μM jeffamine in 70% methanol at a 300 nL/min flow rate. An electrical voltage of 4.8 kV was applied through a metal union right connected in front of the microchip. TIC intensities increased in about 5 - 7 fold from a membrane assisted chip-based emitter than that of from an open chip channel as shown in Figure 3.11. The variation of electrospray signals reduced from 25% to about 5% of RSD. This experiment demonstrated that by simply gluing a piece of porous membrane onto the exit aperture of

a PC microchip, a porous membrane assisted microchip can be coupled to a mass spectrometer as an interface for nano-electrospray.

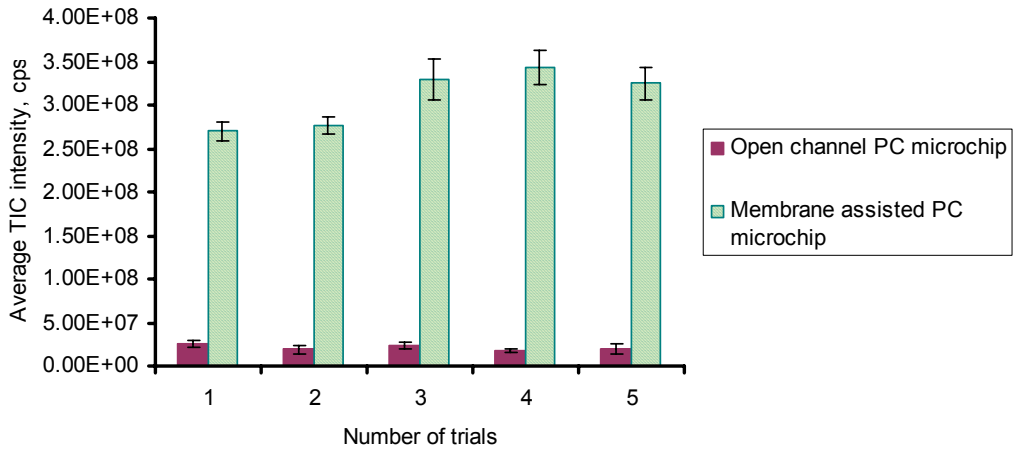

Figure 3.11. Comparison of electrospray sensitivity and stability between a membrane assisted microchip and an open chip channel by infusing 1 μM jeffamine in 70% methanol at 300 nL/min flow rate and 4.8 kV spray voltage.

3.4 Summary

A novel method was introduced to fabricate multiple path electrospray emitters by adhering a piece of porous polymer membrane onto either a fused-silica capillary or a plastic microfluidic chip. Both PSF and PC membranes contain well defined pores to generate multiple paths for electrospray. Emitters with membranes containing pores at different sizes from 0.2 μm to 5.0 μm all demonstrated the improved electrospray performances. The S/N ratio for the 482.4 m/z peak of jeffamine was increased from 6 to 34 for a membrane assisted capillary emitter compared to that of an open tubular emitter. No direct correlation between the pore size and the sensitivity of detection was found.

Reproducible electrospray signals were obtained from five capillary emitters bonded with PC membranes. However, the robustness of membrane assisted emitters is not as good as that of the roughened emitters. The preliminary experiment also demonstrated that TIC intensity was increased by 5 to 7 fold and variation of electrospray signals was reduced from 25% to 5% RSD when comparing a membrane bonded PC microchip to that of an open channel PC microchip. This method provided an alternative for the fabrication of a nano-ESI emitter with more defined multiple electrospray paths/channels.

3.5 References

(1) Koerner, T.; Oleschuk, R. D. *Rapid Communications in Mass Spectrometry* **2005**, *19*, 3279-3286.

(2) Koerner, T.; Turck, K.; Brown, L.; Oleschuk, R. D. *Analytical Chemistry* **2004**, *76*, 6456-6460.

(3) Koerner, T.; Xie, R.; Sheng, F.; Oleschuk, R. *Analytical Chemistry* **2007**, *79*, 3312-3319.Yamashita, M.; Fenn, J. B. *Iyo Masu Kenkyukai Koenshu* **1984**, *9*, 203-206.

(4) Rulison, A. J.; Flagan, R. C. *Review of Scientific Instruments* **1993**, *64*, 683-686.

(5) Hsueh, T.-H.; Huang, H.-W.; Kao, C.-C.; Chang, Y.-H.; Ou-Yang, M.-C.; Kuo, H.-C.; Wang, S.-C. *Japanese Journal of Applied Physics, Part 1: Regular Papers, Brief Communications & Review Papers* **2005**, *44*, 2661-2663.

(6) Tang, K.; Lin, Y.; Matson, D. W.; Kim, T.; Smith, R. D. *Analytical Chemistry* **2001**, *73*, 1658-1663.

(7) Bocanegra, R.; Galan, D.; Marquez, M.; Loscertales, I. G.; Barrero, A. *Journal of Aerosol Science* **2005**, *36*, 1387-1399.

(8) Lee, S. S. H.; Douma, M.; Koerner, T.; Oleschuk, R. D. *Rapid Communications in Mass Spectrometry* **2005**, *19*, 2671-2680.

(9) Oleschuk, R. D.; Shultz-Lockyear, L. L.; Ning, Y.; Harrison, D. J. *Analytical Chemistry* **2000**, *72*, 585-590.

(10) Brown, L.; Koerner, T.; Horton, J. H.; Oleschuk, R. D. *Lab on a Chip* **2006**, *6*, 66-73.

(11) Dahlin, A. P.; Bergstroem, S. K.; Andren, P. E.; Markides, K. E.; Bergquist, J. *Analytical Chemistry* **2005**, *77*, 5356-5363.

(12) Gobry, V.; Van Oostrum, J.; Martinelli, M.; Rohner, T. C.; Reymond, F.; Rossier, J. S.; Girault, H. H. *Proteomics* **2002**, *2*, 405-412.

(13) Tojo, H.; (Japan). Application: WO, 2004, pp 36 pp.

(14) Wang, Y.-X.; Cooper, J. W.; Lee, C. S.; DeVoe, D. L. *Lab on a Chip* **2004**, *4*, 363-367.

(15) www.sterlitech.com/products/membranes/polycarbonate/PCTEMembrane.htm

(16) Yan, X.; Liu, G.; Dickey, M.; Willson, C. G. *Polymer* **2004**, *45*, 8469-8474.

(17) Lee, S.B.; Mitchell, D.T.; Trofin, L.; Nevanen, T.K.; Martin, C.R.; *Science* **2002**,296,2198.

(18) Cabodi, M.; Turner, S.W.P.; Craighead, H.G.; *Analytical Chemistry* **2002**,74,5169.

(19) Grayson, R.C.R.; Choi, I.S.; Tyler, B.M.; Wang, P.P.; Brem, H., Cima, M.J.; Langer, R. *Natural Material* **2003**,2,767.

(20) Bedair, M. F.; Oleschuk, R. D. *Analytical Chemistry* **2006**, *78*, 1130-1138.

(21) Brennen, R. A.; Yin, H.; Killeen, K. P.; (Agilent Technologies, Inc., USA). Application: DE, 2002, pp 24 pp.

(22) Griss, P.; Melin, J.; Sjoedahl, J.; Roeraade, J.; Stemme, G. *Journal of Micromechanics and Microengineering* **2002**, *12*, 682-687.

(23) Song, Y.; Quan, Z.; Liu, Y.-M. *Rapid Communications in Mass Spectrometry* **2004**, *18*, 2818-2822.

Chapter 4

Multi-channel Nano-ESI Emitters Derived from Photonic Crystal Fibers

4.1 Overview

Multi-channel emitters have been found to be an advantageous approach to increase sensitivity by splitting larger flow rates associated with conventional ESI to flows in the nanoelectrospray regime.[1] While the available niche for multi-ESI in mass spectrometry is unquestionable, there have been relatively few multi-ESI platforms mentioned in the literature.[1-3] A multi-emitter array was developed where multiple tapered fused silica emitters were bundled through PEEK (poly ether ether ketone) tubing and positioned in a linear array. Multiplexed emitters have also been prepared using complex microfabrication techniques such as laser machining,[1,3] and photolithography/etching.[2] The use of multi-channel emitters has been found to significantly improve sensitivity as discussed in chapter 3. The sensitivity gain and the improved clogging resistance of multichannel emitters will undoubtedly benefit the "omics" (*e.g.* proteomics, metabolomics, glycomics) communities. However to supplant single tapered emitters, multi-channel emitters will need to be facilely produced, relatively inexpensive, and robust. Porous polymer membrane assisted multiple channel nano-ESI emitters did not fully satisfy these requirements.

In this chapter, a novel nanoelectrospray emitter is presented that uses a commercially available microstructured silica fiber (MSF) as a "shower head" to split the fluidic flow through its multiple channels and enhance sensitivity of electrospray. The

microstructured fibers are a relatively new class of silica optical fiber that confines light through the use of a microstructured cladding. MSF are commercially produced by stacking silica capillaries to a desired preform, followed by heating and pulling (a technique commonly referred to as stack and draw).[4] The micron-sized holes and pattern can be precisely controlled during the manufacturing process. However rather than guiding light, we demonstrate their application as multiple-channel nanoelectrospray emitters for mass spectrometry and utilize the independent channels as fluidic conduits. Two microstructured fibers possessing either 30 or 168 fluidic channels, each with a 4-5 μm diameter individual aperture emanating from a 340 μm outer diameter fiber, were used in this project for the electrospray investigation. The electrospray performance of the MSF emitter is compared directly to a commercially available tapered emitter. The MSF emitters generate stable electrospray at flow rates from 10 to 500 nL/min with a significant sensitivity gain at low nano flow rates (≤ 20 nL/min).

The silica-based MSF emitters were also modified with silylation reagents to improve their nanoelectrospray efficiency for highly aqueous solutions. With simple chemical modification of the MSF emitter exit using chlorotrimethylsilane (CTMS) or 3-(trimethyoxysily)propyl methacrylate (TMSPMA), the emitters can effectively electrospray up to 99.9% aqueous samples with striking stability and sensitivity. Superior emitter robustness (*i.e*. anti-clogging characteristics) is also demonstrated compared to a single-tip tapered emitter by the infusion of Hanks' solution (a balanced salt solution for cell biology).[3] Furthermore, the MSF emitter architecture obviates inter-emitter electric field gradients encountered with linear multi-emitter arrays.[2]

This study demonstrates that a microstructured photonic fiber can be used as a multi-channel nanoelectrospray emitter enabling not only superior sensitivity, but also increased robustness. In addition, the hydrophobic modified MSF emitters greatly improved electrospray efficiency of aqueous samples compared to a conventional tapered emitter. To this end, we believe that we have developed a nano-ESI emitter that improves upon the major drawbacks of single tapered emitters as well as satisfies the features required for a routine analytical device.

4.2. Experimental

4.2.1. Materials and Reagents

Methanol, toluene, glacial acetic acid and acetonitrile (HPLC grade) were purchased from Fisher Scientific (Ottawa, ON, Canada) and used without further purification. Formic acid (analytical reagent, 98%) was purchased from BDH Chemicals, (Toronto, ON Canada). Leucine enkephalin (synthetic acetate salt), chlorotrimethylsilane (CTMS), and 3-(trimethyoxysily)propyl methacrylate (TMSPMA) were from Aldrich (Oakville, ON, Canada). Deionized water (> 18 MΩ·cm) was obtained from a Milli-Q system (Millipore, Bedford, MA, USA).

The Hanks' solution was prepared by adding 0.8 g sodium chloride, 0.02 g calcium chloride, 0.02 g magnesium sulfate, 0.04 g potassium chloride, 0.01 g monobasic potassium phosphate, 0.127 g sodium bicarbonate, 0.01 g dibasic sodium phosphate, and 0.2 g glucose to sufficient Milli-Q water for a 100 mL final volume.[5]

The microstructured fibers (F-SM16 with 30 holes and F-SM20 with 168 holes) were obtained from Newport Corporation (Irvine, CA, USA), and the pulled-tip emitters (non-coated 5 μm internal tip diameter, PicoTip SilicaTip) were from New Objective (Woburn, MA, USA).

4.2.2. Chemical Modification of Microstructured Fibers

The MSF segments were cut to 5 cm in length using a fiber cleaver (FiTel, Furukawa Electric, Japan) to satisfy the length requirement of nanoelectrospray ion source. External polymer coating of MSF emitters was first removed physically or by soaking in toluene (Figure 4.1a and 4.1b show the emitters with partially removed coating). The end of the cleaved fiber without coating was inserted in a silylation reagent solution (20% (v/v) of CTMS or TMSPMA in toluene) overnight for modification. Then, the fibers were rinsed for ten minutes with an acetonitrile/water solution (80/20) using a syringe pump set at 500 nL/min.

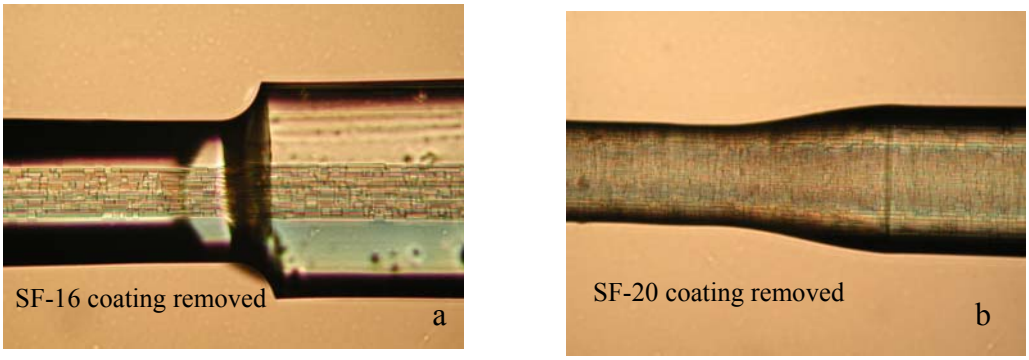

Figure 4.1. Images show partially removed coating from MSF emitters (a) SF-16 with 30 holes, (b) SF-20 with 168 holes.

4.2.3. Mass Spectrometry

Mass spectrometry instrumental setup was described in section 2.2.6 in Chapter 2. Briefly, a Micro-tee was used to connect a MSF emitter and the nano-pump. A MSF emitter was connected to one end of the Micro-tee with the other end of the Micro-tee connecting to a nano-pump through a transferring capillary. Spray voltages were also applied through a metal wire inserted into the liquid junction within the MicroTee. The micro-tee was then mounted on the x,y,z stage, then CCD cameras and the x-y-z stage were used to finely position the emitter. Evaluation of electrospray performance for the MSF emitters was conducted using this instrumental setup.

4.2.4. Offline Electrospray Imaging

Aqueous electrospray samples (99.9% water, 0.1% formic acid) were delivered through a MSF emitter using a 0.5 mL Hamilton syringe driven by an 11 Plus pump (Harvard Apparatus, Holliston, MA, USA). Electrospray was generated offline via an Upchurch MicroTee with a liquid junction electrode using an ESI potential applied with a Trisep^{TM}- 2100 high voltage module (Unimicro Technologies Inc. Pleasanton, CA, USA). A grounded metal plate was placed approximately 5 mm from the emitter. The resulting electrospray plumes were imaged using a Nikon Eclipse TE 2000-U microscope equipped with a direct visualization system, Q-Imaging, QICAM with Simple PCI software (Compix Inc. Imaging Systems, 705 Thomson Park Drive, PA, USA).

4.2.5. Scanning Electron Microscopy

The MSF emitters were mounted on an aluminum stub using copper conductive tape to facilitate imaging of the fiber cross section. SEM images were obtained using a Jeol JSM-840 (Tokyo, Japan) scanning electron microscope.

4.2.6. Emitter Robustness Evaluation

Hanks' solution was used to evaluate emitter's robustness to clogging. As illustrated in Figure 4.2, an emitter was connected first to a 63 cm long 150 μm i.d. fused silica capillary filled with a 5 μM leucine enkephalin solution, for establishing an initial stable TIC trace. This capillary was then connected through a micro-union to a 50 cm long 150 μm i.d. capillary filled with Hanks' solution, which was then connected to a nano-pump through a six-port valve and sample loop. Solutions were sequentially infused through emitters at 300 nL/min. The "time to clog" was used to ascertain the relative robustness of each emitter.

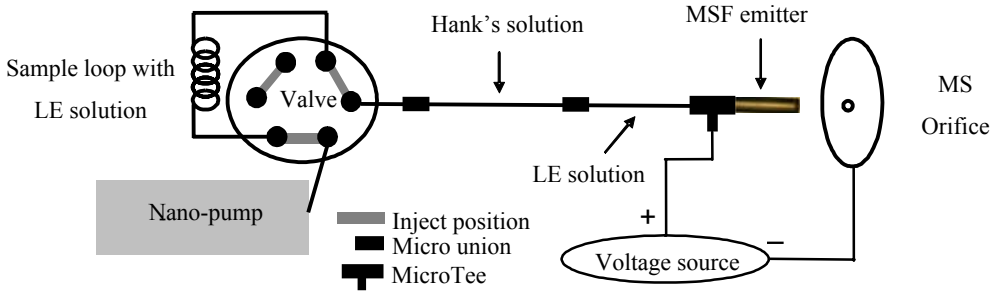

Figure 4.2. Setup for MSF emitter robustness evaluation.

4. 3. Results and Discussion

4.3.1. The architecture of MSF emitters

As an alternative, we have investigated microstructured photonic fibers as multi-channel emitters for nanoelectrospray. SEM images (Figure 4.3) show the cross sections of the two microstructured fibers investigated as emitters.

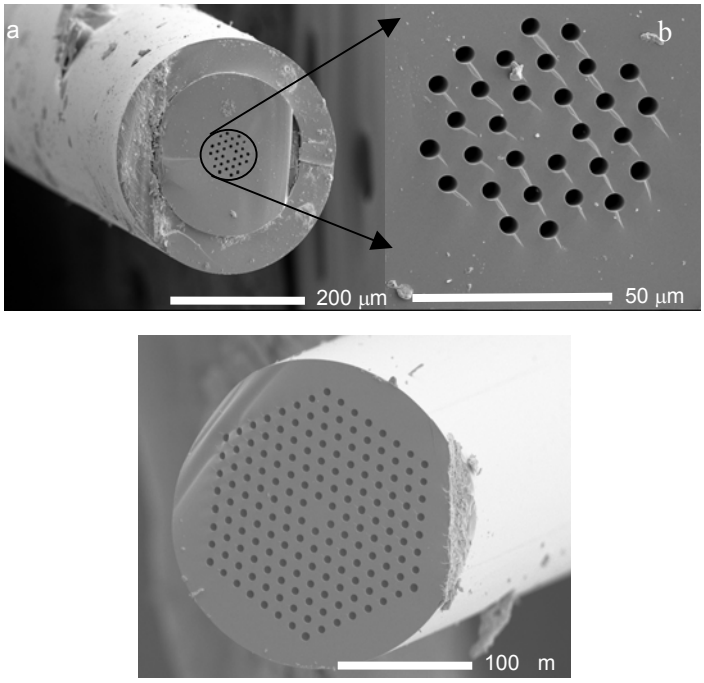

Figure 4.3. SEM images (a) and (b) cross section of a 30 orifice, 4-5 μm, microstructured fiber, at different magnification (c) Cross section of an alternative microstructured fiber with 168 orifices.

The example depicted in Figure 4.3a and 4.3b has 30 independent orifices, each 4-5 μm in diameter. Figure 4.3c shows another microstructured fiber with similarly sized holes, however the array is comprised of 168 independent orifices. The orifice dimensions (4-5 μm) are consistent with the typical aperture sizes of tapered emitters

used for flow rates as low as a few 10's of nL/min. From previous experiences developing non-tapered nanoelectrospray emitters,[6, 7] it was found that minimization of edge effects is crucial for good emitter performance. Several capillary cutting methods were employed, however a commercial fiber cleaver provided the best performance in terms of maintaining the integrity of the microstructured cladding.

4.3.2. Electrospray characteristics of unmodified MSF emitters

Initial testing of an unmodified MSF emitter (schematic drawing shown in Figure 4.4, insert) involved the infusion of a peptide, leucine enkephalin, dissolved in a standard ESI solution (50% water in acetonitrile (0.1% formic acid)).

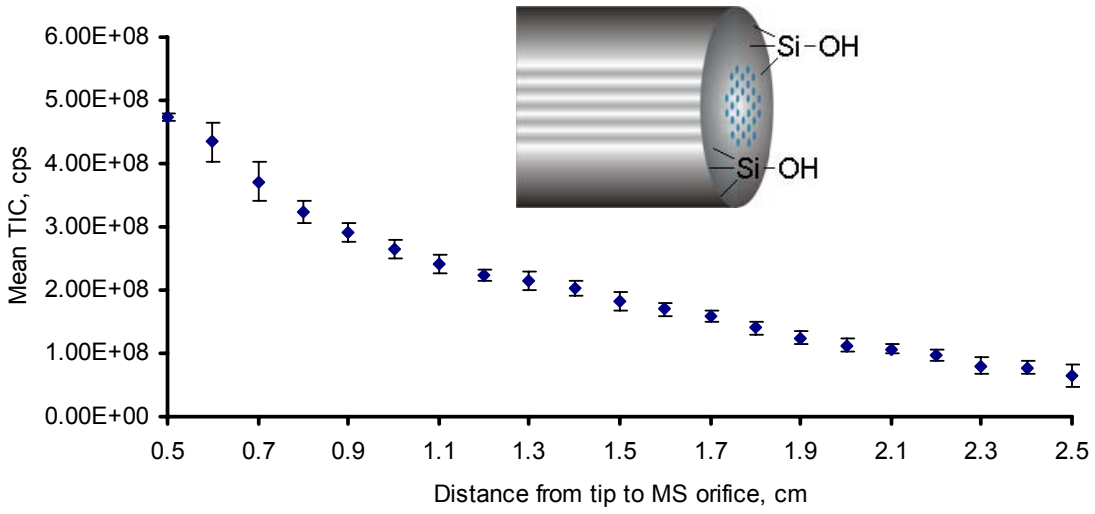

Figure 4.4. Electrospray characteristics for different distances from emitter tip to MS orifice from unmodified MSF emitters obtained from infusing 1.0 μM leucine enkephalin (1:1, v/v, water/acetonitrile (0.1% formic acid)) at 500 nL/min flow rate.

At a flow rate of 500 nL/min, the observed backpressure was below 65 psi for both the 30 and 168-hole emitters. As shown in Figure 4.4, the working distance from the exit apertures of the MSF emitters to the MS orifice, was found to be between 0.5 and 2.5 cm. The TIC intensity was reduced gradually but high stability was maintained over a large range of relative distances. A greater operational distance enables integration of online sample preparation strategies such as desalting and preconcentration, with reduced risk of ion source contamination. However, the MSF emitter seems quite sensitive toward changes in spray voltages from the fluctuation in electrospray stability shown in Figure 4.5a. The detection sensitivity increased gradually upon increasing spray voltage (Figure 4.5b).

Figure 4.6a shows the TIC traces generated using an unmodified MSF emitter with 30 orifices at different flow rates. Stable electrospray signals were obtained with RSD < 10% over a wide range of flow rates. As a comparison, Figure 4.6b shows the same experiment conducted with a standard tapered nanoelectrospray emitter. The TIC intensity was increased greatly for the MSF emitter at lower flow rates compared to that from a tapered emitter.

The 340 μm outer diameter of the MSF enabled all the same capillary tubing transfer lines and MS interface parameters to be employed for both the tapered and MSF emitter thus providing a true side by side comparison. Both emitters produce similar ion current stabilities and demonstrate the sensitivity enhancements characteristic of nanoelectrospray. A direct sensitivity comparison shows that the MSF emitter is more efficient and generates higher ion fluxes per mole of analyte consumed, as the flow rate is

decreased (Figure 4.6c). The increased sensitivity is most marked at a flow rate of 10 nL/min where a roughly two fold increase in ion current is observed.

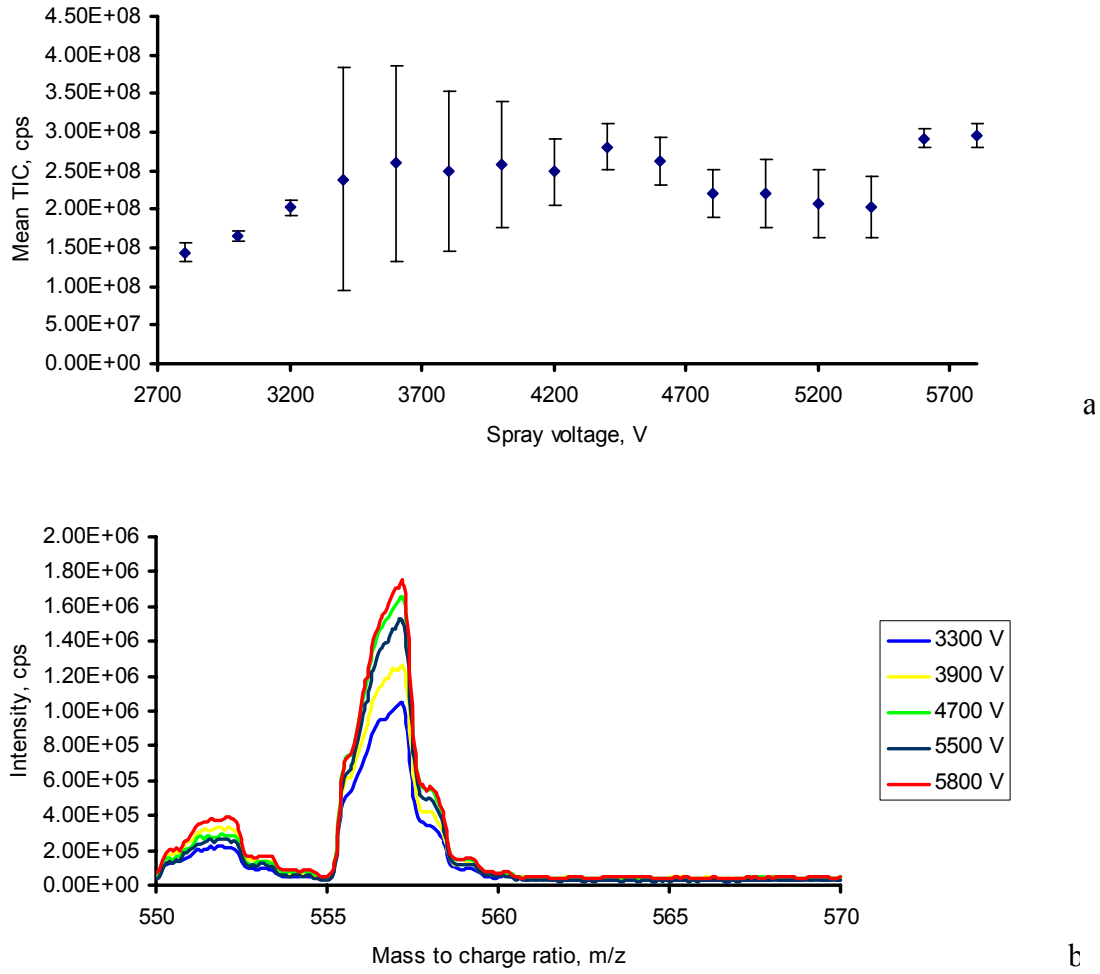

Figure 4.5. Electrospray characteristics of unmodified MSF emitters obtained from infusing 1.0 µM leucine enkephalin (1:1, v/v, water/acetonitrile (0.1% formic acid)) at: (a) different spray voltages; (b) extracted mass spectrum from TIC trace from 4.5a.

Although a sensitivity gain of two was achieved with the unmodified MSF emitter at low flow rates, the gain was not as substantial as theoretically predicted. It has been

shown (equation 4.1) that the increase in electrospray ion current is related to the square root of the number of ESI emitters.[8]

$$I_{total} = \sqrt{n} I_s \qquad (4.1)$$

Where: I_{total} is the total multielectrospray ion current

n is the number of emitters

I_s is the ion current of an individual emitter

In this case, if 30 individual electrospray plumes were generated, an ion current increase of approximately 5.5 (*i.e.* $\sqrt{30}$) would be expected. However, the largest ion current increase obtained is ≈ 2 at 10 nL/min. In addition, the signal enhancement is reduced at higher flow rates suggesting that the MSF emitter is operating as a single emitter in these flow regions with 50% methanol. The relatively poor signal enhancement is attributed to the coalescence of flows into a single or few Taylor cones at the MSF emitter/air interface. The surface of silica is relatively hydrophilic (water contact angle 50^{o}) and as solvent is emitted from the exit apertures (spaced 7 microns apart) it will likely spread across the entire emitter surface. Consequently, individual plumes will result at low flow rates only. Once the flow is substantial enough a single Taylor cone will predominate.

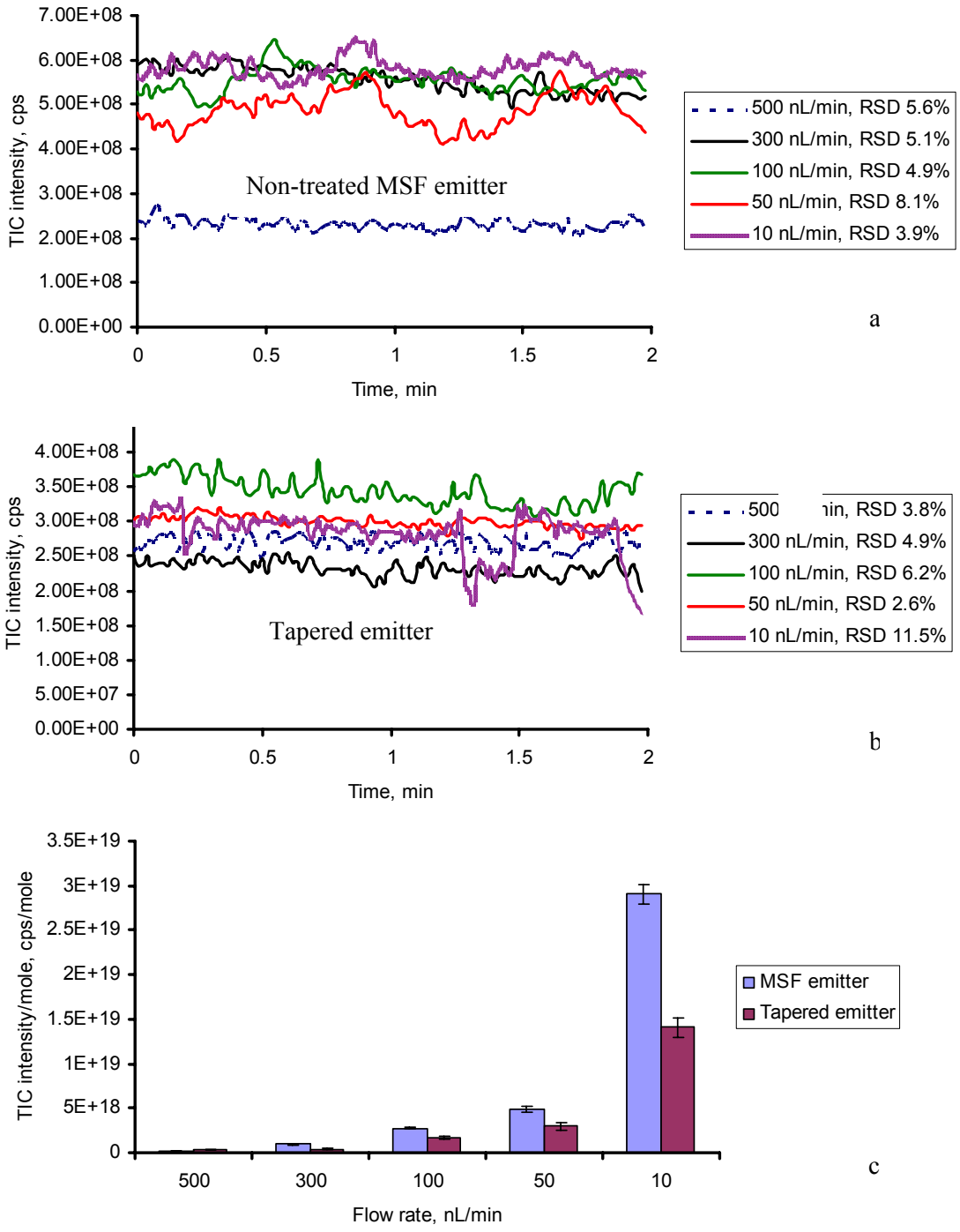

Figure 4.6. MS data obtained from infusing 1.0 µM leucine enkephalin (1:1, v/v, water/acetonitrile (0.1% formic acid)) at different flow rates. a) Silica surface of the unmodified MSF emitter, b) Results from a tapered emitter with a 5 µm aperture, c) Bar graph showing increases in sensitivity as the flow rate is reduced for both MSF and tapered emitters.

4.3.3. Sensitivity gain from hydrophobic modified MSF emitters

The MSF emitter is composed of silica and can be modified with a number of silylation reagents to alter its wetting characteristics to improve the ionization efficiency when spraying highly aqueous solutions. Electrospraying aqueous samples is important for reversed phase LC separation gradients which involve the transition from a highly aqueous solvent to one of higher elutropic strength. Furthermore, in structural proteomics, some samples can not tolerate significant organic solvent content without denaturation, hence necessitating working in aqueous environments.

Chlorotrimethylsilane (CTMS) and 3-(trimethyoxysily)propyl methacrylate (TMSPMA) are both effective at considerably altering the surface wetting characteristics of glass. Contact angle experiments conducted in our laboratory have shown that the water contact angle is increased from 50^{o} to 127^{o} for CTMS derivatized fused silica.[9] To examine the effects of electrospray using a hydrophobic emitter, the exit surfaces of the MSF emitters were modified using CTMS and TMSPMA (schematic drawing shown in Figure 4.7a and 4.7b respectively). Aqueous solutions exhibit a higher contact angle on hydrophobic surfaces relative to that of mixed organic/aqueous compositions. Aqueous samples (i.e. 89.9% and 99.9% H_2O/0.1% formic acid) were used for emitter evaluation to maximize the contact angle of the liquid emanating from the MSF and prevent the exit aperture of the emitter from being wetted. Consequently highly aqueous solutions should promote the formation of multiple electrospray plumes emanating from the multiple channels of MSF emitter, thereby increasing sensitivity.

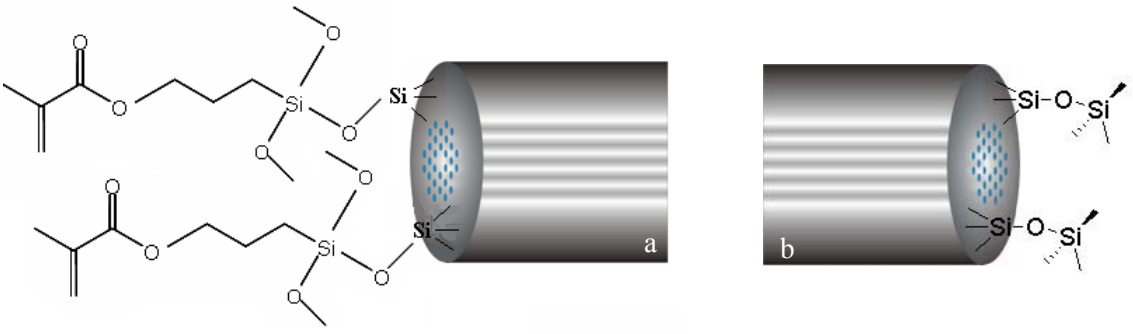

TMSPMA -treated MSF emitter CTMS-treated MSF emitter

Figure 4.7. Schematic diagram showing the CTMS (a) and TMSPMA (b) modified MSF emitters, respectively.

Figure 4.8a summarizes the results obtained for a CTMS derivatized MSF emitter while infusing 1.0 μM leucine enkephalin in 89.9% water (0.1 % formic acid). The modified MSF emitter sprays aqueous samples with remarkable ease and produces stable total ion currents at flow rates ranging from 10-500 nL/min (RSD's 2-11%). Highly aqueous solutions are notoriously difficult to spray with hydrophilic silica tips owing to both the high surface tension and low volatility of water. As shown in Figure 4.7d, the tapered emitter (5μm aperture) generates relatively unstable TIC traces (RSD's 3-68%) over the same flow rate range.

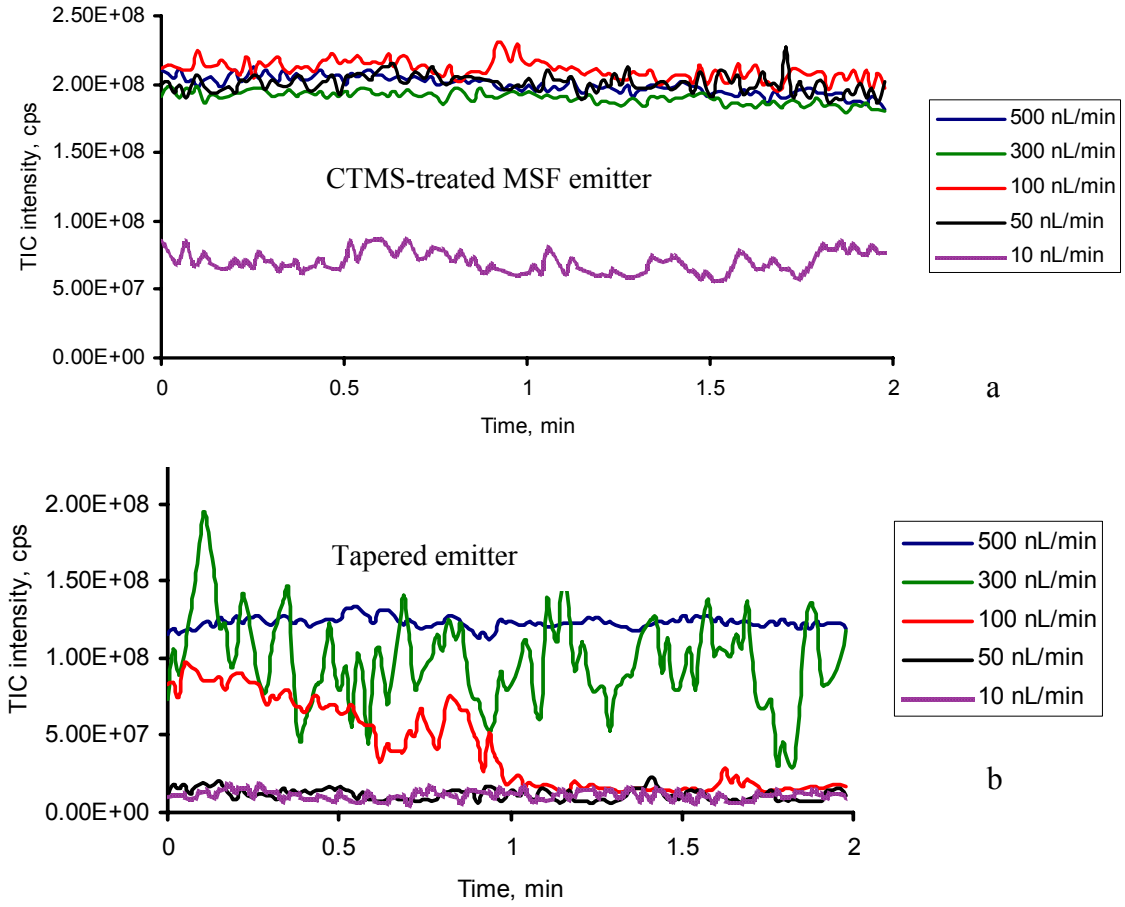

Figure 4.8. Overlaid TIC traces obtained from1.0 µM of leucine enkephalin (in 89.9 % water, 0.1% formic acid) using a CTMS modified MSF emitter (a) and a tapered emitter (b) at 500-10 nL/min flow rates.

Similar to the unmodified MSF emitter (Figure 4.6c), an increase in sensitivity is achieved with the derivatized MSF emitters as well (shown in Figure 4.9), and the sensitivity gains are more dramatic at lower flow rates. Indeed, for a CTMS modified MSF emitter, the increase in sensitivity between the MSF emitter and the single emitter is 6.5 ± 0.2 times when spraying an 89.9% aqueous solution at 10 nL/min (Figure 4.9); while the sensitivity gain is 4.5 ± 0.2 times when using the same emitter to spray a 99.9% aqueous solution at 20 nL/min. Both results are consistent with the theoretical prediction

(≈ 5.5) based on equation 1 that ion count is proportional to the square root of the number of emitters. The relatively greater sensitivity gain when spraying a 89.9% aqueous solution than when spraying a 99.9% aqueous solution may be attributed to the increased desolvation efficiency with higher organic composition.

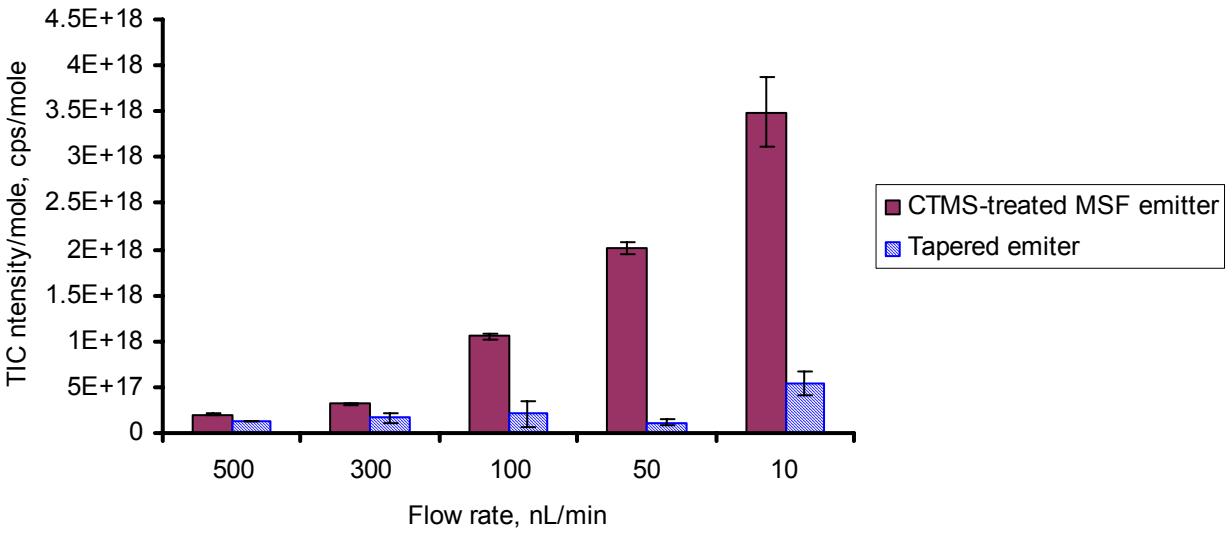

Figure 4.9. Nanoelectrospray performance obtained from1.0 μM of leucine enkephalin (in 89.9 % water, 0.1% formic acid) using a CTMS modified MSF and a tapered emitter at 500-10 nL/min flow rates.

For a 99.9% aqueous solution, the deviation from theoretical prediction may be due to reduced ion transmission and/or coalescing of Taylor cones. Reduced ion transmission efficiency may result from the larger spray "cone" emanating from the MSF emitter exit. For a tapered emitter, the nanoESI plume is generated from a single 5 μm orifice, whereas the MSF emitter produces a spray from multiple channels (30 channels, each 5 μm in diameter with 7 μm gaps between each) representing a total emitting

surface diameter of 60 µm. The larger ionization plume may affect the MS sampling efficiency resulting in lower ion currents.

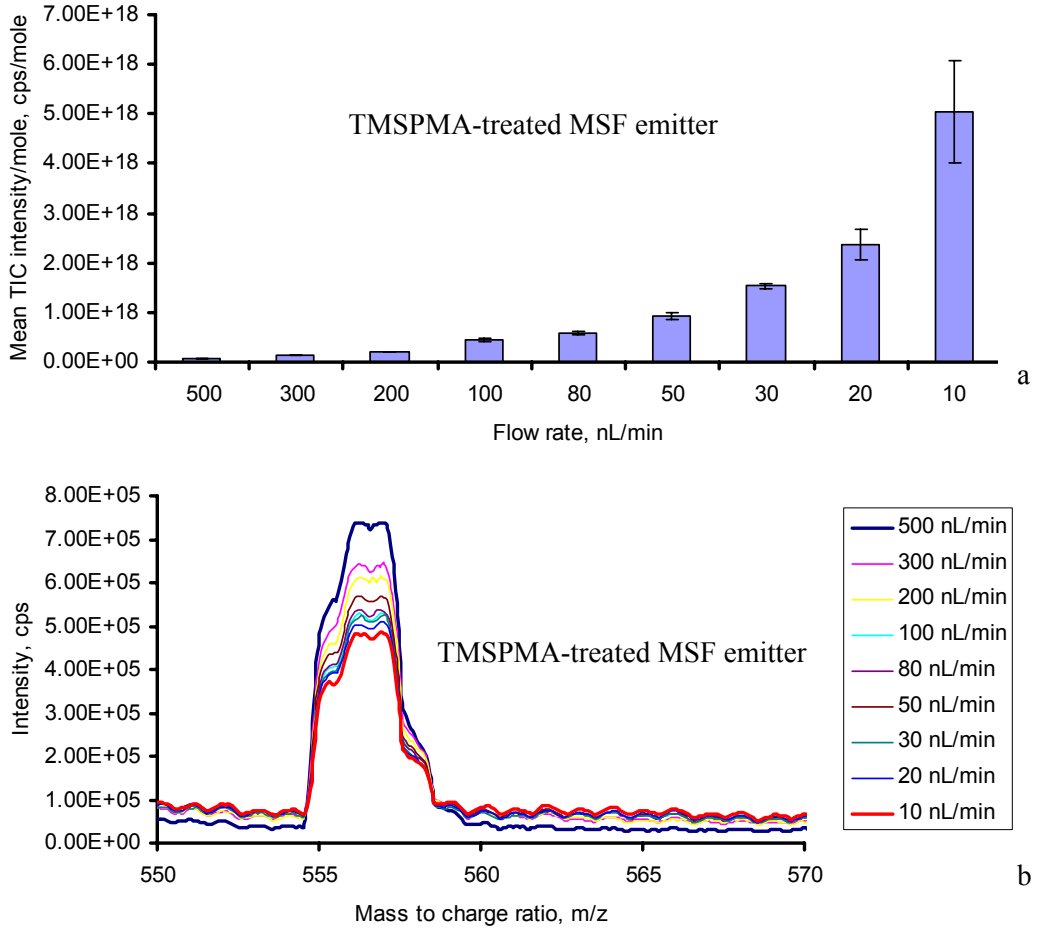

Figure 4.10. Nanoelectrospray performance obtained from1.0 µM of leucine enkephalin (in 89.9 % water, 0.1% formic acid) using a TMSPMA modified MSF emitter at 500-10 nL/min flow rates. (a) Increased sensitivity at lower flow rate demonstrated from a TMSPMA treated MSF emitter, (b) Overlaid mass spectrum showing leucine enkephalin peaks at different flow rates.

Kelly *et al.*[2] have demonstrated that a multiplexed emitter requires the use of a multi MS inlet for best ion transmission. It is therefore envisioned that MSF emitters used

in conjunction with an electrodynamic ion funnel would further increase sensitivity. Alternatively, the observed difference from the theoretical prediction may be attributed to the coalescing of some of the Taylor cones on the emitting surface.

Improved performance was also demonstrated from TMSPMA modified MSF emitter as shown in Figure 4.10a and 4.10b.

4.3.4. Multiple electrospray from MSF emitters

The consistency of the calculated sensitivity gain with the theoretical prediction as discussed above suggests that multiple electrospray may occur from an individual Taylor cone at lower nano flow rates. Further evidence for the multiplicity of MSF emitters is confirmed from the offline electrospray images obtained when spraying 99.9% aqueous solution at different flow rates. An offline electrospray image clearly shows that at relatively high flow rates such as 300 nL/min a single Taylor cone is observed (Figure 4.11a), however a mist (Figure 4.11b) emanates from the exit apertures of the CTMS derivatized MSF emitter if the flow rate is lowered (*e.g.* 25 nL/min). However, imaging analysis has so far not enabled the clear characterization of individual Taylor cones on the emitting surface as we expected. The observations are consistent with the experimental results and sensitivity gain calculations. These images also support the assumption that flow from the individual pores may coalesce at higher flow rates, while at lower flow rates the individual pores act as individual sprayers. For an emitter with 168 channels at 20 nL/min total flow rate, it would yield about 150 pL/min flow rate from each individual channel. Similar behavior has been reported with porous polymer

monolith emitters and entrapped microsphere emitters, however the resulting "hole" patterns were not as well defined.[10]

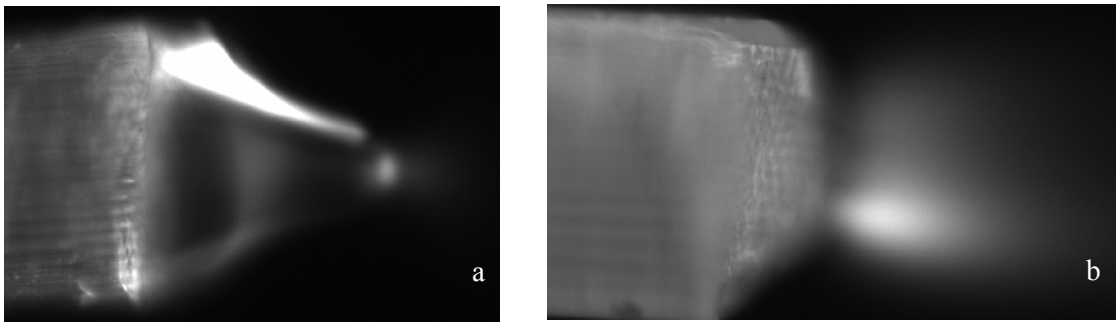

Figure 4.11. Electrospray characteristics of a CTMS modified Multiple channel MSF emitter at different flow rates. (a) Single Taylor cone at 300 nL/min, b) A plume of mist at 25 nL/min.

Based on the multiple electrospray theory, an obvious approach to further enhance sensitivity is to increase the number of orifices emanating from the MSF. A 168-hole MSF emitter (similar hole size and spacing) was used for comparison with a single-tip tapered emitter and a 30-hole MSF emitter. Not surprisingly, infusion of a 1 μM leucine enkephalin solution (89.9% water in acetonitrile (0.1% formic acid)) through a 168-hole CTMS treated emitter, resulted in an increase in sensitivity as compared to a conventional emitter or to the 30-hole MSF as shown in the TIC traces (Figure 4.12). The experimentally determined sensitivity gains from the 30 and 168-hole MSF show the trend in agreement with root n as predicted by 5.5 and 13 times increase, respectively. However, the TIC trace obtained from the 168-hole CTMS derivatized MSF emitter was

found to be less stable (RSD 13%) compared to the 30-hole CTMS derivatized MSF emitter, especially when the flow rate was reduced below 100 nL/min.

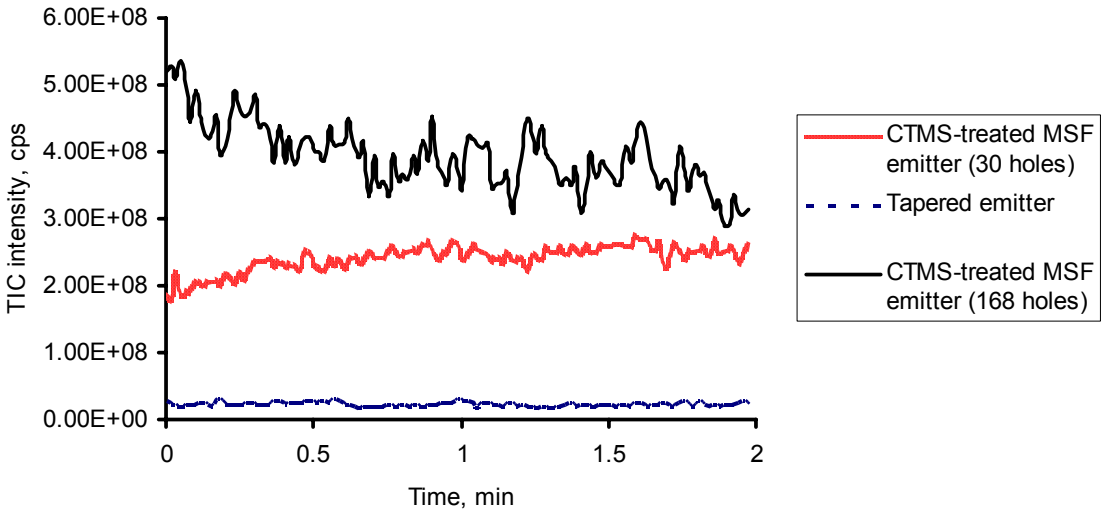

Figure 4.12. Comparison of TIC traces generated with a 168 orifice hydrophobic MSF emitter, a 30 orifice hydrophobic MSF emitter, and a tapered emitter, obtained by infusion of 1 µM leucine enkephalin at a 100 nL/min flow rate (9:1, *v/v,* water/acetonitrile (0.1% formic acid)).

4.3.5. Robustness evaluation

Multiple fluidic channels make MSF emitters more resistant to clogging. The robustness and clogging resistance of the MSF emitters was ascertained by infusing Hanks' solution, a highly concentrated nonvolatile salt mixture (see experimental section 4.2.1). A commercial tapered emitter with a 5 µm tip aperture was used for comparison. The leucine enkephalin and Hanks' solutions were sequentially infused through each of the emitters at 300 nL/min using the setup shown schematically in Figure 4.2. Both induced back pressure (time to clog) and the resulting mass spectra were monitored to gauge the relative robustness of each emitter type.

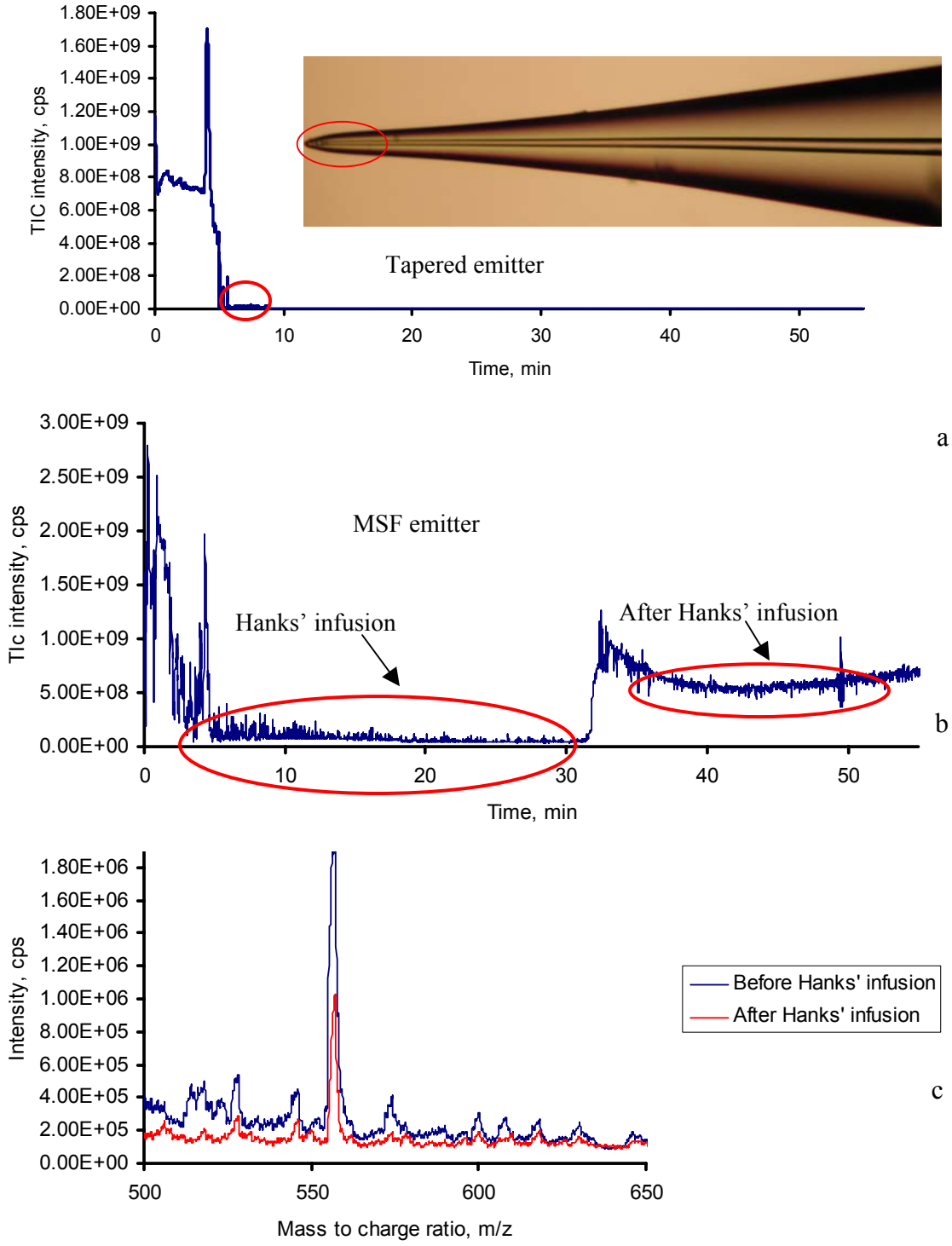

Figure 4.13. Emitter robustness test involves the infusion of Hanks' buffer. (a) TIC trace of a tapered emitter (inset, photomicrograph of the clogged tapered emitter), (b) TIC trace of a MSF emitter; (c) Detected leucine enkephalin peaks from the MSF emitter before and after Hanks' infusion.

With the continuous infusion of Hanks' solution, the tapered emitter experienced a sharp rise in back pressure (> 2000 psi) and was completely clogged in less than 4 minutes (Figure 4.13a inset) resulting in a complete loss of ion intensity. In contrast, the MSF emitter not only survived the clogging test after constantly infusing the Hanks' solution for 25 minutes (Figure 4.13b), but also demonstrated the capability to resume its electrospray performance, indicated by the recovered analyte signal (Figure 4.13c). Although this is an extreme case, it demonstrates the relative robustness of the MSF emitter to clogging.

4.4. Summary

Microstructured fibers have been demonstrated as efficient nanoelectrospray emitters. The sensitivity of these fiber emitters appears to be better comparing to that of porous membrane assisted emitters and roughened emitters. MSF emitters are easily adapted to conventional nanoESI instrumentation due to their dimensional similarity with commonly used capillary tubing diameters. The MSF emitters are shown to be more sensitive using standard electrospray conditions; however, more significant sensitivity enhancements and stabilities are evident when spraying 100% aqueous solutions at flow rates less than 100 nL/minute.

In addition, the MSF emitters are both highly resistant to clogging and compatible with large flow rate regimes with minimal backpressure. Moreover, the MSF emitter's architecture obviates the inter-emitter electric field gradients encountered with linear multi-emitter arrays. The MSF emitters can be used with standard nanoESI-MS

interfaces, however further gains in sensitivity may be possible with improved ion focusing. The MSF utilized were designed and optimized to offer reduced optical loss for photonic applications and not for the delivery of fluids. Consequently, further sensitivity enhancements will be possible through modeling and optimization of the hole size, shape, number and spacing at the exit aperture of a capillary or microfluidic device. The combination of improved nanoESI robustness and enhanced sensitivity will make multi-ESI emitters more attractive for both "omic" practitioners and those that currently shun nanoelectrospray because of robustness concerns.

4.5. References

(1) Kelly, R. T.; Page, J. S.; Tang, K.; Smith, R. D. *Anal. Chem.* **2007,** *79*, 4192-4198.

(2) Kim, W.; Guo, M.; Yang, P.; Wang, D. *Anal. Chem.* **2007,** *79*, 3703-3707.

(3) Kelly, R. T.; Page, J. S.; Zhao, R.; Qian, W.-J.; Mottaz, H. M.; Tang, K.; Smith, R. D. *Anal. Chem.* **2008,** *80*, 143-149.

(4) Russell, P. *Science* **2003,** *299*, 358-362.

(5) Humason, G. L., In *Animal Tissue Techniques*, 4th ed.; W.H. Freeman and Co.: San Francisco, 1979; pp 546.

(6) Bedair, M. F.; Oleschuk, R. D. *Anal. Chem.* **2006,** *78*, 1130-1138.

(7) Koerner, T.; Xie, R.; Sheng, F.; Oleschuk, R. *Anal. Chem.* **2007,** *79*, 3312-3319.

(8) Tang, K.; Lin, Y.; Matson, D. W.; Kim, T.; Smith, R. D. *Anal. Chem.* **2001,** *73*, 1658-1663.

(9) Gibson, G. G. T.; Mugo, S. M.; Oleschuk, R. D. *Polymer* **2008**, In press.

(10) Koerner, T.; Turck, K.; Brown, L.; Oleschuk, R. D. *Anal. Chem.* **2004,** *76*, 6456-6460.

Chapter 5

Integrated Nano-ESI Emitters with ODS Microspheres

5.1. Overview

Nano-ESI emitters with either a larger aperture or multiple channels were developed to successfully cope with problems associated with tapered emitters such as frequent clogging, large flow resistance, limited flow rate range, and difficulty in spraying highly aqueous solutions, as discussed in chapters 2, 3 and 4. However, these emitters feature only a single function as an electrospray ion source. In the case of online sample preparation (desalting, pre-concentration, and separation) before conducting a MS analysis (such as using nano-LC/nano-ESI-MS), these types of hollow emitters need to be coupled with reverse phase LC columns in a hyphenated fashion.[1] Multiple connections in addition to the hollow emitter after the separation column in a hyphenated configuration add more dead volume leading to increased band broadening. One of the trends for the development of advanced nano-ESI emitters is to integrate multiple functions onto a single emitter by filling the emitter exit with reverse phase materials.[2]

In general, integrated nano-ESI emitters can be fabricated by forming porous polymer monolith, packing chromatographic microspheres against a frit, or entrapping microspheres in one end of a fused silica capillary channel.[3-6] In this chapter, integrated emitters were fabricated by packing ODS spheres against a PPM frit, and entrapping ODS spheres by photo initiated polymerization to yield a frit-free emitter. Entrapping ODS beads yields a frit-free emitter with spheres fixed in a desirable position, which

largely enhances the robustness and the reproducibility of the integrated emitters with only a moderate induced back pressure.

The objectives of this chapter are to characterize an entrapped ODS emitter for its utility as a nanoelectrospray ion source for routine analysis, and to evaluate the potential of using integrated emitters for online sample preparation (*e.g.* preconcentration). Most fundamental studies on how operational factors affect nanoelectrospray behavior have been conducted using only tapered emitters due to their dominance in nano-ESI.[7-10] However, we have seen earlier in this thesis that non-tapered emitters have shown potential to share the same merits as tapered emitters while overcoming tapered emitter drawbacks.[7, 11] Unlike a tapered emitter, these non-tapered emitters were fabricated without tapering either internal or external diameters (75 μm i.d. and 360 μm o.d.). Since a non-tapered emitter has dramatically different architecture compared to a conventional tapered emitter, the operational parameters established based on the understanding and characterization of tapered emitters may not be fully applicable to non-tapered emitters.

In this chapter, the nanoelectrospray behaviour of entrapped-microsphere emitters is investigated. The characterization of nanoelectrospray from entrapped emitters was conducted over a wide range of flow rates (10 -500 nL/min), spray voltages (2.4 - 5.0 kV), and relative distances (5 - 25 mm) from emitter tip to MS orifice. The converted signal response factor and signal to noise ratio (S/N) was used for the comparison of sensitivity under different conditions. The stability and reproducibility of electrospray were also evaluated. To visually distinguish the different electrospray behaviors of an entrapped emitter and a tapered emitter, offline electrospray experiments were designed

to capture the electrospray image at low nano flow rates. Additionally, the robustness of entrapped emitters was evaluated by infusing a highly concentrated salt mixture (Hank's solution) through the emitter and its resistance to clogging was compared to that of a tapered emitter.

Furthermore, the potential of using integrated emitters (both packed and entrapped ODS emitters) for online sample manipulation and purification was evaluated. The binding characteristics of protein/peptides on both bare and entrapped ODS spheres was investigated. Different types of salts such as sodium chloride, sucrose, urea, potassium phosphate, and Tris were used to test the capability of these emitters for handling high salt containing samples online. Proteins/peptides (bradykinin, leucine enkephalin, cytochrome c, and insulin) with different molecular masses and hydrophobicity were used for the evaluation of separation efficiency.

A packed emitter, an entrapped emitter, and a roughened emitter were used as an interface to couple an HPLC pump with a quadrupole time-of-flight (q-TOF) tandem mass spectrometer (MS/MS) to demonstrate their application potentials in protein identification by the analysis of trypsin digested BSA using direct infusion.

5.2. Experimental

5. 2.1. Reagents

Bradykinin acetate (BK, $C_{50}H_{73}N_{15}O_{11} \cdot xC_2H_4O_2$, formula weight: 1060.21), leucine enkephalin acetate hydrate (LE, $C_{28}H_{37}N_5O_7 \cdot xC_2H_4O_2 \cdot yH_2O$, formula weight: 555.62), cytochrome c (Cyt-c, Mol. Wt. 12,384) from equine heart, insulin from bovine

pancreas (Ins, $C_{254}H_{377}N_{65}O_{75}S_6$, formula weight: 5733.49), bovine serum albumin (BSA, Mol. Wt. 71244), and trypsin were purchased from Sigma (Oakville, ON, Canada) and also used without purification. Sodium chloride, sucrose, urea, monobasic potassium phosphate (KH_2PO_4), and tris(dimethylphenylphosphine)(2,5-norbornadiene)rhodium(I) hexafluorophosphate (Tris) were also purchased from Sigma (Oakville, ON, Canada). The Hank's solution was prepared as described in section 4.2.1 of Chapter 4. Glacial acetic acid, methanol and acetonitrile (HPLC grade) were all from the same source as described previously.

3-(Trimethoxysilyl)propyl methacrylate ($H_2C=C(CH_3)CO_2(CH_2)_3Si(OCH_3)_3$) (saline), butyl acrylate (monomer), 1, 3-butanediol diacrylate (BDDA) (cross linker), and benzoin methyl ether (BME) (initiator) were all obtained from Aldrich and used as received. The buffer salt potassium phosphate was purchased from Fisher Scientific. Buffers were prepared using 18.2 MΩ•cm deionized water filtered through a Milli-Q Gradient water purification system (Millipore S.A. Molsheim, France). Ethanol was purchased from Commercial Alcohols Inc. (Brampton, ON, Canada). Three-micrometer octadecyl silane (ODS) microspheres (Microsorb 100-3 C18) were received as a gift from Varian Canada Inc. (Mississauga, ON, Canada).

5.2.2. Fabrication of packed ODS emitters

Each packed ODS emitter was fabricated individually. A 10 cm UV transparent fused silica capillary channel (75 μm i.d. and 360 μm o.d.) was first pretreated at room temperature by filling with a solution of 3-(trimethoxysilyl)propyl methacrylate

(20%,v/v), glacial acetic acid (30%, v/v), and deionized water (50%, v/v) for 3 h to graft the inner wall with vinyl groups as shown in the following diagram (Figure 5.1).

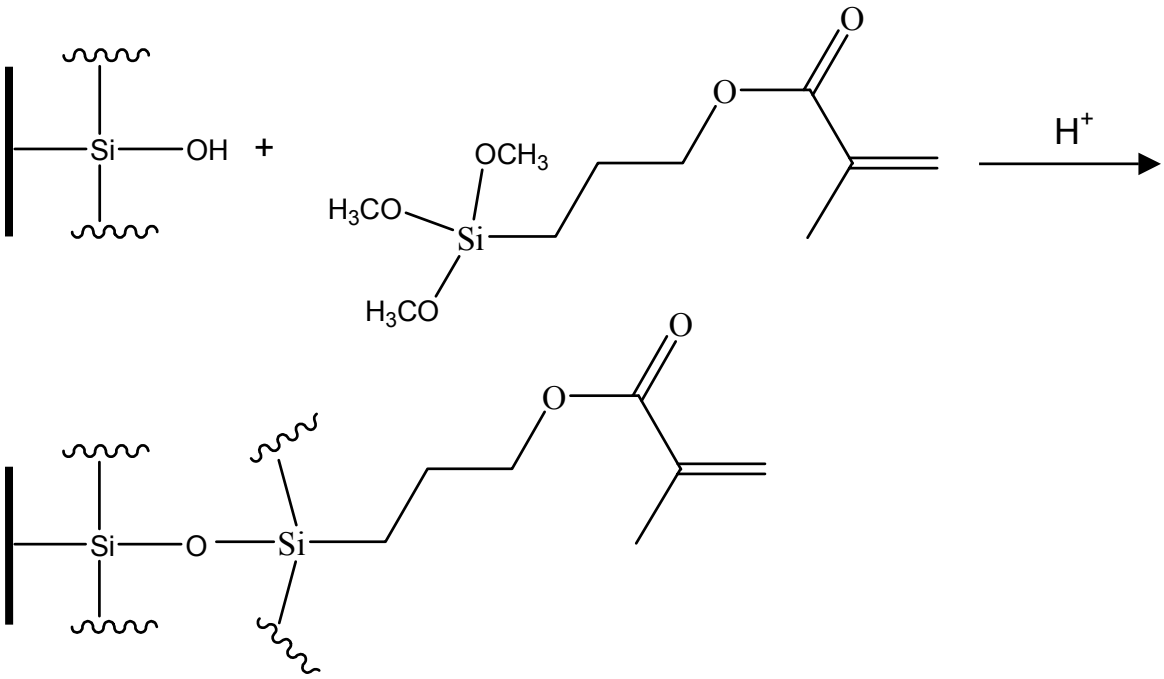

Figure 5.1. Illustration of silica wall treatment.

The treated capillary (5 cm cut from the 10 cm length) was then flushed using 80% acetonitrile and 20% water at 20 μL/min for 10 min. The capillary was then filled with a polymerization mixture consisting of 23% butyl acrylate monomer, 10% BDDA as the cross-linker, 0.5% (5 – 6 mg/mL) BME as initiator, 13.25% ethanol, 40% acetonitrile, and 13.25% 5 mM phosphate buffer at pH 6.8 as porogenic solvent with a syringe pump. The capillary was then covered by a mask with a 1.5-mm window and exposed to the 254-nm UV light (Mineralight UV lamp, UVG-11) for 1.5 min to generate a porous

polymer frit following the reactions as illustrated below. Then, a slurry of 3-µm ODS microspheres in acetonitrile (5 mg/mL) was introduced into the capillary with a HPLC pump. Once we obtained about 1 cm of packed microspheres, a mixture of ethanol, acetonitrile, and 5 mM phosphate buffer, pH 6.8 (20:60:20) was flushed through the capillary column against the frit with an HPLC pump to remove unreacted monomeric materials. The frit end was trimmed leaving a 1 mm frit and a flat edge. The fabrication process is shown in the schematic diagram in figure 5.2. The cross sections with PPM frit of a packed ODS emitter at different magnifications are shown in figure 5.3.

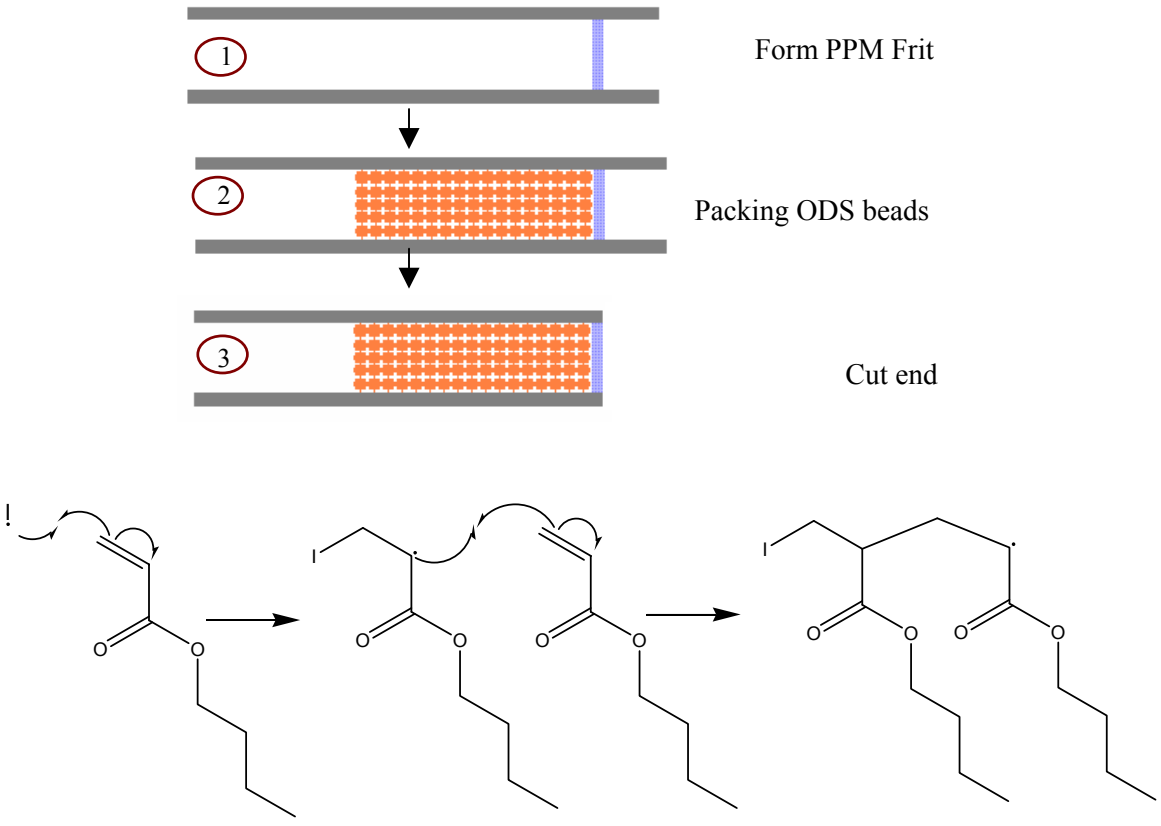

Figure 5.2. Schematic diagram of fabrication procedure of packed ODS emitter and the mechanism of polymerization for making the PPM frit.

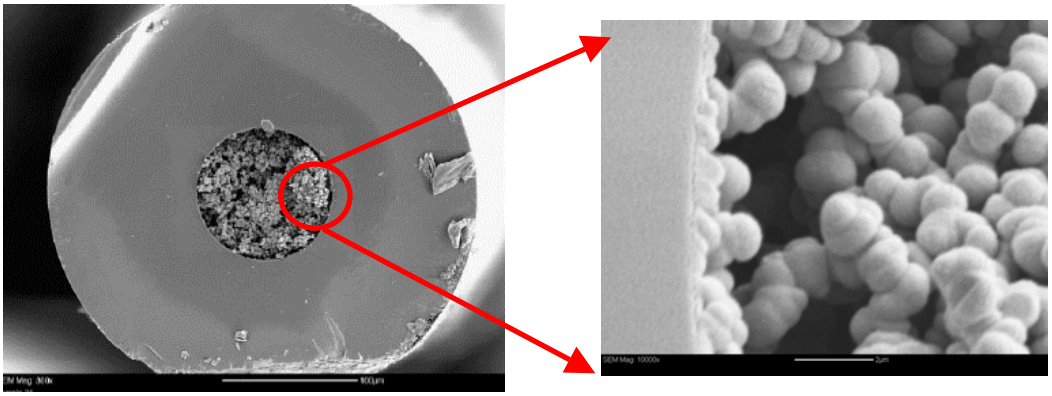

Figure 5.3. Cross section of frit section of the packed ODS emitter at different magnifications.

5.2.3. Fabrication of entrapped ODS emitters

All entrapped emitters were fabricated individually according to the procedures (schematic diagram shown in Figure 5.4) developed by our group.[5]

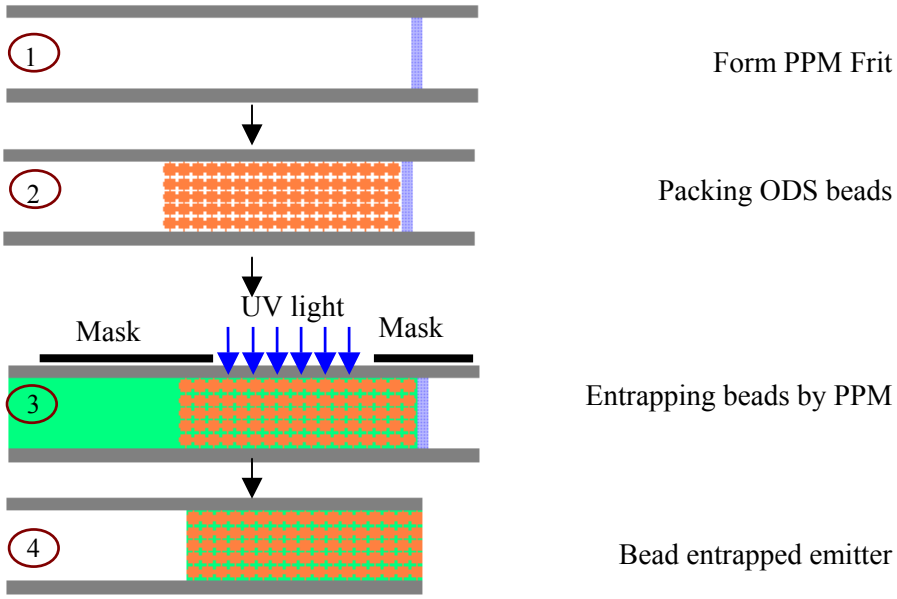

Figure 5.4. Schematic diagram of fabrication procedure of entrapped ODS emitter.

Briefly as described for a packed ODS emitter, a 1 mm length of porous polymer monolith (PPM) frit was formed by a photo-initiated polymerization at the end of a fused silica capillary (75 μm i.d. and 360 μm o.d.). A slurry of 3 μm octadecyl silane (ODS) coated silica particles was packed under pressure into the capillary against the frit until at least a 1 cm length of microsphere bed was obtained. The same polymerization mixture as used for making the frit was reintroduced into the column at a maximum pressure of 2500 psi to ensure that the microspheres were tightly packed during immobilization procedure. After several column volumes of the polymerization mixture had passed through the capillary, the HPLC pump was turned off. Then, a 1 cm long microsphere packed region was exposed to the 254 nm UV light (Spectroline UV lamp, ENF-280C) from a distance of approximately 1.5 cm from the retaining frit through a mask to facilitate microsphere entrapment. The polymer not only anchors microspheres to the capillary wall but also builds a network among ODS spheres as shown by the following illustration (shown in Figure 5.5). The temporary retaining frit was then cut off, and a mixture of ethanol, acetonitrile, and 5 mM phosphate buffer, pH 6.8 (20:60:20) was flushed through the capillary column back and forth with an HPLC pump to remove un-reacted monomeric materials and non-entrapped microspheres.

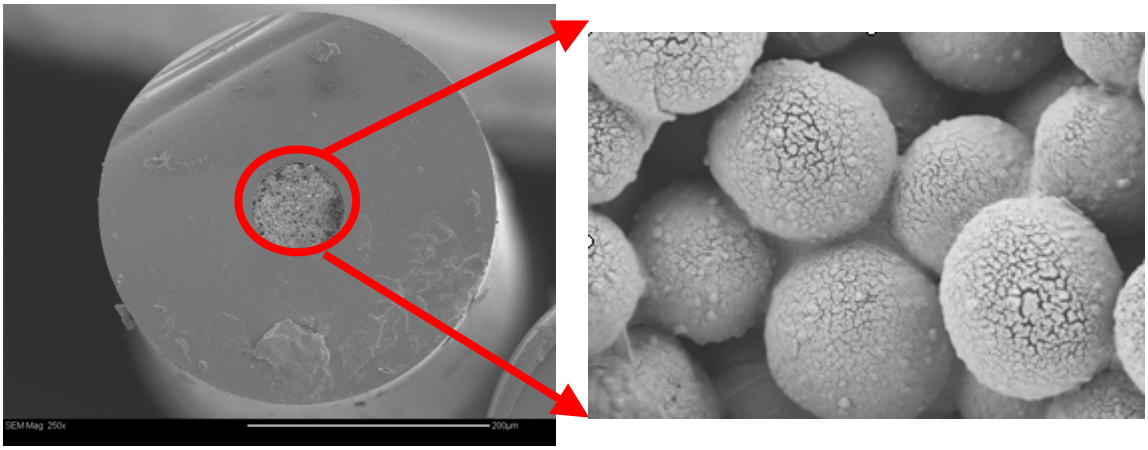

Figure 5.5. Illustration of the formation of network webbing among the ODS spheres.

5.2.4. Operation procedures of an entrapped-microsphere emitter

Mass spectrum acquisition was conducted using the same setup as described in section 2.2.6. An entrapped-microsphere emitter was mounted onto the MicroTee (Upchurch, SPE Ltd, North York, ON, Canada) and in turn held on an x-y-z stage. Two CCD cameras and the x-y-z stage were used to finely position the emitter. Before applying flow and electrospray voltage, the emitter was positioned 1-2 mm from the centre of the MS orifice for alignment, it was then moved back precisely in-line by turning the micrometer screw of the stage to 5 to 25 mm away from the MS orifice. One end of the MicroTee was connected to a nano-LC pump (Eksigent, Dublin, CA, USA) with 15 cm of capillary (360 μm o.d. and 30 μm i.d.), which provided flow rates from 10 nL/min to 1000 nL/min corresponding to backpressures of about 10 to 1000 psi

respectively. After adjusting the emitter position to a desired distance, a designated flow rate was applied until a droplet appeared at the tip of the emitter aperture. A spray voltage was then applied onto the tip to initiate an electrospray.

5.2.5. Offline and online electrospray set-up

The offline and online electrospray setup is as the same as described in section 4.2.4 as well as section 2.2.6 respectively.

5.2.6. Electrospray characterization

The trends of intensity of the total ion current (TIC), the signal response factor (RF), and the signal to noise ratio (S/N) from electrospray of leucine enkephalin standard were investigated as a function of the relative distance (5 mm and 25 mm) between emitter tip and MS orifice, spray voltages from 2.4 kV to 4.9 kV, and flow rate from 10 nL/min to 500 nL/min. The influence of these factors on electrospray stability, sensitivity and reproducibility was evaluated. The intensity of TIC was used as an index for sensitivity at the same flow rate with the same analyte concentration. For different flow rates, a signal response factor was calculated using the average TIC/XIC intensity (TIC in this experiment) divided by the amount of analyte consumed over an acquisition period using the following equation:

$$RF = I/[c*(dV/dt)*t], \quad (1)$$

Where: RF is the response factor; I is the average intensity of TIC/XIC (TIC in this case); c is the concentration of analyte; d*V*/d*t* is the flow rate; and t is the acquisition time.

Signal to noise ratio (S/N) was calculated by dividing the background subtracted analyte peak heights against the standard deviation of the background signals. The stability of the electrospray was indicated by the relative standard deviation (RSD %) of the TIC intensities calculated by dividing the standard deviation (SD) of the TIC data points against the average of TIC intensities.

5.2.7. Robustness evaluation

See details in section 4.2.6.

5.2.8. Protein/peptide binding and separation

A protein/peptide solution mixture was prepared containing 23 μM BK, 7.1 μM LE, 4.6 μM Cyt-C, and 9.4 μM Ins in water. The solution (400 nL to 1000 nL in volume) was loaded onto the ODS sphere bed using a gradient of 99% of mobile phase A (aqueous) and 1% of mobile phase B (acetonitrile). A gradient (see Table 1) with increasing organic content was used to elute different protein/peptides at different retention times, followed by detection with mass spectrometry at 500 nL/min flow rate using the instrument setup as described in section 2.2.6.

Table 5.1. Gradients used for proteins/peptides separation

Time (min)	B%
0	2
2	2
3.3	24
3.7	50
4.7	80
8	80

5.2.9. Desalting

Solutions were prepared with a mixture of 23 μM BK, 7.1 μM LE, 4.6 μM Cyt-C, and 9.4 μM Ins containing sodium chloride, sucrose, urea, potassium phosphate (pH 4-5), and tris (pH 8-9) at 400 mM, 300 mM, 900 mM, 150 mM, and 200 mM, respectively, in water. Each solution (400 nL to 1000 nL in volume) was loaded onto the ODS sphere bed using a gradient of 99% of A and 1% of B. It was then washed by continually infusing using 99% A and 1% B from 0.5 min to 4 min giving 10 to 80 column volume wash. A gradient with increasing organic content was used to elute different protein/peptides at different retention times, followed by detection with mass spectrometry using the instrument setup as described in section 2.2.6.

5.2.10. Protein identification by direct infusion

Analysis of a digested protein was conducted using a non-tapered emitter as an interface coupling an HPLC pump (Agilent, HP 1100, USA) to a hybrid QStar (Q-TOF XL) (MDS, Sciex, ON, Canada) (schematic diagram shown in Figure 5.6). Trypsin digested BSA was prepared as described elsewhere[12] and an online nanospray interface (MDS, Sciex, ON, Canada) was installed with two CCD cameras, a metal emitter holder and an x-y-z stage. A tested emitter was inserted into the metal holder and the relative distance between the emitter and mass spectrometer orifice was maintained between 0.5 cm and 1.5 cm. Spray voltages of 4.0 kV to 4.5 kV were applied through the connection with the metal holder. One end of the emitter opposing the tip was connected through a trapping column with an HPLC pump operated at a 1 μL/min flow rate. The trapping

column (OPTI-PAK, Optimize Technologies Inc., Brockville, ON, Canada) was installed to provide the necessary backpressure required for valve actuation within the pump. A length of capillary similar to the transfer line (30 μm i.d.) was used to split the flow from the HPLC pump, which allows one to deliver a solution to the emitter tip at a flow rate of less than 500 nL/min. A 2.5 μL sample loop was used to bypass the trapping column for the direct delivery of sample solutions to the electrospray emitter (Figure 5.6). An isocratic solvent program was used to infuse the BSA digest using 1:1 (v/v) acetonitrile/water with 0.1% formic acid.

An information dependent data acquisition program in the Analyst QS software was used for TOF spectra and product ion spectra data acquisition. The TOF MS mass range was set as 300-2000 m/z, while that for MS/MS was set as 65-1500 m/z. Former target ions were always excluded during the ion acquisition. A TOF MS precursor ion spectrum was accumulated at 1 Hz followed by three product ion spectra, each for 3s. Positive ion mode was used to acquire +2 to +4 charged ions.

The peptide ESI-MS/MS spectra were searched against the Swiss-Prot database using the MASCOT search engine[13] with a mass tolerance of 0.2 Da and 2 allowed missed cleavages. Search parameters allowed for variable modification of the oxidation of methionine and fixed modification of carbamidomethylation. Unambiguous protein identification was judged by the number of peptides, probability based MOWSE score, sequence coverage and the quality of the MS/MS spectra.

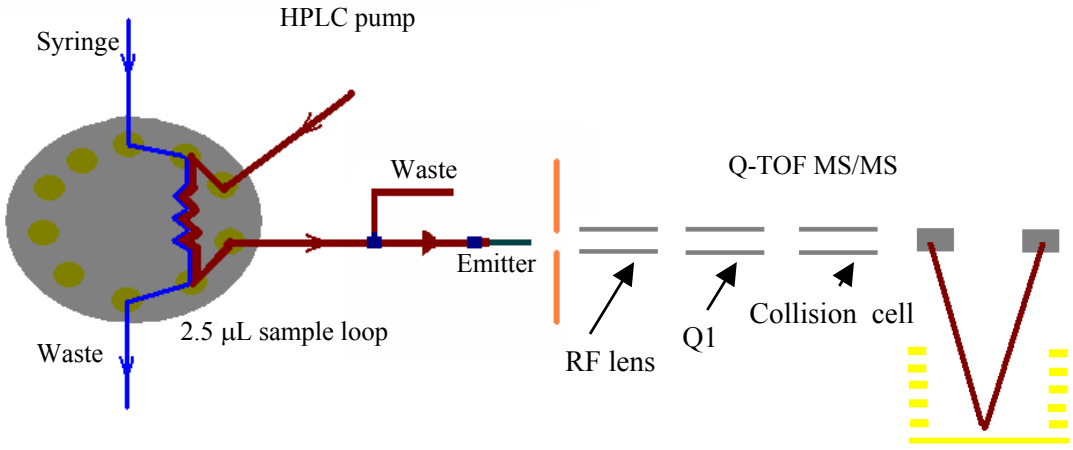

Figure 5.6. Schematic diagram of LC-ESI/MS/MS system used for protein identification.

5.3. Results and discussion

5.3.1. Characterization of an entrapped emitter

We have previously studied the nanoelectrospray behavior and performance of non-tapered nano-ESI emitters such as a roughened open tubular emitter, a membrane assisted emitter, and a microstructured fiber emitter. Those emitters all contain hollow channels, and function only as an ion source. The distinguishing feature of an entrapped emitter discussed in this chapter includes a bed of 3 µm sized ODS microspheres entrapped with a butyl acrylate porous polymer positioned at the end of the emitter as shown in Figure 5.7a. Instead of functioning only as a nano-ESI emitter as shown in Figure 5.7b, the chromatography bead bed was also expected to function as a column for solid phase extraction and separation. Moreover, because of the multiple channels formed from the voids between the ODS beads, a plume of mist instead of a regular Taylor cone

was also observed at low nano flow rates (25 nL/min) (illustrated in Figure 5.7b) as that of observed from a MSF multi-channel emitter discussed in chapter 4.

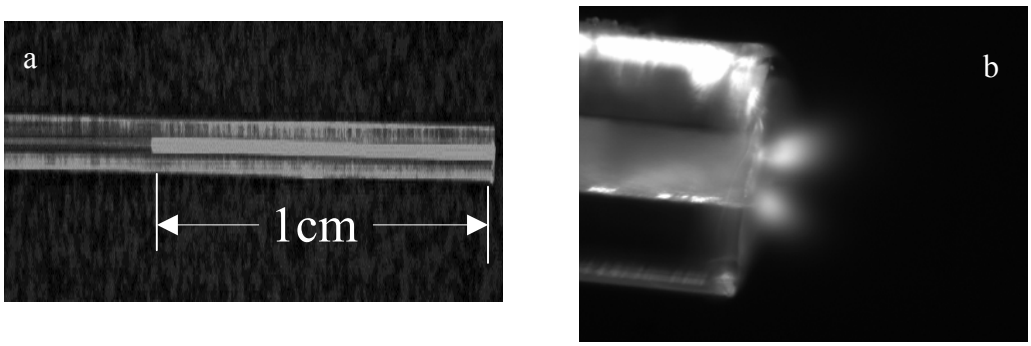

Figure 5.7. Distinguishing features of an entrapped emitter (a) optical image of an entrapped emitter with 1 cm entrapped ODS microspheres; (b) image of a mist from offline electrospraying at 25 nL/min flow rate (Image b courtesy of Dr. Samaul Mugo).

The fine droplets of mist at low nano flow rates from such an entrapped emitter potentially enhance the ionization efficiency thus enabling high sensitivity. When an emitter was positioned at 10 mm from the MS orifice and 3.2 kV spray voltage was applied, the TIC intensity at 100 nL/min was only about 1.3 fold higher compared to that of at 10 nL/min flow rate as shown in Figure 5.8a. The moderate reduction in TIC intensities when lowering the flow rates is attributed to the formation of mist thus a characteristic improvement in sensitivity at low nano flow rates. A stable electrospray trace was obtained with less than 10% of RSD at a flow rate of 10 nL/min. Figure 5.8b shows the equivalent S/N ratios of a leucine enkephalin peak at *m/z* 556.7 from 100 nL/min and 10 nL/min flow rate under these conditions.

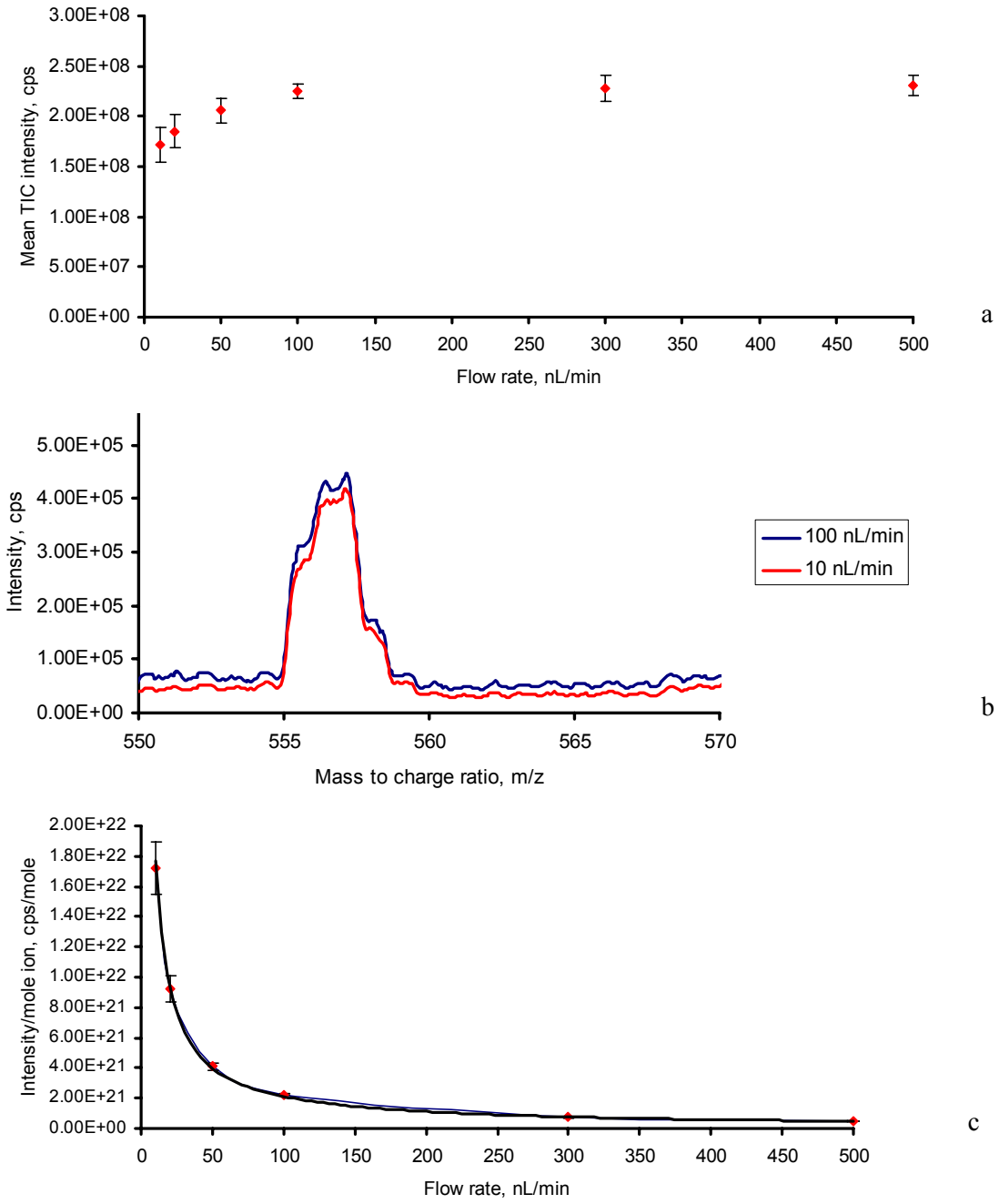

Figure 5.8. Improved sensitivity at low nano flow rates from an entrapped emitter by spraying a 1 μM leucine enkephalin solution with 3.2 kV spray voltage at 10 mm relative distance from the emitter tip to a MS orifice. (a) TIC intensities at different flow rates; (b) comparison of S/N ratio of the leucine enkephalin peak at *m/z* of 556.7 at 10 nL/min and 100 nL/min flow rate; (c) TIC counts per mole of analyte as a function of flow rate corresponding to 5.8a.

Various approaches have been used to measure, compare or simply demonstrate the sensitivity of detection from nanoelectrospray. For example, electrospray ion current was used for the quantitative measurement of ionization efficiency and transmission efficiency individually. Practically, for a comparison of sensitivity at the same flow rate with the same analyte concentration, the intensity of the total ion current (TIC) or extracted ion current (XIC) are the simplest methods. In these experiments, a signal response factor was also used for the sensitivity comparison at different flow rates as shown in Figure 5.8c. As theoretically predicted, the curve of the signal response factor as a function of flow rate shows that sensitivity increases exponentially as flow rates are reduced, especially at low nano flow rates.

Another interesting feature is that when comparing with a tapered emitter, a non-tapered emitter is usually positioned with a significantly larger gap between the emitter tip and the MS orifice. For a typical tapered emitter, the recommended relative distance for achieving 10 to 40 nL/min flow rates is within 1 mm to 2 mm of the MS orifice as shown in a schematic drawing in Figure 5.9. Accurately positioning a tapered emitter is a big challenge. Different apparatus or programs (as shown in Figure 5.10) were developed to accurately control the emitter position.

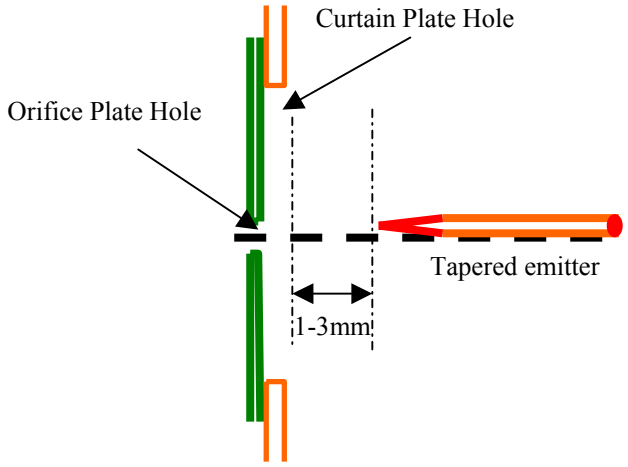

Figure 5.9. Schematic drawing of positioning a tapered emitter tip.

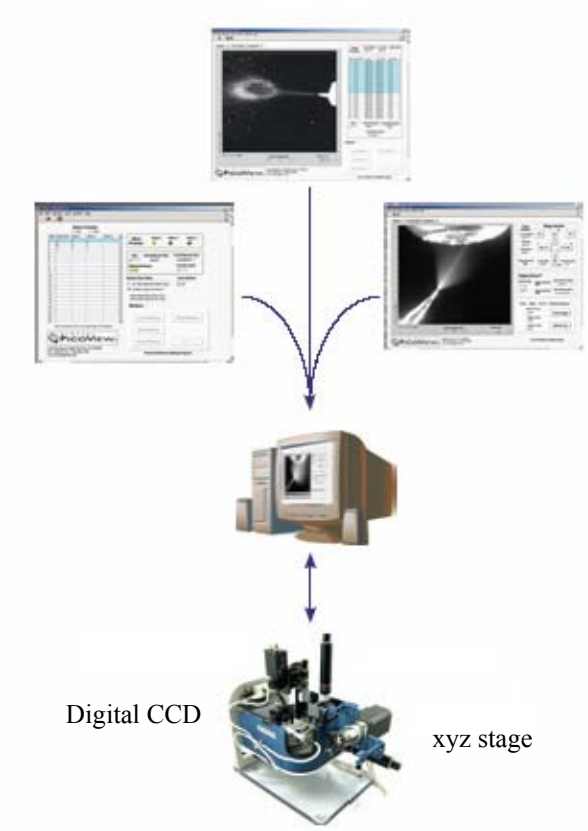

Figure 5.10. Schematic diagram of a program controlled emitter positioning for a tapered emitter.

However, when using an emitter that generates multiple electrospray, the plume obtained from a multiple electrospray is larger than that of from a single Taylor cone mode as illustrated in Figure 5.11a and 5.11b. At lower flow rates, the larger spray plume provides a better chance of ionized analytes being sucked into the mass chamber. This explains why an entrapped emitter can be positioned farther (schematic drawing shown in Figure 5.12) and positioning of an entrapped emitter is not as critical to the nanoelectrospray performance. The capability of being positioned farther is important while conducting an online sample manipulation (e.g. desalting) because it will largely eliminate the chance of ion source contamination.

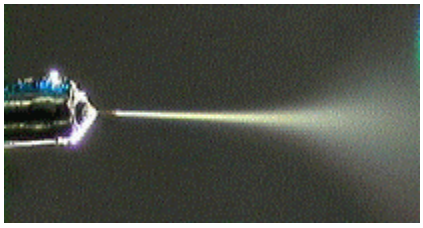

a

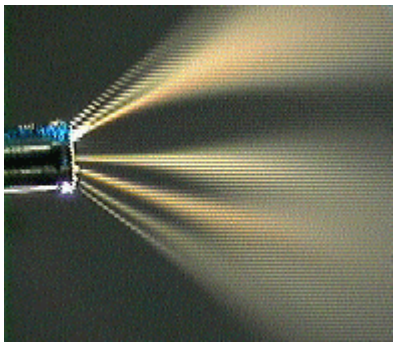

b

Figure 5.11. Electrospray images of a single Taylor cone mode (a) and a multiple electrospray mode (b).[14]

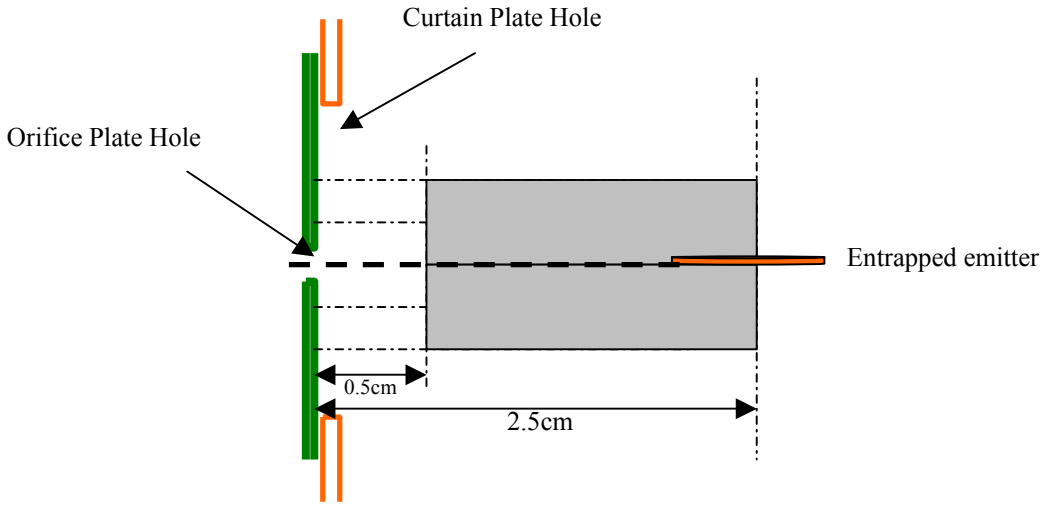

Figure 5.12. schematic drawing of positioning an entrapped emitter.

To further investigate the effect of electrospray performance at different positions, an entrapped emitter was positioned from 5 mm to 25 mm relative distance between the emitter tips to the MS orifice. The position of the emitter was accurately monitored with the x, y, and z actuators on the ion source stage. The average TIC intensities versus relative distance were obtained by electrospraying 1 μM leucine enkephalin standard at 500 nL/min (shown in Figure 5.13a). A 3.2 kV spray voltage was maintained during the full range of the tested distances. The distance between an emitter tip and the MS inlet was increased at 1 mm intervals. No electrospray was initiated during this experiment with the emitter tip being positioned closer than 5 mm to MS orifice in order to avoid ion source contamination. Further optimization was not necessary to obtain a stable electrospray at different distances.

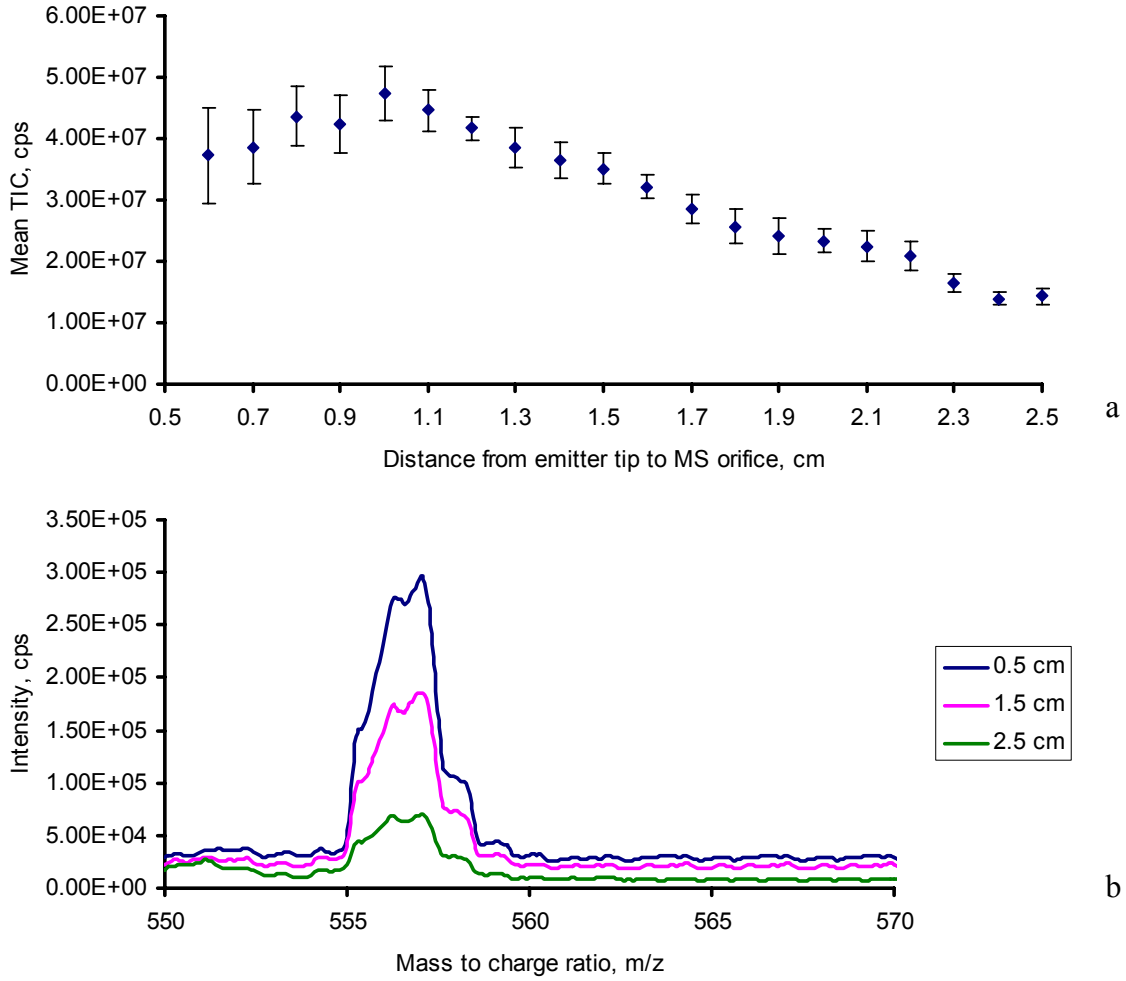

Figure 5.13. Characterization of TIC intensity as a function of distance from emitter tip to MS orifice by constantly infusing 1 μM leucine enkephalin solution (1:1 water/methanol): (a) TIC intensity at different relative distance from an emitter tip to MS orifice, 3.2 kV spray voltage was applied; (b) signal to noise ratio at 5 mm, 15 mm and 25 mm distance from emitter tip to MS orifice.

It was found that when an emitter was positioned at the distance of 5 mm to the MS orifice, the electrospray signal was not very stable (20% RSD) due to pulsation of the Taylor cone. With increasing distance (5 mm to 10 mm), the TIC intensity increases slightly and the electrospray becomes more stable (< 10% RSD) as well. This is partially due to a stabilized Taylor cone at the increased distance as well as the enhanced

desolvation efficiency with longer evaporation time. When the distance is increased further from 10 mm to 25 mm, the TIC intensity was reduced about 3.5 fold. The relatively smaller change in TIC intensity with such a large range of distances provides more flexibility for positioning an emitter without worrying about significant ion losses. As distance increased, the signal to noise ratio of the leucine enkephalin peak was also decreased correspondingly by about 1.5 fold from 5 mm to 15 mm and 2 fold from 15 mm to 25 mm as shown in figure 5.13b.

Since the onset spray voltage was determined mainly by the external diameter of an emitter, an entrapped emitter with non-tapered external diameter requires a relatively high spray voltage compared to a conventional tapered emitter. An investigation of electrospray behaviour at spray voltages ranging from 2.4 kV to 5.0 kV provides a reference for choosing a working spray voltage when using an entrapped emitter. Positioning the emitter tip 10 mm relative to the MS orifice, while constantly infusing 1 μM leucine enkephalin solution (1:1 water/methanol) at 500 nL/min flow rate, average TIC intensities were plotted against different spray voltages as shown in Figure 5.14a. The onset spray voltage was found to be close to 2.4 kV. Stable electrosprays (RSD% <5%) were maintained up to about 4.0 kV. TIC intensity increased slightly as the spray voltage increased within this range (1.5 fold). When the applied voltage was higher than 4.0 kV, the TIC intensity started to decrease and the signal became less stable. The S/N ratio of the leucine enkephalin peak increased about 1.5 fold when the spray voltage increased from 3.5 kV to 4.0 kV, while S/N ratio dropped to about the same level as that of 2.5 kV to 3.5 kV due to the poor electrospray stability at spray voltages higher than 4.0

kV as shows in Figure 5.14b. Based on the characterization results, six entrapped emitters were used to test the reproducibility of their electrospray performance without further optimization using a 100 nL/min flow rate, 3.2 kV spray voltage and centrally positioned at 10 mm from the MS orifice. The variation of TIC intensities from the 6 emitters was less than 7% with less than 5% RSD for each emitter tested as shown in Figure 5.15.

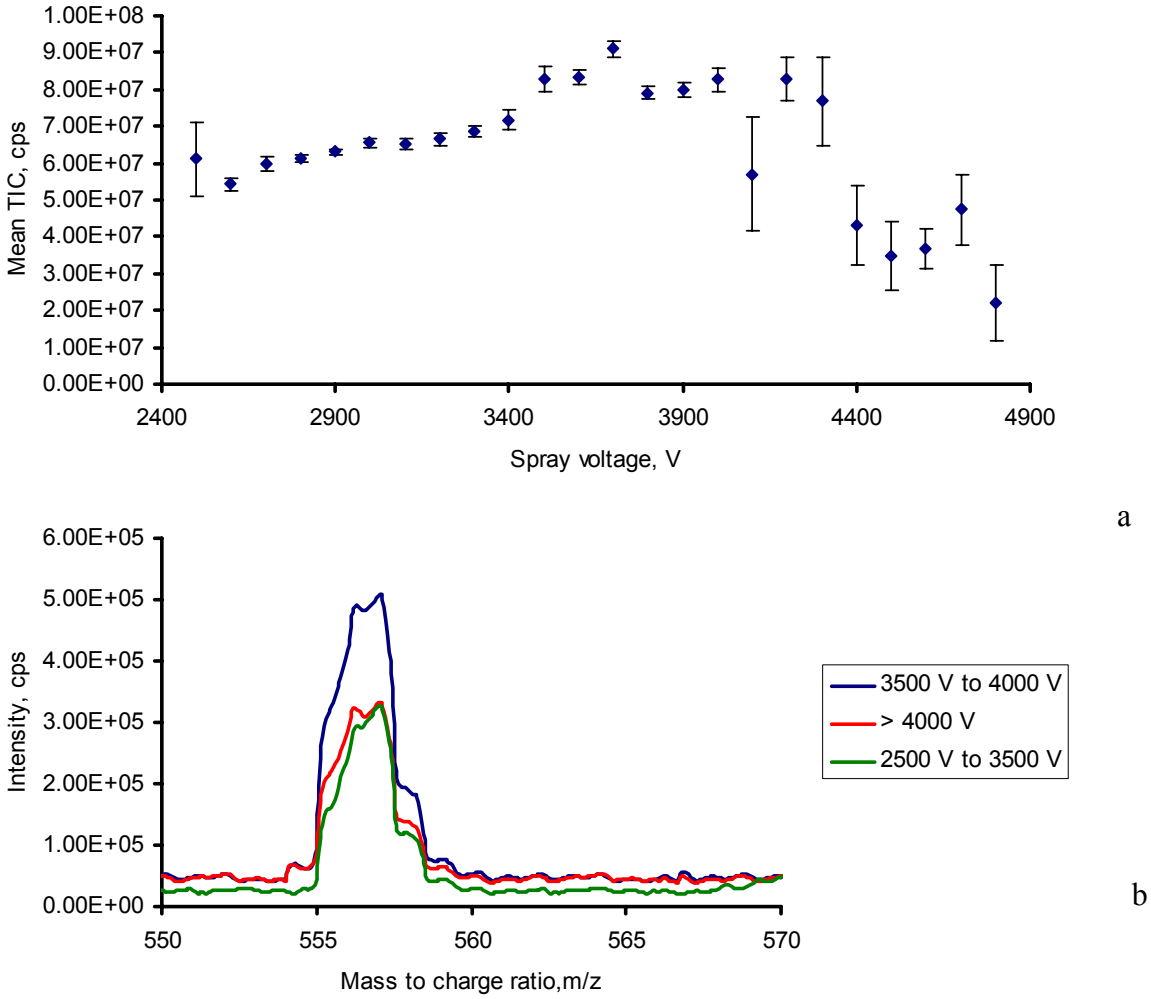

Figure 5.14. Characterization of TIC intensity as a function of electrospray voltages by constantly infusing 1 μM leucine enkephalin solution (1:1 water/methanol): (a) Overlaid TIC trace at different electrospray voltages with 10 mm relative distance from the emitter tip to a MS orifice at 500 nL/min flow rate; (b) S/N ratio at 3.0 kV, 3.5 kV and 4.0 kV spray voltages.

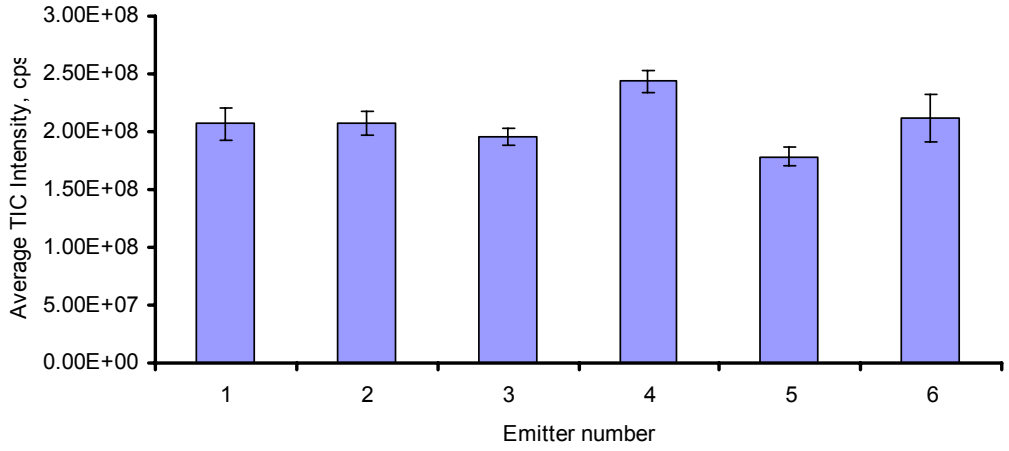

Figure 5.15. Reproducibility of electrospray from six entrapped emitters at 100 nL/min flow rate, 3.2 kV spray voltage and being positioned at 10 mm from the MS orifice.

5.3.2. Robustness evaluation of entrapped emitters

Entrapped emitters show superior resistance to clogging compared to tapered emitters. The robustness of entrapped emitters has been demonstrated from their day to day utilization, where clogging never occurred under regular electrospray conditions. Furthermore, a robustness evaluation was conducted by infusing Hank's solution, a highly concentrated salt mixture, in an attempt to rapidly induce clogging. Hank's buffer was pushed into emitters (both entrapped and tapered) at a 300 nL/min flow rate. As shown in Figure 4.11a, the tapered emitter with 5 μm aperture was completely clogged in less than 4 minutes after the start of Hanks infusion, with the back pressure surging to above 2000 psi., accompanied by a complete disappearance of the leucine enkephalin peak.

The same experiment was carried out using an entrapped emitter. It was remarkable that an entrapped emitter not only survived the clogging test after constantly infusing the

Hank's solution for 25 minutes, but also demonstrated the capability to resume its normal electrospray performance after completely flushing out the salt residue from the microsphere bed of the tested entrapped-emitter. During 25 minutes of Hank's solution infusion, the induced back pressure was initially increased from about 500 psi to about 600 psi within a short period of time. However, it then quickly dropped to lower than 500 psi (about 300 psi) during the rest of the Hank's infusion and returned to the normal level at average of 500 psi after the Hank's infusion (shown in Figure 5.16a). While this aspect of the behavior was similar to the tapered emitter, the leucine enkephalin peak disappeared. It was detected 10 minutes after the Hank's was replaced with leucine enkephalin, however the S/N ratio was reduced about 5 fold compared to before the Hank's infusion. This was expected due to ion suppression from the salt residues remaining on the emitter's microsphere bed. With increased flushing time, the S/N ratio of leucine enkephalin peak continued to increase. After 30 minutes of online flushing with leucine enkephalin solution (1:1 water/methanol), the TIC intensity was close to the initial levels before and complete recovery occurred after 40 minutes (Figure 5.16b). The emitter was then conditioned by constantly infusing a mobile phase (1:1 water/acetonitrile) for another 1 hour to establish a blank TIC trace. Following the clogging evaluation the entrapped emitter functioned normally. The stability and the sensitivity of the electrospray were similar to those from a fresh entrapped emitter with the RSD of the average TIC intensity at 2.5% for a 60 minutes run (shown in Figure 5.17).

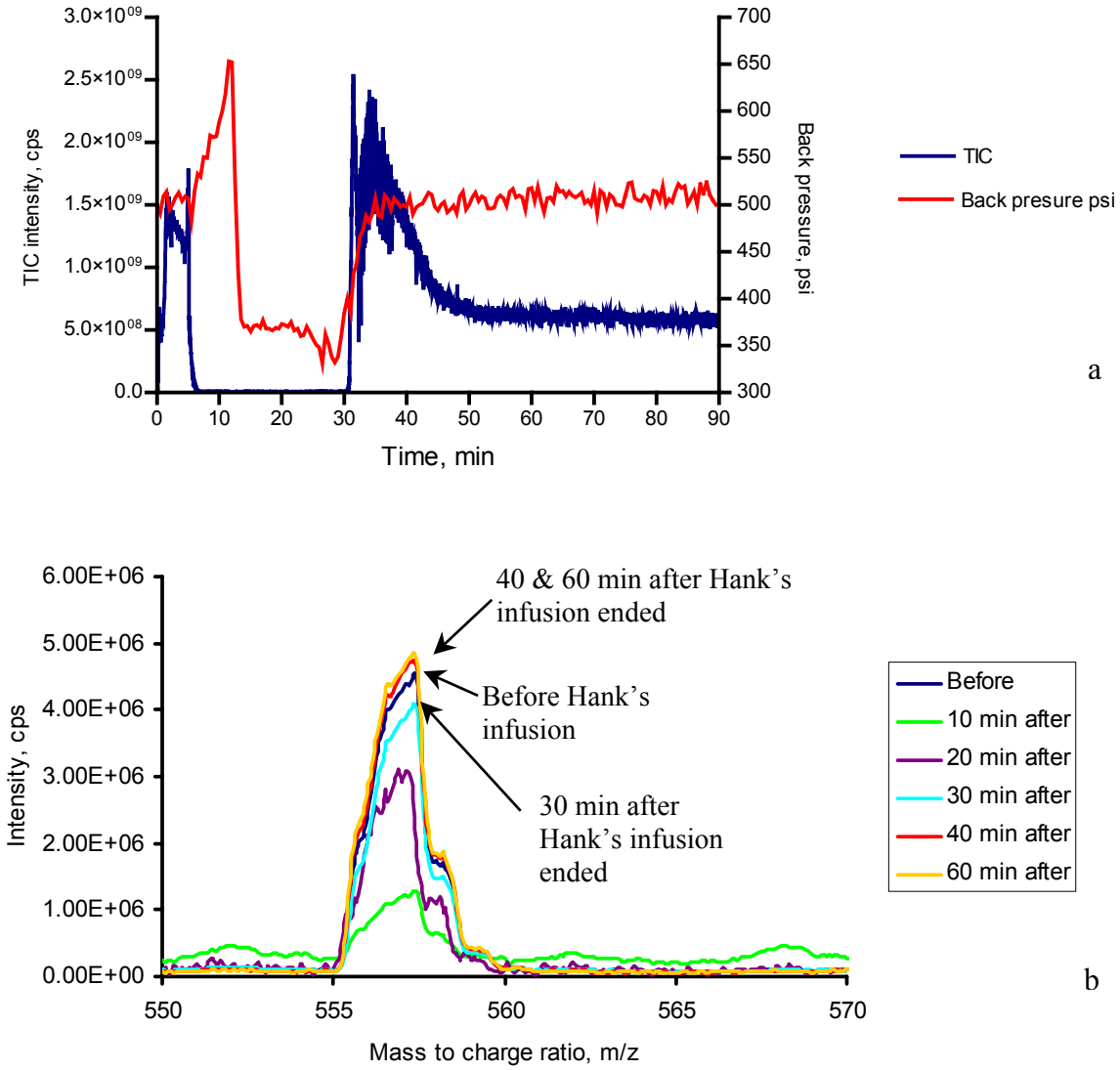

Figure 5.16. The robustness of an entrapped emitter demonstrated by infusing a Hank's solution at 300 nL/min flow rate (a) TIC trace and backpressure observed for an entrapped emitter before, during and after infusing a Hank's buffer; (b) leucine encephalin peak at 556.7 *m/z* before and after infusing a Hank's buffer to an entrapped emitter.

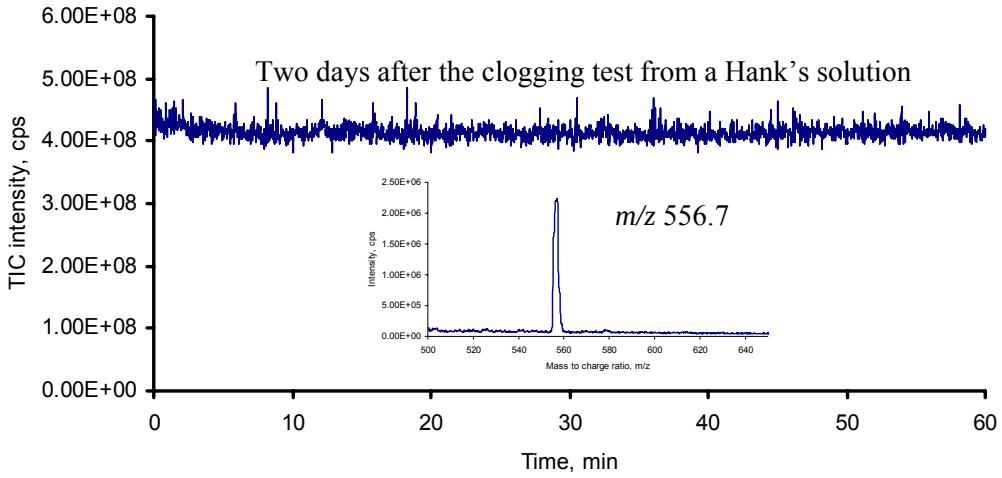

Figure 5.17. 60 minutes of TIC trace and leucine enkephalin peak (insert) from an entrapped emitter at 300 nL/min by infusing a 1 μM leucine enkephalin solution two days after the test of Hank's solution infusion.

5.3.3. Preconcentration

A packed and an entrapped ODS emitter with 2 cm microsphere bed were used for studies on protein binding and separation. Without pre-concentration, the detection limit for leucine enkephalin was determined by a plot of different concentrations versus their corresponding LE XIC intensities obtained with constant infusion. Leucine enkephalin solutions were prepared in 1:1 (v/v) water and methanol with concentrations ranging from 0.03 μM to 1.0 μM. Each solution was directly infused through a packed emitter at 500 nL/min flow rate. Mass spectra were extracted from 1 min of TIC trace obtained from each run at different concentrations. The average peak heights at 556.5 m/z (leucine enkephalin peak) from three replicates were used to plot against the concentration (shown in Figure 5.18a). Figure 5.18b overlays the LE peaks at different concentrations, which shows a signal to noise ratio (S/N) less than 10 at 0.03 μM.

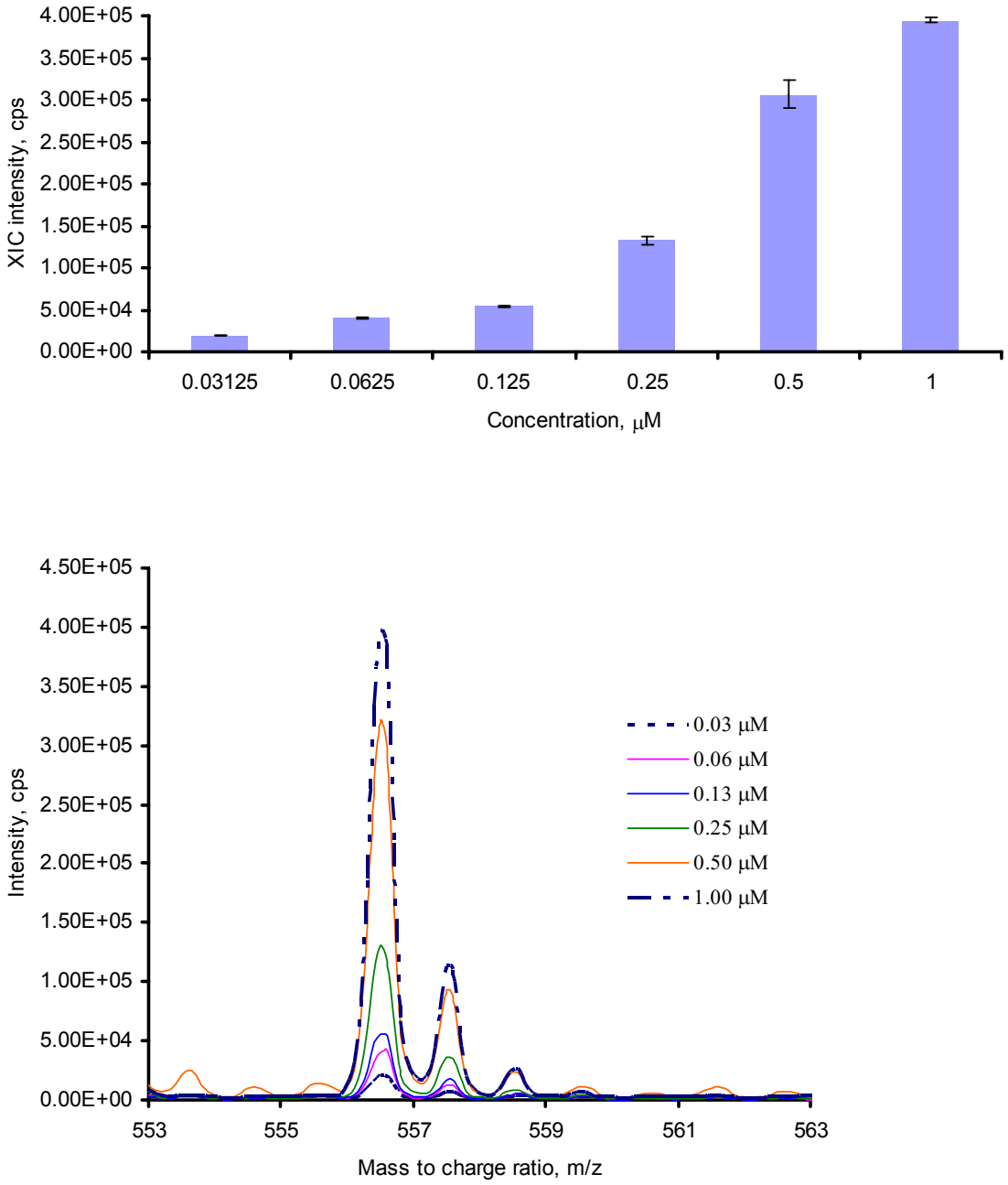

Figure 5.18. Detection limit of LE without pre-concentration by constant infusion from a packed ODS emitter: (a) plot of LE concentrations versus their peak heights; (b) overlaid of mass spectra showing changes in LE peak height at different concentrations.

To test the binding capability of a packed ODS emitter, 1 μM LE solution was prepared in aqueous solution and diluted 10 fold several times down to 0.0001 μM. A metered injection with the nano-pump was used to automatically load 50 nL, 500 nL and 1500 nL of 0.0001 μM LE solution, respectively, onto the emitter ODS bed. After 4 min washing with 98% aqueous solution, the stacked peptide was then eluted using 70% of acetonitrile (Figure 5.19).

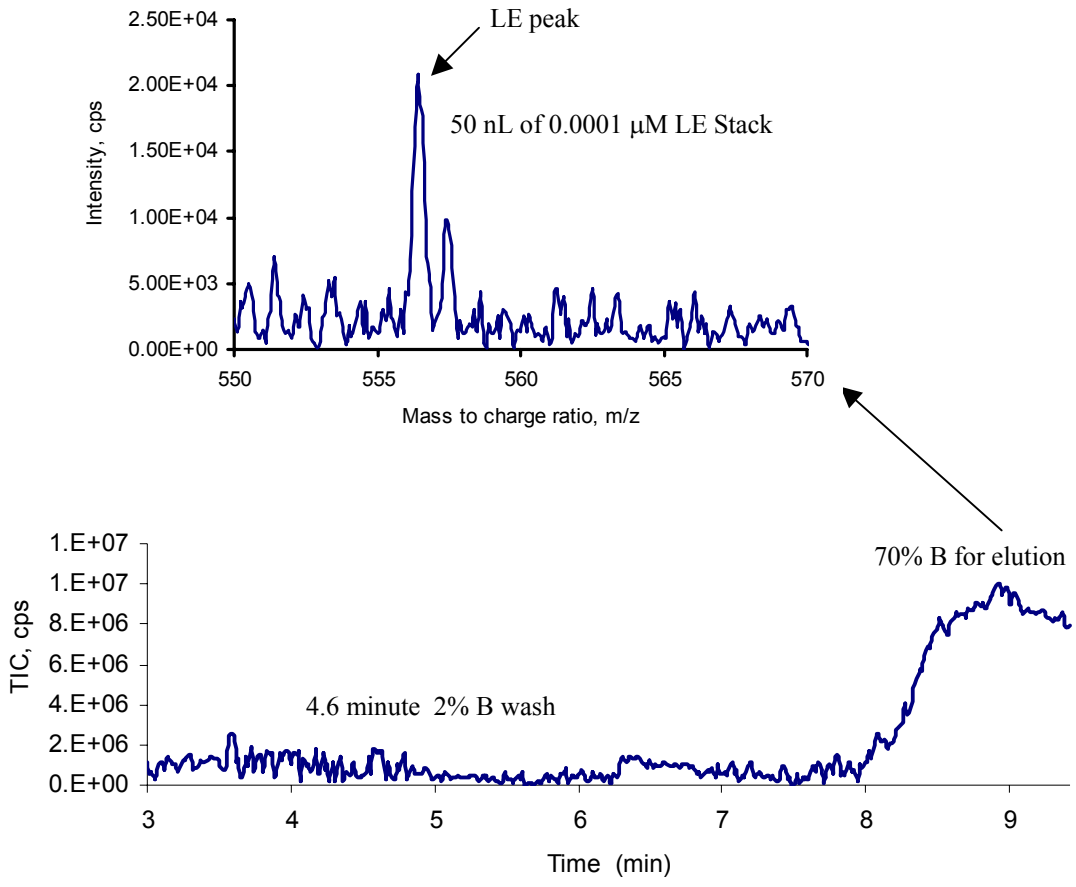

Figure 5.19. Stack and elution of 50 nL of 0.0001 μM LE solution (the insert is a mass spectrum at 70% ACN elution).

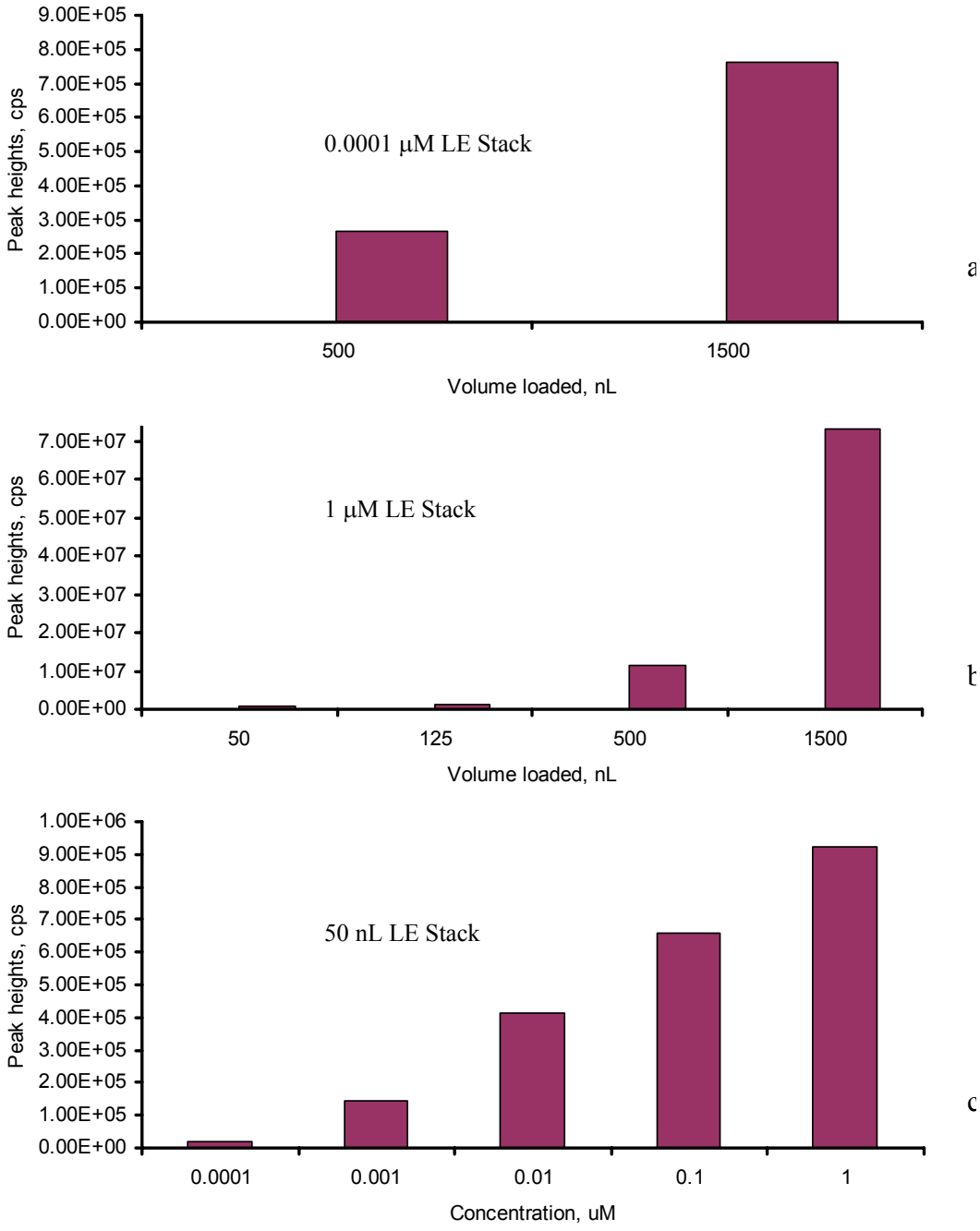

Figure 5.20. LE pre-concentration: (a) peak heights by stacking 500 nL and 1500 nL of 0.0001 μM LE solutions; (b) peak heights by stacking different volumes of 1 μM LE solutions; (c) peak heights by stacking 50 nL of LE solutions with different concentrations.

The S/N ratio of leucine enkephalin peak was close to 3 for a 50 nL injection of 0.0001 μM stacking with enhanced signals for the 500 nL and 1500 nL sample volumes as shown in Figure 5.20a. The same technique was used to stack various volumes of 1 μM LE solutions onto the ODS bed, respectively, shown in Figure 5.20b. A similar trend was obtained as that of from the lower concentration. The same sample volume (50 nL), with different concentrations from 0.0001 μM to 1 μM LE, were loaded onto the same emitter respectively. The results shown in Figure 5.20c, confirmed those obtained in Figure 5.18a. In this case, the detection limit of leucine enkephalin was reduced down to 0.0001 μM compared to 0.031 μM without pre-concentration (shown in Figure 5.18a).

However, when the same experiment was carried out on the entrapped emitter, instead of observing stacking and concentrated elution, a somewhat "on-off" elution was observed at different solvent composition as shown in Figure 5.21. With 50% mobile phase B, leucine enkephalin was detected, which indicated some retention (on) on the entrapped microspheres. However, when increased the phase B to 70%, the leucine enkephalin peak dispersed (off) showing insignificant retention. The "on-off" phenomenon repeated with switching of the mobile phase compositions. No concentrated elution was achieved after trying different gradients as expected, which indicated an overall poor binding capability of an entrapped emitter. It is not clear what causes the "on-off" phenomenon. One of the possible causes may be the swelling of the entrapping polymer. The swollen polymer may trap peptides at one solvent composition and release it at a composition that deswells the polymer.

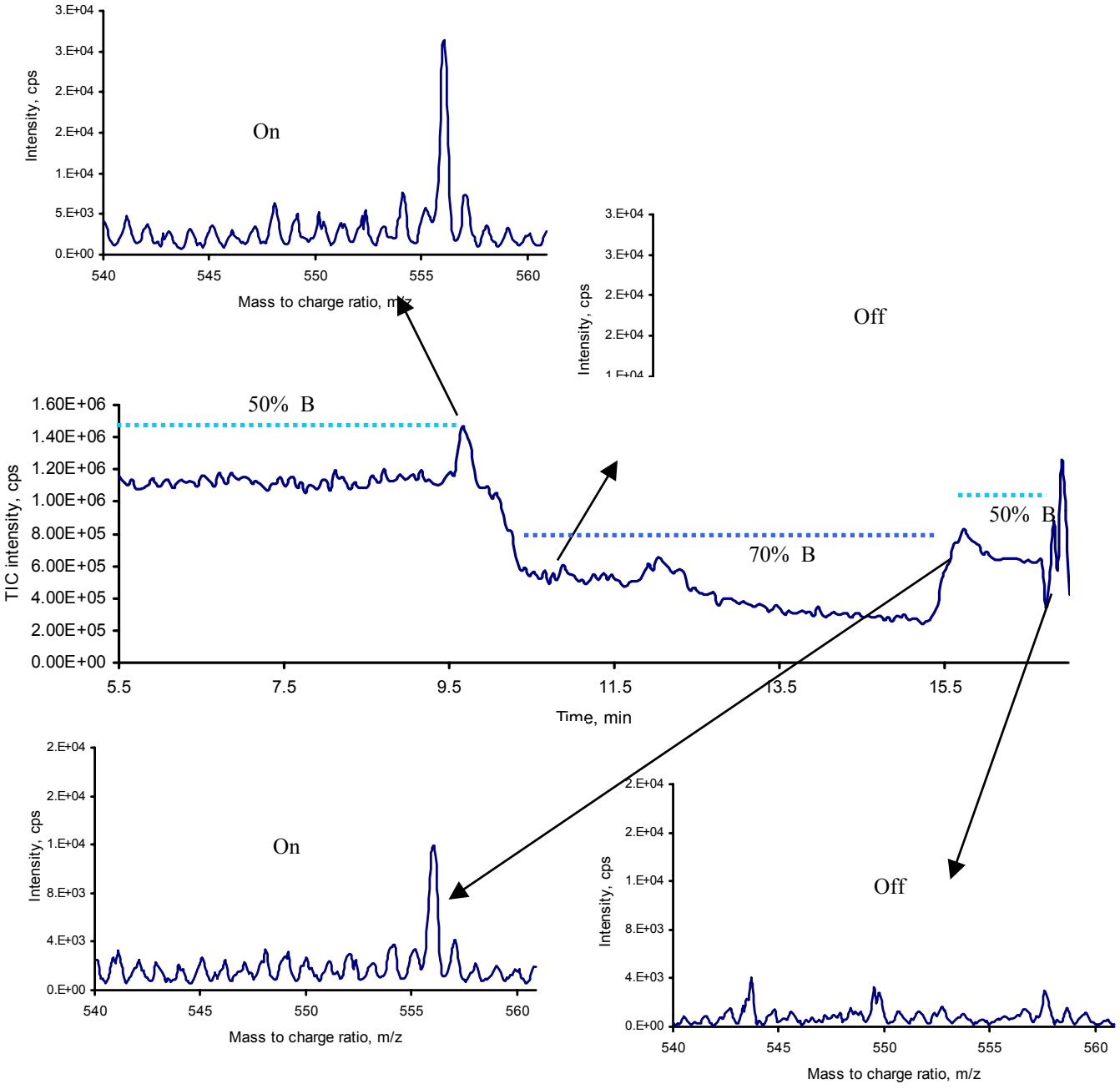

Figure 5.21. "On-off" phenomena shown in the elution of leucine enkephalin solution from an entrapped ODS emitter by stacking 1000 nL of 1 μM LE solution. LE peak appears when it is "on" and disappear when it is "off".

5.3.4. Separation

The poor binding of protein on an entrapped emitter was also confirmed with a protein separation experiment. A protein mixture was prepared with 23 μM BK, 7.1 μM LE, 4.6 μM Cyt-C, and 9.4 μM Ins in 100% aqueous. A 600 nL protein mixture was loaded onto the emitter bed automatically through an Eksigent nano-pump. Figure 5.22 shows a TIC trace for a 2 min washing with 2% B flowing by a gradient with gradually increasing B composition. However, only minimal binding of BK, LE, and Ins was observed. Cyt-c was not detected with the elution showing no binding at all.

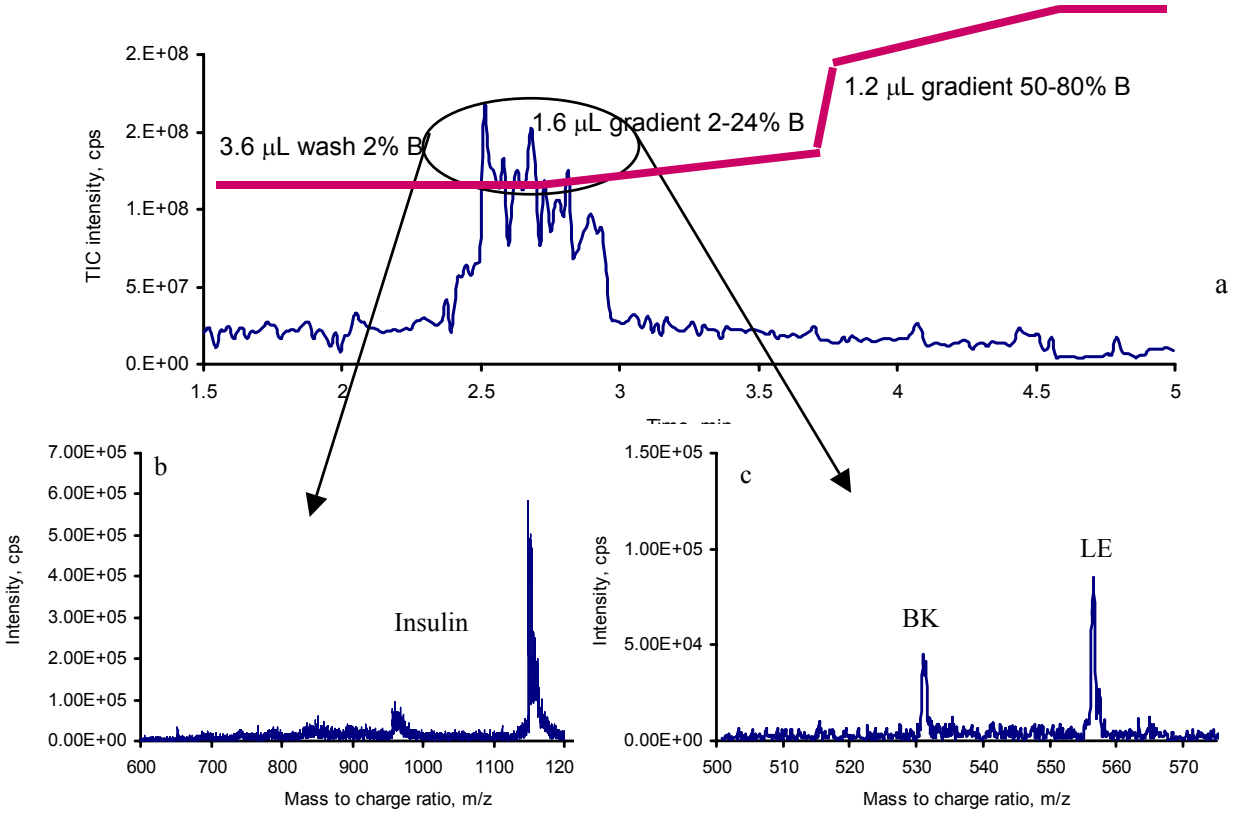

Figure 5.22. Separation of proteins by an entrapped ODS emitter: (a) TIC trace of a protein mixture containing BK, LC, Cyt-c, and Ins. from a gradient; (b) extracted mass spectrum of insulin, (c) extracted mass spectrum of unseparated BK and LE.

The same protein separation experiment was conducted using a packed ODS emitter. Bradykinin and leucine enkephalin were separated from each other as well as from Cyt-c and insulin. Cyt-c and insulin had an overlap, but individual peaks were still resolved with great sensitivity as shown in Figure 5.23.

5.3.5. Desalting

The same protein mixture as above was prepared with different types of salts respectively for the testing of desalting efficiency. Salts such as sodium chloride, urea, potassium phosphate, and Tris can be effectively removed from the range of 150 mM to 900 mM with as little as a 10 column volume wash (see Figure 5.24a and 5.24b for a comparison of a 10 and 80 column volume wash). Sucrose, which is a commonly used media in bio-samples, was also removed efficiently. The evaluation of emitter performance after removal of salts was conducted using a 10 column volume wash (Figure 5.24c to 5.24f). Except for potassium phosphate, both intensity and retention time of each resolved protein peak was not affected significantly after washing away the salts. Although the peak intensity was reduced, the four proteins were still resolved as shown in Figure 5.24c. An indicator (pH paper) was also used to confirm the complete removal of monobasic potassium phosphate by observing the color of the pH paper changing from pink to beige, and for Tris from blue to beige. An entrapped emitter showed similar capability for removal of salts.

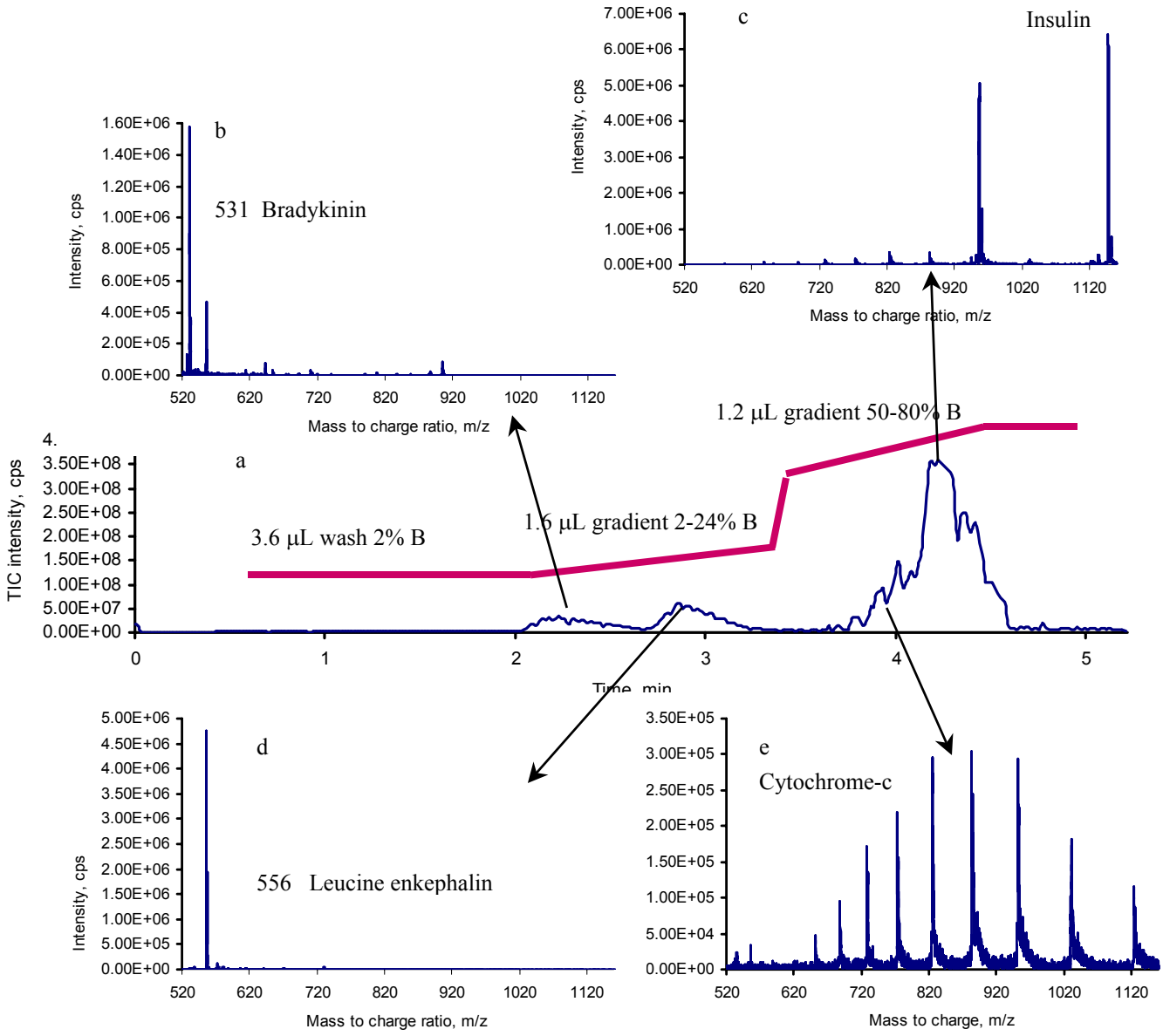

Figure 5.23. Separation of proteins by a packed ODS emitter: (a) TIC trace of a protein mixture containing BK, LC, Cyt-c, and Ins. from a gradient; (b) extracted mass spectrum of resolved BK, (c) extracted mass spectrum of solved insulin, (d) extracted mass spectrum of solved LE, (e)extracted mass spectrum of resolved Cyt-c.

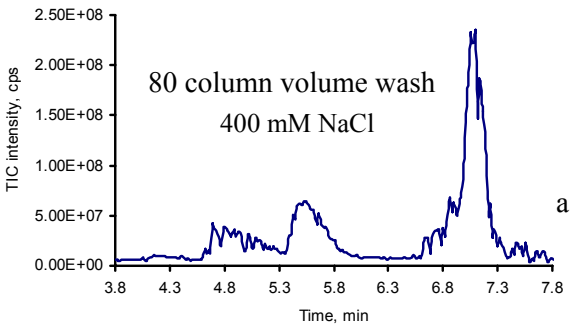
80 column volume wash
400 mM NaCl
TIC intensity, cps
Time, min
a

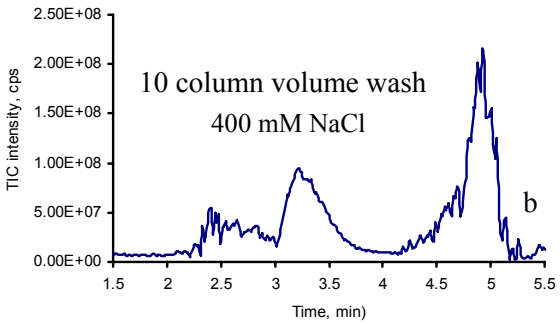
10 column volume wash
400 mM NaCl
TIC intensity, cps
Time, min)
b

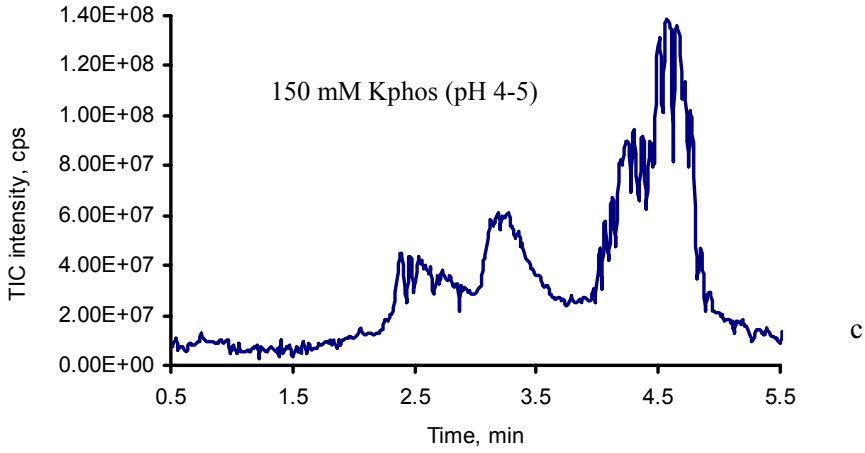
150 mM Kphos (pH 4-5)
TIC intensity, cps
Time, min
c

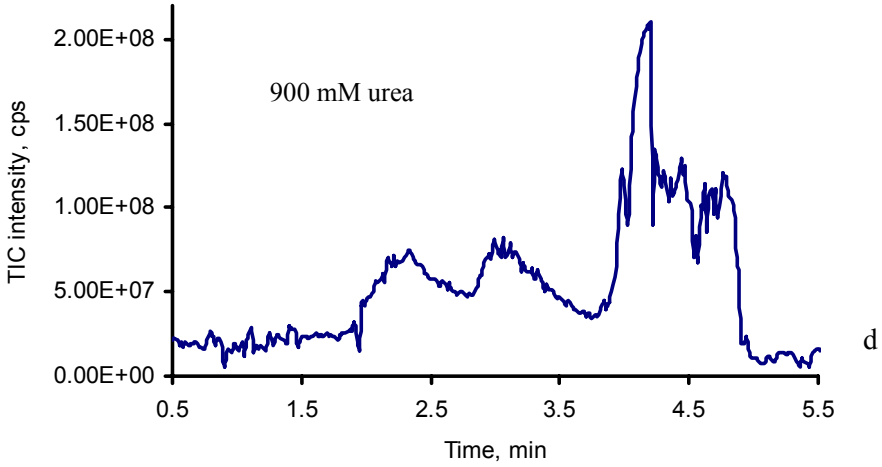
900 mM urea
TIC intensity, cps
Time, min
d

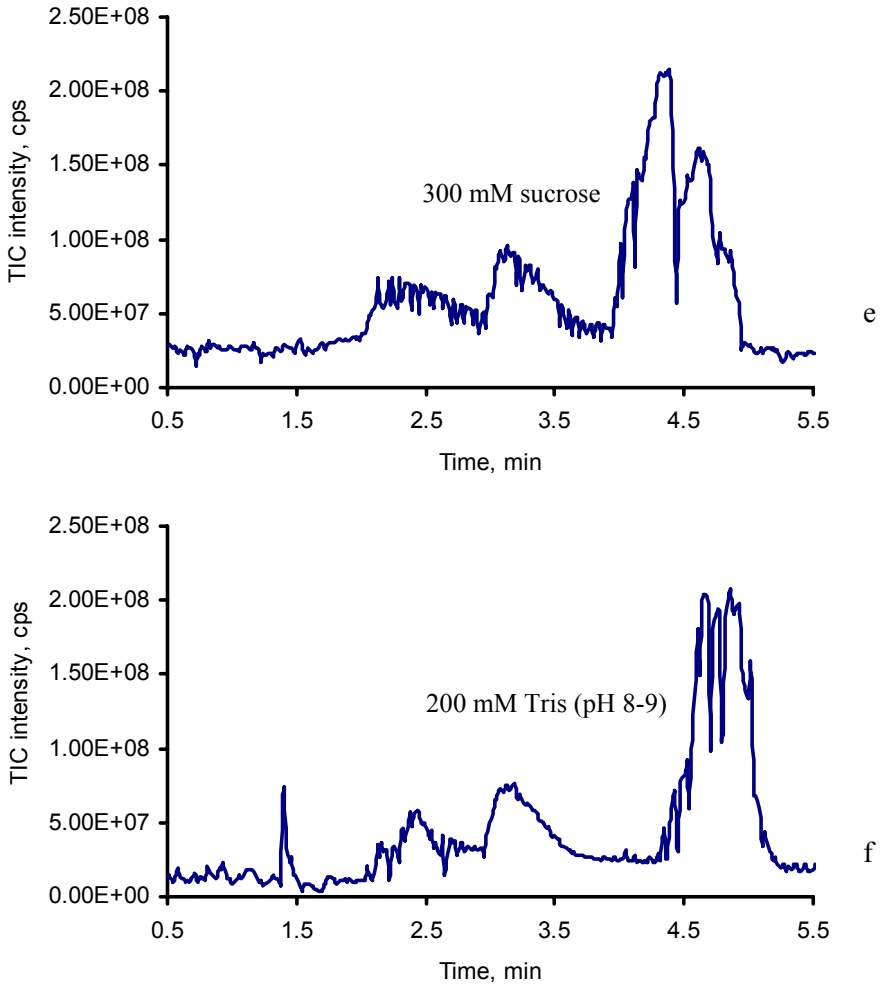

Figure 5.24. Removal of various salts from a protein mixture: (a) removal of 400 mM NaCl by 80 column volume wash; (b) removal of 400 mM NaCl by 10 column volume wash; (c) removal of 150 mM Kphos by 10 column volume wash; (d) removal of 900 mM urea by 10 column volume wash; (e) removal of 300 mM sucrose by 10 column volume wash; (f) removal of 200 mM Tris by 10 column volume wash.

5.3.6. Protein identification

An entrapped emitter, a packed ODS emitter, and a roughened emitter were used as a nano-ESI/MS/MS interface for protein identification, respectively. Nano-ESI/MS/MS has been demonstrated as a promising system for the identification of

proteins, especially those proteins of low abundance. However, the traditional tapered emitters suffer from continuous clogging, which has impeded their routine application. In this study, a 2.5 μL sample of trypsin digested BSA (100 fmol) was sprayed from a non-tapered emitter through constant infusion at 500 nL/min for MS/MS analysis by a Q-TOF instrument. The majority of the peptide ions were collected within 20 minutes as shown in Figure 5.25a. Figure 5.25b shows a representative mass spectrum extracted from Figure 25a. The MS/MS data were searched against the Swiss-Prot database which gives a total of 46 peptides matched with a MOWSE score of 1620 and sequence coverage of 72% (Table 5.2 and 5.3, Figure 5.26). MOWSE score is a probability based ion score expressed by -10*Log(P), where P is the probability that the observed match is a random event. Table 5.4 and Figure 5.27 and 5.28 give an example showing the MS/MS searching and matching using fragmentation of RHPEYAVSVLLR that was found in ALBU_BOVIN, serum albumin precursor (Allergen Bos d 6) (BSA) - Bos taurus (Bovine).

The summarized sequence coverage obtained from different non-tapered emitters was listed in Table 5.5. The results show that entrapped emitters as well as the non-tapered emitters developed here give reasonable sequence coverage that can be used for protein identification. The sequence coverage from an open tubular emitter, an entrapped emitter and a packed emitter are 62%, 72%, and 78% respectively. The reduced concentration of BSA digests was also used for the experiment using an entrapped emitter. Sequence coverage of 35% and 20% were obtained from a 10 femtomole and 1 femtomole BSA digest, respectively.

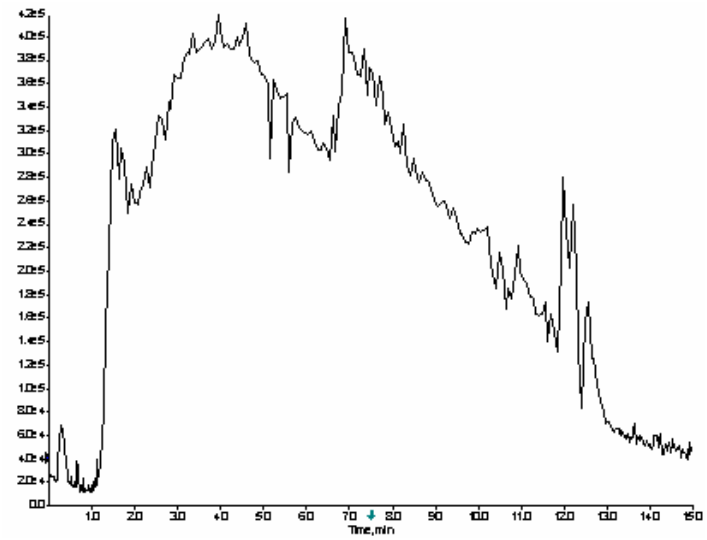

a

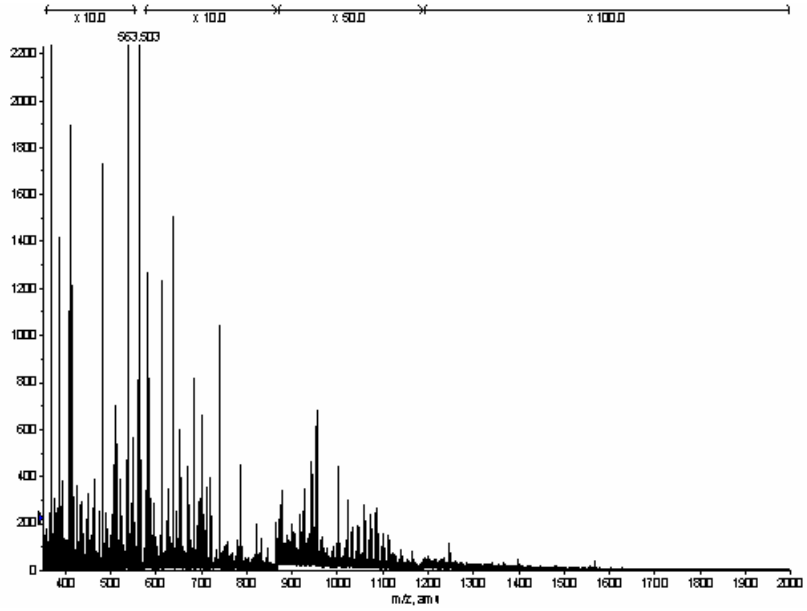

b

Figure 5.25. Direct infusion of 2.5 μL trypsin digested BSA (100 fmol) in 50% ACN (0.1% of formic acid) from an entrapped emitter at 500 nL/min and 4.5 kV spray voltage: (a) TIC trace of precursor ions of trypsin digests; (b) mass spectrum extracted from 20a at 8.74 min.

Table 5.2. Mascot Search Results

Type of search	MS/MS Ion Search
Enzyme	Trypsin
Fixed modifications	Carbamidomethyl (C)
Variable modifications	Deamidated (NQ),Gln->pyro-Glu (N-term Q),
	Glu->pyro-Glu (N-term E),Oxidation (M)
Mass values	Monoisotopic
Protein Mass	Unrestricted Peptide
Mass Tolerance	± 0.2 Da
Fragment Mass Tolerance	± 0.2 Da
Max Missed Cleavages	2
Instrument type	Q-TOF
Number of queries	647

Table 5.3. Protein view

Match to	ALBU_BOVIN
Score	1620
Serum albumin precursor	(Allergen Bos d 6) (BSA) - Bos taurus (Bovine)
Nominal mass (Mr):	71244
Calculated pI value	5.82
Taxonomy	Bos taurus
Fixed modifications	Carbamidomethyl (C)
Variable modifications	Deamidation (NQ),N-Acetyl (Protein),
	Oxidation (M),Pyro-glu (N-term E),Pyro-glu (N-term Q)
Cleavage by Trypsin	cuts C-term side of KR unless next residue is P
Sequence coverage	72%

Matched peptides shown in **Bold Red**

```
  1 MKWVTFISLL LLFSSAYSRG VFRRDTHKSE IAHRFKDLGE EHFKGLVLIA
 51 FSQYLQQCPF DEHVKLVNEL TEFAKTCVAD ESHAGCEKSL HTLFGDELCK
101 VASLRETYGD MADCCEKQEP ERNECFLSHK DDSPDLPKLK PDPNTLCDEF
151 KADEKKFWGK YLYEIARRHP YFYAPELLYY ANKYNGVFQE CCQAEDKGAC
201 LLPKIETMRE KVLASSARQR LRCASIQKFG ERALKAWSVA RLSQKFPKAE
251 FVEVTKLVTD LTKVHKECCH GDLLECADDR ADLAKYICDN QDTISSKLKE
301 CCDKPLLEKS HCIAEVEKDA IPENLPPLTA DFAEDKDVCK NYQEAKDAFL
351 GSFLYEYSRR HPEYAVSVLL RLAKEYEATL EECCAKDDPH ACYSTVFDKL
401 KHLVDEPQNL IKQNCDQFEK LGEYGFQNAL IVRYTRKVPQ VSTPTLVEVS
451 RSLGKVGTRC CTKPESERMP CTEDYLSLIL NRLCVLHEKT PVSEKVTKCC
501 TESLVNRRPC FSALTPDETY VPKAFDEKLF TFHADICTLP DTEKQIKKQT
551 ALVELLKHKP KATEEQLKTV MENFVAFVDK CCAADDKEAC FAVEGPKLVV
601 STQTALA
```

Figure 5.26. The MS/MS data searched against the Swiss-Prot database which gives a total of 46 peptides matched with a MOWSE score of 1620 and sequence coverage of 72%.

Table 5.4. Peptide View

Match to Query 398	1438.817655 from(480.613161,3+)
Elution	6.16 min
Period	1
Cycle(s)	139 (Experiment 4)
Monoisotopic mass of neutral peptide Mr(calc)	1438.8
Fixed modifications	Carbamidomethyl (C)
Ions Score	96
Expect	2.70E-07
Matches (Bold Red):	26/132 fragment ions using 27 most intense peaks

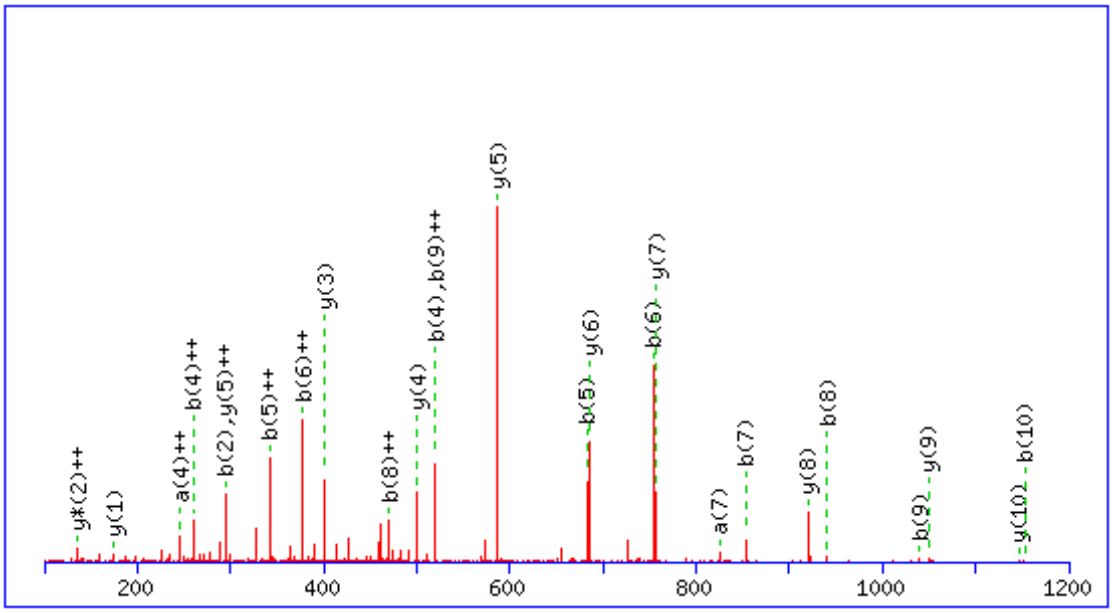

Figure 5.27. An example showing MS/MS searching and matching using fragmentation of RHPEYAVSVLLR that was found in ALBU_BOVIN, serum albumin precursor (Allergen Bos d 6) (BSA) - Bos taurus (Bovine).

#	a	a^{++}	a^{*}	a^{*++}	b	b^{++}	b^{*}	b^{*++}	Seq.	y	y^{++}	y^{*}	y^{*++}	#
1	129.11	65.06	112.09	56.55	157.11	79.06	140.08	70.54	R					12
2	266.17	133.59	249.15	125.08	294.17	147.59	277.14	139.07	H	1283.71	642.36	1266.68	633.85	11
3	363.23	182.12	346.20	173.60	391.22	196.11	374.19	187.60	P	1146.65	573.83	1129.63	565.32	10
4	492.27	246.64	475.24	238.12	520.26	260.63	503.24	252.12	E	1049.60	525.30	1032.57	516.79	9
5	655.33	328.17	638.30	319.66	683.33	342.17	666.30	333.65	Y	920.56	460.78	903.53	452.27	8
6	726.37	363.69	709.34	355.17	754.36	377.69	737.34	369.17	A	757.49	379.25	740.47	370.74	7
7	825.44	413.22	808.41	404.71	853.43	427.22	836.40	418.71	V	686.46	343.73	669.43	335.22	6
8	912.47	456.74	895.44	448.22	940.46	470.74	923.44	462.22	S	587.39	294.20	570.36	285.68	5
9	1011.54	506.27	994.51	497.76	1039.53	520.27	1022.51	511.76	V	500.36	250.68	483.33	242.17	4
10	1124.62	562.81	1107.59	554.30	1152.62	576.81	1135.59	568.30	L	401.29	201.15	384.26	192.63	3
11	1237.71	619.36	1220.68	610.84	1265.70	633.35	1248.67	624.84	L	288.20	144.61	271.18	136.09	2
12									R	175.12	88.06	158.09	79.55	1

Figure 5.28. List of fragment masses showing sequence match.

Table 5.5. Summary of sequence coverage obtained from different non-tapered emitters

	Sequence Coverage, %			Amount, fmole
Emitter ID	Run 1	Run 2	Mean	
Packed ODS emitter	75	81	78	100
Entrapped ODS emitter	71	72	72	100
	35			10
	20			1
Roughened open tubular	60	64	62	100

5.4. Summary

The characterization of nanoelectrospray from integrated emitters made of both packed and entrapped ODS emitters provides a guideline for the utilization of these emitters for online sample manipulation and purification. Nanoelectrospray characterization was mainly conducted with an entrapped emitter. A mist of fine droplets

instead of a Taylor cone was formed at low nano flow rate using an entrapped emitter, which results in increased sensitivity at lower nano flow rates. In particular, the capability of enabling nanoelectrospray at larger operational distance will be beneficial for protection of the ion source from contamination when using the emitter for online sample preparation. Entrapped emitters also demonstrate extraordinary resistance to clogging as demonstrated from a robustness test using a Hank's solution. In addition, this study shows that this type of entrapped emitter allows relatively flexible operational parameters with moderate change in sensitivities compared to conventional tapered emitters. It was also found that under certain operational conditions, near equivalent peak intensities of a peptide standard leucine enkephalin can be obtained from electrosprays at 10 nL/min to 500 nL/min flow rates without further optimization. Even though the optimal conditions may vary for different instrument configurations, the operation of an entrapped emitter at nano flow rates is in general very robust and minimal effort for optimization is required.

The potential of using an integrated emitter for multiple functions was investigated for both packed and entrapped emitters. Both emitters show strong capability for online desalting leaving negligible ion suppression after the salt is removed. Although our previous study indicated some difficulties in achieving reproducible electrospray performance from a PPM emitter, the packed ODS emitter (which spray from a PPM frit) shows its capability of binding proteins with different strengths according to their hydrophobicity. The experiments show that the packed ODS bed can be used for stacking proteins for pre-concentration. Four proteins were also separated sufficiently through a solvent gradient when using a packed ODS emitter. Entrapped ODS emitters, however,

found difficulty in protein binding even though excellent nanoelectrospray performance was demonstrated from this type of emitter. Further studies in polymer chemistry are needed in order to explore the possibility of enabling proper protein binding so that it can combine the benefit from entrapping as well as the merits of bare ODS for chromatography.

Both packed and entrapped emitters as well as an open tubular emitter were used to successfully demonstrate the utilization of non-tapered emitter for protein identification through a direct infusion followed by MS/MS analysis and Mascot searching.

5.5. References

(1) Pelzing, M.; Neususs, C. *Electrophoresis* **2005**, *26*, 2717-2728.

(2) Peh, T. K. G.; (Avago Technologies General Ip (Singapore) Pte. Ltd., Singapore). Application: US, 2005, pp 6 pp.

(3) Luo, Q.; Page, J. S.; Tang, K.; Smith, R. D. *Analytical Chemistry* **2007**, *79*, 540-545.

(4) Robins, R. H.; Guido, J. E. *Rapid Communications in Mass Spectrometry* **1997**, *11*, 1661-1666.

(5) Xie, R.; Oleschuk, R. *Analytical Chemistry* **2007**, *79*, 1529-1535.

(6) Koerner, T.; Turck, K.; Brown, L.; Oleschuk, R. D. *Analytical Chemistry* **2004**, *76*, 6456-6460.

(7) Lee, S. S. H.; Douma, M.; Koerner, T.; Oleschuk, R. D. *Rapid Communications in Mass Spectrometry* **2005**, *19*, 2671-2680.

(8) Smith, D. R.; Moy, M. A.; Dolan, A. R.; Wood, T. D. *The Analyst* **2006**, *131*, 547-555.

(9) Skazov, R. S.; Nekrasov, Y. S.; Kuklin, S. A.; Simenel, A. A. *European Journal of Mass Spectrometry* **2006**, *12*, 137-142.

(10) Eshraghi, J.; Chowdhury, S. K. *Analytical Chemistry* **1993**, *65*, 3528-3533.

(11) Koerner, T.; Xie, R.; Sheng, F.; Oleschuk, R. *Analytical Chemistry* **2007**, *79*, 3312-3319.

(12) Bruce, J. E.; Anderson, G. A.; Wen, J.; Harkewicz, R.; Smith, R. D. *Analytical Chemistry* **1999**, *71*, 2595-2599.

(13) www.matrixscience.com (last visited in May 2007)

(14) http://www.gwu.edu (last visited in September 2008)

Chapter 6

Conclusions and Outlook

6.1 Overview

This chapter highlights the main findings from the thesis study and also outlines some interesting research areas that may be explored further.

6.2 Conclusions

6.2.1 Practical aspects of developing non-tapered nano-ESI emitters

Five types of non-tapered nanoelectrospray emitters (listed in table 6.1) were developed during the thesis study. Two general approaches, using either a larger emitter exit aperture or multiple spray channels, were followed. One of the study objectives was to improve the robustness of nano-ESI emitters. The non-tapered emitters greatly improved the clogging resistance due to a larger aperture or multiple spray channels compared to traditional tapered emitters. In addition, flow resistance from open tubular emitters, membrane emitters, and MSF fiber emitters is negligible. Moderate backpressures were generated from the chromatographic materials filled in either packed or entrapped ODS emitters. For example, a 1 cm entrapped ODS bed yields about 500 psi induced backpressure at 500 nL/min flow rate at the emitter head. Chemical resistance was another property assessed for each emitter type. For a membrane assisted emitter, epoxy resin bonded membrane tended to peel from the emitter exit after exposure to solvents (*i.e.* methanol and acetonitrile). The polyacrylate coating for the MSF fiber

emitter tended to soften when in contact with methanol and acetonitrile, and dissolved in toluene during the hydrophobic modification treatment.

The other goal of the study was to achieve equivalent electrospray performance to that of a conventional tapered emitter. Stable nanoelectrospray at flow rates as low as 10 nL/min from MSF fiber emitters and entrapped ODS emitters, and 50 nL/min from an open tubular emitter and a membrane emitter were obtained. These emitters all demonstrated good electrospray performance in terms of stability and sensitivity with at least 20% organic solvent. The hydrophobic modified MSF emitter shows excellent performance when spraying a highly aqueous solution even with 100% water. The sensitivity gain from a MSF emitter comparing to that of a tapered emitter is about $\sqrt{N}$ (N is the number of individual orifices on MSF emitter).

The impacts of operational parameters on nanoelectrospray behaviour and performance were also investigated for these non-tapered emitters. It was found that unlike tapered emitters, non-tapered emitters can be positioned at a further distance relative to the MS orifice (5 to 25 mm versus 1-2 mm). The optimization of emitter position was not as critical as that required for tapered emitters. This results in faster turn around when replacing an emitter, and greater flexibility in its positioning. The greater positioning distance prevents the MS ion source from becoming contaminated when conducting online sample treatment and purification.

Furthermore, the ease of fabrication was also taken into consideration during the development of non-tapered emitters. Our group has demonstrated an efficient and reliable method to fabricate entrapped emitters as integrated emitters. Although the

chromatographic performance obtained from an entrapped emitter is not as good as that of a packed ODS emitter, the road has been paved for the further study of polymerization chemistry to eliminate the impact of polymer on the chromatographic properties.

Table 6.1. Summary of non-tapered emitters developed during the thesis study

Characterizations	**Roughened Emitter**	**Membrane Emitter**	**Modified MSF Emitter**	**Packed ODS Emitter**	**Entrapped ODS Emitter**
ESI performance					
Flow rates, nL/min	> 50	> 50	> 10	> 50	> 10
Stability, %RSD	Good	Good	Excellent	Good	Excellent
Reproducibility	Good	Good	Excellent	OK	Excellent
Sensitivity	Good	Good	Excellent	Good	Excellent
High aqueous spray	Poor	ND	Excellent	ND	ND
Robustness					
Clogging resistance	Excellent	Good	Excellent	Good	Good
Flow resistance	Negligible	Negligible	Negligible	Moderate	Moderate
Chemical resistance	Excellent	Limited	Limited	Limited	Limited
Solution degasing	Sensitive	ND	ND	Moderate	Moderate
Functionalities					
Function	Emitter	Emitter	Emitter	Emitter/Multi-functionalities	Emitter/Multi-functionalities
Chromatography	None	None	None	Good	Need optimized polymerization
Fabrication					
Easiness of fabrication	Yes	No	Yes	OK	OK
Relative cost of production	Low	Moderate	Low	High	High

6.2.2 Theoretical aspects of multiple nanoelectrospray

In addition to the traditional nanoelectrospray theory proposed from a single-tip tapered emitter, the fundamental aspects of nanoelectrospray were discussed based on non-tapered emitters. It was found that when spraying from a large open tubular emitter, the trend of reducing the size of emission zone with the reduced flow rates agrees with theoretical predication. A stable electrospray with a roughened open tubular emitter with 75 μm i.d. dimensions was maintained at a 50 nL/min flow rate. It suggests that in addition to parameters such as emitter geometry, spray voltage, flow rates, solvent composition, and the relative distance between the emitter tip to MS orifice, the surface roughness (*i.e.* modified wettability) also affects the stability of the electrospray signals.

The fundamental theory of nanoelectrospray was also investigated for multiple channeled emitters. Unlike a single Taylor cone generated from a single-tip tapered emitter, a plume of mist was observed at low nano-flow rates from both entrapped emitters and MSF emitters. The plume of mist was attributed to multiple Taylor cones formed from multiple channels. The assumption was supported by the fact that a sensitivity gain was related to the square root of emitter number as obtained using a 30 orifice MSF emitter. The multiple channels split the flow into multiple streams providing a means of spraying a relatively large volume in a more efficient manner, but also reduces the tendency to clog.

6.2.3 Application potential of the robust nano-ESI emitters

The application potential of the developed non-tapered emitters was investigated. Protein identification experiments were carried out using a roughened open tubular emitter, a packed, and entrapped ODS emitter. It was found that non-tapered emitters not only show good electrospray performance at low flow rates yielding sequence coverage between 60% to 72% by a direct infusion of a tryptic digested BSA, but also demonstrate greater ease of use, and enhanced robustness to clogging.

The potential of using integrated emitters for preconcentration, desalting, and separation was also discussed. The protein binding capability of both bare ODS beads and ODS beads with entrapping polymer was compared. The performance obtained from a packed ODS emitter showed better binding capabilities than that of entrapped ODS beads. The bare ODS bead bed is able to bind different proteins with different strengths so that individual proteins were eluted at different solvent strength and retention time. However, when entrapping ODS beads with the butyl-acrylate polymer, the surface morphology is likely changed (i.e. the micro-pores might be masked by polymer). The retention capability of proteins on bare ODS beads enables desalting. Proteins were eluted following complete salt removal which significantly reduced ion suppression.

With hydrophobic modification, the MSF emitters demonstrated excellent electrospray efficiency with highly aqueous solutions. The modified emitters can potentially be used in applications such as the study of non-covalent protein binding, where spraying highly aqueous solutions is necessary.

6.3 Outlook

6.3.1 Mechanism studies of multiple nanoelectrospray

Although multiple nanoelectrospray was proposed from multiple channel-emitters, individual Taylor cones could not be clearly observed (schematic drawing in Figure 6.1). However, the development of well defined microstructured MSF emitters may make it possible to further study the mechanism of nanoelectrospray from multiple channels.

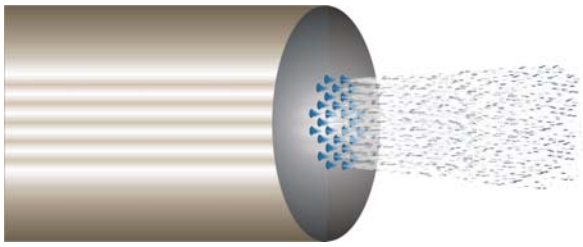

Figure 6.1. Schematic cartoon showing ideal multiple nanoelectrospray from individual Taylor cones (Image courtesy of Dr. Dale Marecak).

Furthermore, in addition to the two MSF emitters investigated in this study, there are various photonic architectures available with different spacing between individual holes and a variety of hole-patterns (shown in Figure 6.2). The availability of various MSF emitter choices provides an opportunity for further study of the effects of emitter geometry on electrospray behaviour and performance. These patterns may also be used to generate computer models to simulate the nanoelectrospray from different geometries.

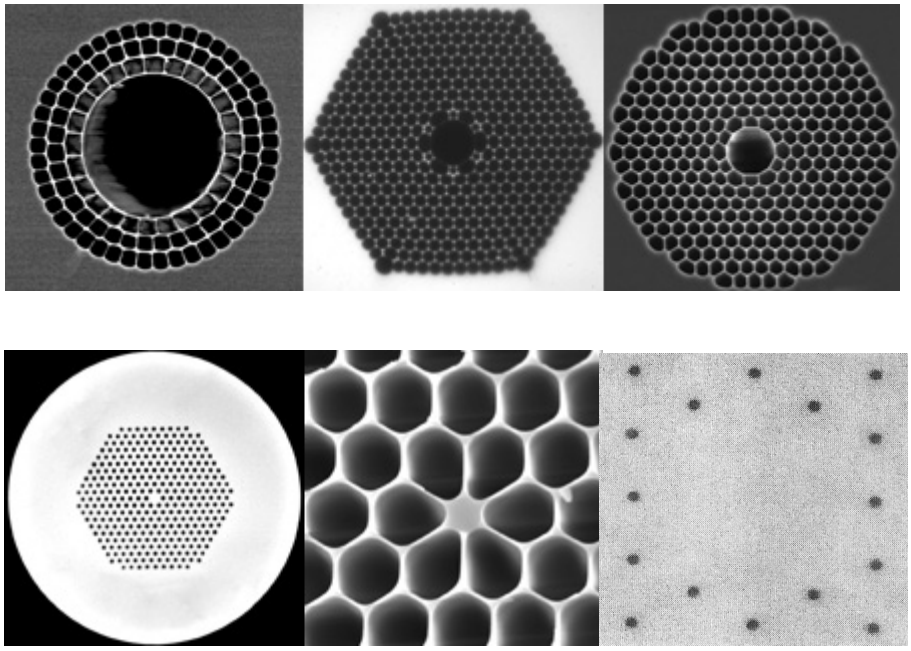

Figure 6.2. Different architectures designed for photonic crystal fibers that are used to efficiently guide light.[1]

6.3.2 Extending applications to non-proteomics

The problems associated with traditional tapered nano-emitters have largely impeded the wide application of the nano-LC/nano-ESI/MS technology. The exception is in research areas such as proteomics, which value the benefits from nano-ESI more than its drawbacks, due to the nature of the analytical work involved in this field. Non-proteomic labs usually prefer regular LC/ESI/MS operation rather than nano-LC/nano-ESI/MS because of the ease of operation and the higher reliability.[2] With the availability of the robust nano-ESI emitters with integrated functions, it may be feasible to operate a nano-LC/nano-ESI/MS as easily as a regular LC/ESI/MS. This means that nano-LC/nano-ESI/MS or MS/MS technologies can be promoted to broader application areas where larger scale LC-ESI/MS is currently employed.

Some interesting research areas regarding this direction include but are not limited to pharmaceutical environmental contamination, the bio-diesel industry and the food industry, where a day-to-day monitoring and analysis of chosen analytes is necessary.[3-5] By implementing miniaturized nano-LC/nano-ESI systems, the better analytical performance will be achieved not only with the improved sensitivity due to better sample utilization efficiency and ionization efficiency but also with more environmentally friendly fashion due to the reduced sample consumption and saved time, labour, space and energy.

6.3.3 Promoting "green" analytical chemistry

The concept of "green" analytical chemistry was proposed in 2001 by Namiesnik who highlighted the top four priorities to achieve "green" based on the 12 principles suggested for green chemistry. The main actions towards "green" based on this concept are primarily the elimination or at least reduction in the amounts of reagents and solvents consumed during analytical laboratory work.[6] Recently, a review article on "green" analytical chemistry systematically outlined more detailed aspects on where and what advanced technologies may be applied during the entire analytical processes to make analytical chemistry greener, where both spectroscopic methods and the miniaturized "Micro Total Analysis System" (μ-TAS) are highlighted.[7]

Miniaturized analytical devices such as microfluidic (also refer to μ-TAS) devices are probably among the most suited instrumentation for achieving "green" analytical chemistry. The idea is to integrate all routine and repetitive laboratory work including

sample introduction, pretreatment, separation, and detection on a microchip platform as small as 2 cm^2 or less.[8] This will significantly reduce sample and reagent consumption, enhance analytical throughput, and decrease costs. While the ultimate aim of μ-TAS is to include sample manipulation and detection on a single chip-sized device, simpler devices with partially integrated functionalities may have more advantages due to their robustness and better reliability.

Compared to a chip-based device, a capillary-based device is simpler and can integrate functions such as sample clean-up, desalting and separation.[9] Following nano-LC, the analytes can be delivered through electrospray ionization into a mass spectrometer (MS) for enhanced detection. By shrinking to "nano-scale" operations, the equivalent or better analytical performance may be achieved in a "greener" manner. The availability of different types of robust nano-ESI emitters will encourage the broader application of nano-ESI technology to make the analytical lab operation more efficient and more environmental friendly.

6.4. References:

(1) www.crystal-fibre.com/products

(2) Covey, T. R.; Pinto, D. *Practical Spectroscopy* **2002**, *32*, 105-148.

(3) Richardson, S. D. *Analytical Chemistry* ***2007,*** 79, 4295-4323.

(4) Rodrigo R. C.; Aline O. F. Elizete M. P. *Journal of Mass Spectrometry.* **2006,** 41, 185-190.

(5) Flamini, R. *Journal of Mass Spectrometry* **2005**, *40*, 705-713.

(6) Namiesnik, J. *Journal of Separation Science* **2001**, *24*, 151-153.

(7) He, Y.; Tang, L.; Wu, X.; Hou, X.; Lee, Y.-I. *Applied Spectroscopy Reviews* **2007**, *42*, 119-138.

(8) Oleschuk, R. D. *Trends in Analytical Chemistry* **2000**, *19*.

(9) Koerner, T.; Xie, R.; Sheng, F.; Oleschuk, R. *Analytical Chemistry* **2007**, *79*, 3312-3319.